



**Republic of Iraq**

**Ministry of Higher Education and Scientific Research  
Kerbala University / College of Veterinary Medicine  
Physiology, Pharmacology and Biochemistry Department**

**Investigation Of Osteogenesis And The Role Of Treadmill Exercise  
In Osteoporotic Male Rats By RANKL/RANK-OPG Pathway**

**A thesis**

Submitted to the Council of the College of Veterinary Medicine, University of  
Kerbala in Partial Fulfillment of the Requirements for the Master Degree of  
Science in Veterinary Medicine / Physiology

**Written by**

**Tabarak Baseem bulibus**

**Supervised by**

**Prof.Dr. Wefak Jbori AI-Bazi**

**Prof. Dr. Rana Fadhil Mousa**

**1445A.H**

**2024A.D**

بِسْمِ اللّٰهِ الرَّحْمٰنِ الرَّحِیْمِ

﴿قَالَ رَبِّ إِنِّي وَهَنَ الْعَظْمُ مِنِّي وَأَشْتَعَلَ الرَّأْسُ شَيْبًا وَلَمْ  
أَكُنْ بِدُعَائِكَ رَبِّ شَقِيًّا﴾

صدق الله العلي العظيم

سورة مريم (الاية 4)

### Committee Certification

This is certify this thesis (Investigation Of Osteogenesis And The Role Of Treadmill Exercise In Osteoporotic Male Rats By RANKL/RANK-OPG Pathway ) was prepared by (Tabarak Baseem bulibus), We the members of the examining Committee, certify that after reading and examining the student in its content, it is adequate for the ward for the degree of Master in Veterinary Medicine/ Physiology.

  
Asst.Prof.

**Dr. Wafaa kadhum jasim**

College of Veterinary Medicine/ University of Kerbala

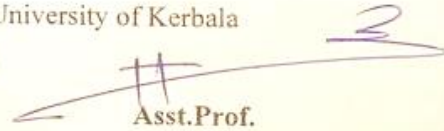
(Chairman)

  
Prof.

**Dr. Tahreer M. Al-Thuwaini**

College of Veterinary Medicine/  
University of AL-Qasim Green

(Member)


  
Asst.Prof.

**Dr. Haider mohammed ali**

College of Veterinary Medicine/  
University of Kerbala

(Member)


  
Prof. Dr. Wefak Jbori Al-Bazi

  
Prof. Dr. Rana Fadhil Mousa

College of Veterinary Medicine/ University of Kerbala

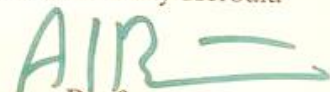
(Member & Supervisor)

Approved by the concile of the college of Veterinary Medicine /University Kerbala

  
Prof.

**Dr. Rana Fadhil Mousa**

Head of Department of Physiology,  
Biochemistry and Pharmacology

  
Prof.

**Dr. Wefak Jbori Al-Bazi**

The Dean of the College of Veterinary  
Medicine


Date: / / 2024

## **Supervisor Certification**

We certify that thesis entitled( **Investigation Of Osteogenesis And The Role Of Treadmill Exercise In Osteoporotic Male Rats By RANKL/RANK-OPG pathway** ) has been prepared by **Tabarak Baseem bulibus** under our supervision at the college of Veterinary Medicine, University of Kerbala in partial fulfillment of the requirements for the Master of Degree in the Sciences of Veterinary Medicine in Veterinary Physiology, Biochemistry and Pharmacology.

### **Supervisor**

**Prof. Dr. Wefak Jbori Al-Bazi**

**Prof. Dr. Rana Fadhil Mousa** 

College of Veterinary Medicine

University of Kerbala

### **The recommendation of the Department**

In view of the above recommendation, I forward this thesis for scientific discussion by the examining committee

**Prof. Dr. Ihab Ghazi Mahdi** 

**Vice Dean for Postgraduate studies and scientific Affairs**

College of Veterinary Medicine

University of Kerbala

## Certification of Linguistic Evaluator

I certify that thesis entitled « **Investigation Of Osteogenesis And The Role Of Treadmill Exercise In Osteoporotic Male Rats By RANKL/RANK-OPG Pathway** » for the student ( **Tabarak Baseem bulibus** ) was linguistically reviewed by me and the necessary correction has been made. Thus, it is linguistically ready for examination.

Linguistic Evaluator

Name: Asst. Prof. Dr. Hamed Qattan Jawad



Signature

## ***Declaration***

I hereby declare that this dissertation is my original work except for equations and citations which have been fully acknowledged. I also declare that it has not been previously, and is not concurrently, submitted for any other degree at University of Kerbala or other institutions.

***Tabarak Baseem bulibus***

***/ / 2024***

*Dedication*

**All Thanks to Allah firstly and finally, then to our prophet Mohammed and his family.**

**To my wounded homeland.... IRAQ**

**I present fragments of my humble research as a gift to my family who supported me and encouraged me in every step**

**To my friends and colleagues in my studies and all my teachers, to my companions in my path**

**I would like to thank everyone who supported me to successfully complete my research**

*Tabarak Baseem bulibus*

## Acknowledgements

Praised be God Almighty, first and foremost, who directed me to prepare this research

I would like to express my sincere thanks and gratitude to ( **Dr. Wefak Jbori Al-Bazi.**) She taught me a lot and helped me build my academic background with broad knowledge, and her strong support and patience is what made this thesis possible.

I would also like to thank (**Dr. Rana Fadhil Mousa**) for her supervision, constant interest, encouragement and advice.

I extend my sincere thanks to the Deanship of **the College of Veterinary Medicine, University of Kerbala**, for help me in postgraduate studies in the branch of physiology, biochemistry, and pharmacology, I also extend my thanks and appreciation to all the teaching staff in the college, including doctors and professors, through their support for me during my postgraduate studies.

Thank you very much to (**Dr. Haider Ali Mohammed** ) for helping me in gene expression assay.

Thank you very much to (**Dr. Hussein Bashir and Dr. Ali Jalil** ) for helping me in scanning electron microscope .

Thank you very much to (**Dr. Falah Mahmood** ) for helping me in X-ray reading.

*Tabarak Baseem bulibus*



## Summary

Osteoporosis is bone loss density and deterioration of bone tissues, osteoclasts are generally regarded as the only cells capable of resorbing to bone, physical exercise by Treadmill has positive preventive and therapeutic effects on osteoclast activity.

The experiment employed 24 male rats, randomly divided equally three groups (8each group), the first group as control group, and the second group rats were given daily 200 mg/kg BW (D-gal) injected intraperitoneally for sixty days. The third group, animals were given daily 200mg/kg BW D-galactose with use of a treadmill at 25 m/min for 5 days weekly for sixty days. First day,30 and 60 days of the experiment was performed to evaluate the bone mineral density (BMD) at the femur of rats. Blood samples were drawn for biochemical analysis to by measuring bone restoration and formation biomarkers represented by Receptor Activator of Nuclear Factor Kappa-B (RANK), Receptor Activator of Nuclear Factor Kappa-B ligand (RANK-L), Cathapsin K, and osteoprotegrin (OPG), serum electrolyte (Ca, Na ,K,and P) , serum hormones(serum PTH, and calcitonin) , and serum Vit D. The femur bone following synthesis of cDNA, gene specific primers used to determine the level of gene Runx2. After preserving the femoral bone to examined by use light microscope and scanning electron microscope(SEM).

The results investigate a significant increase in serum RANK, RANK-L, and cathapsin-K levels in osteoporotic rats with D-gal, while OPG analysis revealed a significant decline in this groups. while the impact of the (treadmill+D-gal) showed a significant decrease in the levels of serum, RANK, RANKL, and Cathepsin K compared with the D-gal group. A significant increase of serum in the PTH, Vit D, calcitonin & Ca in the osteoporotic rats compare with other groups,

while serum Na and K showed a significant decline in osteoporotic rats group as compare with other groups. While impact of (treadmill+D-gal) showed a significant decrease in the level of the serum PTH, Vit D , calcitonin & Ca compare with control group. The D-gal case imbalance in the Ca related hormone (PTH & calcitonin ) which lead to imbalance in the Ca an the mineral in the body treadmill exercise stimulates bone formation and suppresses bone resorption. The gene expression (Runx 2) showed a significant increase in the D-gal group as compare with the other two group. The X-ray photography showed a significant decrease in the bone density in the D-gal group as compare with the (treadmill+D-gal) and the control group.

The femur rats histological examination of osteoporotic group showed resorption and marked thinning of trabecular with numerous osteoclasts while the (D-gal +treadmill) groups showed newly added lamellar structure and number of osteocytes with fewer cavities in the bony plates and reduction in micro-fissure in femur compact bone by using electron microscope, exercise increases cancellous bone mass through increased bone formation decreased bone absorption, and increased cortical bone mass due to increased periosteal bone formation. results of the bone examined under the light microscope showed a differences between the control group and the D-gal group, as the D-gal group has activated osteoclast cells, which cause bone necrosis and failure to perform their functions properly, which leads to weakness in the bone tissue while the (D-gal +treadmill) groups showed thicker trabecular and denser bone lamellae within the haversian canals (cavities within the bone) of the treadmill exercising rates.

In conclusion treadmill sport can emolliate the level of serum RANKL-RANK OPG pathway and decrease level of the serum Cathepsin K with up regulation of the Runx2 gene expression on the osteoporosis induced by D-galactose.

## List of Contents

<b>No.</b>	<b>Subject</b>	<b>Page No.</b>
	<b>Summary</b>	<b>I</b>
	<b>List of Contents</b>	<b>III</b>
	<b>List of Tables</b>	<b>VIII</b>
	<b>Table of Figures</b>	<b>VIII</b>
	<b>List of abbreviations</b>	<b>XI</b>
	<b>Chapter One: Introduction</b>	
	<b>Introduction</b>	<b>1</b>
	<b>Aim of the study</b>	<b>4</b>
	<b>Chapter Two: Literature Review</b>	
<b>2</b>	<b>Literature Review</b>	<b>5</b>
<b>2.1</b>	<b>Bones</b>	<b>5</b>
<b>2.2</b>	<b>Bone cells</b>	<b>6</b>
<b>2.2.1</b>	<b>Osteoblast</b>	<b>6</b>
<b>2.2.2</b>	<b>Osteocyte</b>	<b>7</b>
<b>2.2.3</b>	<b>Osteoclast</b>	<b>8</b>
<b>2.3</b>	<b>Osteoporosis</b>	<b>9</b>
<b>2.3.1</b>	<b>Classification of osteoporosis</b>	<b>10</b>
<b>2.3.2</b>	<b>Causes of osteoporosis</b>	<b>10</b>
<b>2.3.3</b>	<b>Mechanism of osteoporosis</b>	<b>11</b>

<b>2.3.4</b>	<b>Risk of osteoporosis</b>	<b>12</b>
<b>2.3.5</b>	<b>Diagnosis of osteoporosis</b>	<b>12</b>
<b>2.3.6</b>	<b>Weight loss</b>	<b>13</b>
<b>2.4</b>	<b>Process of Bone Remodeling</b>	<b>13</b>
<b>2.5</b>	<b>D-galactose (D-gal)</b>	<b>14</b>
<b>2.5.1</b>	<b>D-gal chemical properties</b>	<b>14</b>
<b>2.5.2</b>	<b>D-galactose metabolism</b>	<b>16</b>
<b>2.5.3</b>	<b>Role of D-galactose on Aging</b>	<b>17</b>
<b>2.5.4</b>	<b>Effect of D-galactose on bone</b>	<b>18</b>
<b>2.6</b>	<b>Treadmill effect on bone health</b>	<b>19</b>
<b>2.7</b>	<b>Osteoporotic parameters</b>	<b>20</b>
<b>2.7.1</b>	<b>1Receptor Activator of Nuclear Factor kappa-B Ligand (RANKL)</b>	<b>20</b>
<b>2.7.2</b>	<b>Receptor Activator of Nuclear Factor kappa-B (RANK)</b>	<b>21</b>
<b>2.7.3</b>	<b>Osteoprotegerin (OPG)</b>	<b>22</b>
<b>2.7.4</b>	<b>Cathepsin K</b>	<b>23</b>
<b>2.8</b>	<b>RUNX2 gene</b>	<b>24</b>
	<b>Chapter Three: Methodology</b>	
<b>3.</b>	<b>Materials and Methods</b>	<b>27</b>
<b>3.1</b>	<b>Materials</b>	<b>27</b>
<b>3.1.1</b>	<b>Instruments and Equipment</b>	<b>27</b>
<b>3.1.2</b>	<b>Chemicals and Kits</b>	<b>28</b>

<b>3.2</b>	<b>Examination methods</b>	<b>29</b>
<b>3.2.1</b>	<b>Experimental protocol</b>	<b>29</b>
<b>3.2.1.1</b>	<b>Experimental Design</b>	<b>30</b>
<b>3.2.1.2</b>	<b>Treadmill</b>	<b>31</b>
<b>3.2.1.3</b>	<b>Collect of the blood samples</b>	<b>33</b>
<b>3.3</b>	<b>Ethical approve</b>	<b>33</b>
<b>3.4</b>	<b>Detection of serum Biomarkers of Bone</b>	<b>33</b>
<b>3.4.1</b>	<b>Detection of serum RANK</b>	<b>33</b>
<b>3.5</b>	<b>Detection of serum Hormones that effect on bone</b>	<b>34</b>
<b>3.5.1</b>	<b>Detection of serum Calcitonin</b>	<b>34</b>
<b>3.5.2</b>	<b>Detection of serum parathyroid (PTH)</b>	<b>34</b>
<b>3.5.3</b>	<b>Detection of serum Vit D</b>	<b>34</b>
<b>3.6</b>	<b>Detection of serum Electrolytes</b>	<b>34</b>
<b>3.6.1</b>	<b>Detection of serum Calcium (Ca)</b>	<b>34</b>
<b>3.6.2</b>	<b>Detection of serum phosphorus (P)</b>	<b>34</b>
<b>3.6.3</b>	<b>Detection of serum sodium (Na)</b>	<b>34</b>
<b>3.6.4</b>	<b>Detection of serum potassium (K)</b>	<b>35</b>
<b>3.7</b>	<b>Bone parameters</b>	<b>35</b>
<b>3.7.1</b>	<b>Examination of bone mineral density by X-ray</b>	<b>35</b>
<b>3.7.2</b>	<b>Histopathological study</b>	<b>36</b>
<b>3.7.3</b>	<b>Scanning Electron Microscope(ESM)</b>	<b>36</b>
<b>3.8</b>	<b>Gene expression</b>	<b>36</b>

<b>3.8.1</b>	<b>RUNX2 gene expression</b>	<b>36</b>
<b>3.8.2</b>	<b>Quantitative Reverse Transcriptase Real-Time PCR</b>	<b>37</b>
<b>3.9</b>	<b>Statistical analysis</b>	<b>38</b>
<b>Chapter Four: Results &amp; Discussion</b>		
<b>4.1</b>	<b>Effect of D-gal and treadmill on femoral bone X-Ray</b>	<b>39</b>
<b>4.2</b>	<b>Effect of D-galactose and treadmill on serum biomarkers</b>	<b>44</b>
<b>4.2.1</b>	<b>Effect of D-galactose and treadmill on serum RANK/RANKL</b>	<b>44</b>
<b>4.2.2</b>	<b>Effect of D-galactose and treadmill on serum OPG</b>	<b>49</b>
<b>4.2.3</b>	<b>Effect of D-galactose and treadmill on serum cathapsin K (Cat-K)</b>	<b>52</b>
<b>4.3</b>	<b>Effect of D-galactose and treadmill on serum electrolyte (Na, Ca, P &amp; K)</b>	<b>54</b>
<b>4.4</b>	<b>Effect of D-galactose and treadmill on serum bone related hormones and Vit D</b>	<b>57</b>
<b>4.5</b>	<b>Effect of D-galactose and treadmill on femoral bone histology</b>	<b>60</b>
<b>4.6</b>	<b>Effect of D-galactose and treadmill on femoral bone examined by scanning electron microscope</b>	<b>65</b>
<b>4.7</b>	<b>Effect of D-galactose and treadmill on Runx-2 gene expression</b>	<b>68</b>
<b>Chapter five : Conclusions and Recommendation</b>		
<b>5.</b>	<b>Conclusions &amp; Recommendation</b>	<b>71</b>
<b>5.1</b>	<b>Conclusions</b>	<b>71</b>

<b>5.2</b>	<b>Recommendation</b>	<b>72</b>
	<b>Chapter six :References</b>	

### List of Tables

<b>Table No.</b>	<b>Title</b>	<b>Page No.</b>
<b>3.1</b>	<b>Apparatus and equipment with their manufactures</b>	<b>27</b>
<b>3.2</b>	<b>Chemicals and Kits with their suppliers</b>	<b>28</b>
<b>3.3</b>	<b>Nucleotides sequences for RUNX2 gene and Housekeeping gene</b>	<b>38</b>
<b>4.1</b>	<b>Effect of 200 mg/kg of D-gal daily for 1st , 30 and 60 days day s and 25m/min days treadmill sport in the bone density on the male rats</b>	<b>41</b>

### Table of Figures

<b>Figure No.</b>	<b>Title</b>	<b>Page No.</b>
<b>2.1</b>	<b>Chemical structure of D-galactose</b>	<b>15</b>
<b>2.2</b>	<b>Disorders of galactose metabolism</b>	<b>17</b>
<b>2.3</b>	<b>different bases upon which CQ inhibits osteoclastogenesis</b>	<b>19</b>
<b>2.4</b>	<b>RANKL/RANK/OPG pathway</b>	<b>23</b>
<b>2.5</b>	<b>Cathepsin K - A new molecular target for osteoporosis</b>	<b>24</b>
<b>3.1</b>	<b>Experimental Design</b>	<b>30</b>

3.2	The treadmill machine (25m/min ) that was used in the experiment	32
3.3	Hologic dual-energy X-ray absorptiometry scan machine	35
4.1	Radiographic image of the bones with white arrow of control group showing normal bone density (A). Radiographic image of the bones with black arrow of D-galctose group (B) and treadmill group (C) with yellow and black arrow showing normal bone density,	39
4.2	Radiographic image of the bones at day 30 of the experiment with white arrow of control group showing normal bone density (A). While Radiographic image of the bones with treadmill group (C) with yellow arrow showing significantly improved more than D-galctose group (B) with brown arrow, abnormal bone density, decrease osteoporosis with increase in bones mineral density around the vertebral ,femoral and pelvic bones especially at the middle and epiphysis of bones ( after one month).	40
4.3	Radiographic image of the bones with white arrow of control group showing normal bone density (A). While Radiographic image of the bones with treadmill group show a lees bone density as comper with control (C) the D-gal group showing a significant sclerosis with reduce in bones mineral density around the vertebral ,femoral and pelvic bones with a high radiopaque area (B) brown arrow ( after two month).	41



<b>4.4</b>	<b>Effect of 200 mg/kg of D-gal and 25m/min for 1hr/5 days treadmill sport for 8 weeks in the serum RANK concentration on male rats.</b>	<b>45</b>
<b>4.5</b>	<b>Effect of 200 mg/kg of D-gal and 25m/min for 1hr/5 days treadmill sport in the serum RANKL concentration on male rats.</b>	<b>45</b>
<b>4.6</b>	<b>Effect of 200 mg/kg of D-gal daily for 8weeks and 25m/min days treadmill sport in the serum OPG concentration on the male rats</b>	<b>49</b>
<b>4.7</b>	<b>Effect of 200 mg/kg of D-gal daily for 8weeks and 25m/min days treadmill sport in the serum Cathepsin k concentration on the male rats</b>	<b>52</b>
<b>4.8</b>	<b>Effect of 200mg/kg of D-gal and 25m/min for 1hr/5 days treadmill sport for 8weeks on the serum Na ,Ca,P &amp; K concentration on male rats</b>	<b>55</b>
<b>4.9</b>	<b>Effect of 200mg/kg of D-gal and 25m/min for 1hr/5 days treadmill sport for 8weeks on the serum calcitonin and PTH concentration on male rats</b>	<b>58</b>
<b>4.10</b>	<b>Effect of 200mg/kg of D-gal and 25m/min for 1hr/5 days treadmill sport for 8weeks on the serum Vit.D concentration on male rats .</b>	<b>58</b>
<b>4.11</b>	<b>Photomicrograph of bone tissue section for a control animal (H and E,4X)</b>	<b>61</b>
<b>4.12</b>	<b>Photomicrograph of bone tissue section for D-gal treated animal (H and E,40X)</b>	<b>61</b>
<b>4.13</b>	<b>Photomicrograph of bone tissue section for D-gal treated animal (H and E,100X)</b>	<b>62</b>

<b>4.14</b>	<b>Photomicrograph of bone tissue section for D-gal treated animal with exercise (H and E,4X)</b>	<b>63</b>
<b>4.15</b>	<b>Photomicrograph of bone tissue section for D-gal treated animal with exercise (H and E,40X)</b>	<b>64</b>
<b>4.16</b>	<b>Electron microscope photograph of the control group showed a reversible of the histological alterations manifested by marked thickness of trabeculae and lamellars with emularte in the space of the Haversian canal (cavities in bony plate) and improve in the bone matrix</b>	<b>65</b>
<b>4.17</b>	<b>Electron microscope photograph of the D-gal group showed a significant histological alteration manifested by marked thinning and irregular of trabeculae and lamellar with enlarged in the space of the Haversian canal (cavities in bony plate) resorption in the bone matrix</b>	<b>65</b>
<b>4.18</b>	<b>Electron microscope photograph of the D-gal + treadmill group showed a reversible of the histological alterations manifested by marked thickness of trabeculae and bone lamellar in the space of the Haversian canal (cavities in bony plate) in the bone matrix</b>	<b>66</b>
<b>4.19</b>	<b>amplification curve of the tested samples represented the runx-2 gene. this indicate a successful RNA extraction and cDNA synthesis</b>	<b>68</b>
<b>4.20</b>	<b>fold change comparison between the group expressed runx-2 gene . and show a significant increase in the D-gal group as compeer with the control group and treadmill group.</b>	<b>69</b>

## List of Abbreviations

<b>Abbreviations</b>	<b>Meaning</b>
<b>ADAM</b>	<b>Disinterring and metalloprotease domain</b>
<b>AGE</b>	<b>Advanced Glycation End Products</b>
<b>AGEs</b>	<b>Advanced glycation end-products</b>
<b>AP-1</b>	<b>Activator protein-1</b>
<b>BMD</b>	<b>Bone mineral density</b>
<b>BW</b>	<b>Body Weight</b>
<b>Ca</b>	<b>Calcium</b>
<b>CaSR</b>	<b>Calcium-sensing receptors (CaSR)</b>
<b>Cat K</b>	<b>Cathepsin K</b>
<b>CCD</b>	<b>Cleidocranial Dysplasia</b>
<b>D-gal</b>	<b>D-galactose</b>
<b>DXA</b>	<b>Dual X-ray absorptiometry</b>
<b>DXA</b>	<b>Dual-energy X-ray Absorptiometry</b>
<b>ERK</b>	<b>extracellular signal-regulated kinase</b>
<b>FAK</b>	<b>focal adhesion kinase</b>
<b>GAPDH</b>	<b>Glyceraldehyde 3-phosphate dehydrogenase</b>
<b>H&amp;E</b>	<b>hematoxylin and eosin</b>
<b>HCD</b>	<b>High cholesterol diet</b>
<b>I/M</b>	<b>I/M</b>
<b>IGF-1</b>	<b>Insulin growth factor 1</b>

<b>IL-1</b>	<b>Interleukin-1</b>
<b>JNK</b>	<b>Jun N-terminal kinase</b>
<b>g/kg</b>	<b>Gram per Kilogram</b>
<b>m/s</b>	<b>Meters per second</b>
<b>MAPK</b>	<b>Mitogen-activated protein kinase</b>
<b>M-CSF</b>	<b>Macrophage-colony stimulating factor</b>
<b>MMPs</b>	<b>Matrix metallo proteinases</b>
<b>mRNA</b>	<b>messenger RNA</b>
<b>NADPH</b>	<b>Nicotinamide Adenine Dinucleotide Phosphate Hydrogen.</b>
<b>NF-<math>\kappa</math>B</b>	<b>Nuclear factor-kappa B</b>
<b>OPG</b>	<b>osteoprotegrin</b>
<b>OS</b>	<b>Oxidative stress</b>
<b>PI3K</b>	<b>activating phosphoinositide 3-kinase</b>
<b>PTH</b>	<b>Para thyroid Hormone</b>
<b>RANKL</b>	<b>Receptor Activator of Nuclear Factor kappa-B Ligand</b>
<b>ROS</b>	<b>reactive oxygen species.</b>
<b>RPM</b>	<b>rotations per minute</b>
<b>SEM</b>	<b>Scanning Electron Microscope</b>
<b>TGF- <math>\beta</math>1</b>	<b>Transforming Growth Factor Beta1</b>
<b>TNF-<math>\alpha</math></b>	<b>Tumor necrosis factor-alpha</b>

<b>TRAP</b>	<b>Tartrate resistant acid phosphatase</b>
<b>UDP</b>	<b>Uridine diphosphate</b>
<b><math>\Delta\Delta C_t</math></b>	<b>Delta-Delta C<sub>t</sub></b>

# **Chapter One**

## **Introduction**

## ***Introduction***

Bones are a support tissue of the body that are highly specialized and provide structural support, protect vital organs, provide an environment for bone marrow, and act as a mineral reservoir for calcium and the bone is composed of osteoblasts and osteocytes (support cells), osteoclasts (remodeling cells), osteoid cells that are composed of a non-mineral collagen matrix and non-collagenous proteins, and inorganic mineral salts, such as calcium, that are found within the matrix (**Briot , 2015 ; Wawrzyniak *et al* .,2022**).

Osteoporosis is a systemic skeletal disease characterized by low bone mass, the deterioration of the microarchitecture of bone tissue, a consequent increase in bone fragility and a susceptibility to fractures (**Aibar-Almazán *et al* ., 2022**). Osteoporosis has been reported to occur when there is an imbalance in bone cell function (**Letarouilly *et al* ., 2019**). This disease has been called “the silent epidemic of the 21st century” because of its public health implications. It is a severe, chronic, progressive and clinically silent disease and the most common of the metabolic bone diseases (**González *et al* ., 2009**).

Three important proteins, Receptor Activator of Nuclear Factor kappa-B (RANK), Receptor Activator of Nuclear Factor Kappa-B ligand (RANK-L), and osteoprotegerin (OPG), work together to regulate the development and activation of osteoclasts (**Wada *et al* ., 2006**). In addition, osteoclast-mediated bone resorption is aided by the cysteine protease cathepsin K, which is involved in the breakdown of proteins that make up the bone matrix (**Grimaud *et al* ., 2003 ; Deaton *et al* ., 2005**) RANKL is produced by cells of the osteoblast lineage, including matrix-embedded osteocytes. Membrane bound RANKL is cleaved by proteases to form soluble RANKL. OPG is predominantly secreted by osteoblasts to bind to RANKL to suppress its activity and regulate osteoclastic bone resorption .

Aging is a multifactorial process associated with physiological decline. There is a substantial amount of data supporting the positive relation between the process of

aging and the progressive decline in antioxidant function combined with increased mitochondrial ROS (reactive oxygen species) generation and increased accumulation of oxidant products (**Wickens, 2001**).

D-gal is a monosaccharide that has the same chemical formula as glucose, i.e., C<sub>6</sub>H<sub>12</sub>O<sub>6</sub>. It is similar to glucose in its structure, differing only in the position of one hydroxyl group, this difference gives galactose different chemical and biochemical properties to glucose (**Shahroudi et al ., 2017**). D-gal a reducing sugar, induces oxidative stress resulting in alteration in mitochondrial dynamics and apoptosis of neurons ( **Qu et al., 2016**).D-gal is converted to galactitol, which accumulates in the cells and then induces osmotic stress and generates ROS, (**Woo et al ., 2014**). When an exogenous dose of D-gal is given beyond normal concentration, this can induce aging effects in several organs by increasing oxidative stress, apoptosis and inflammation. (**Ullah et al ., 2015; Wang, 2022**). Long-term injection of D-gal can induce chronic inflammation and oxidative stress, accelerating aging. The model of accelerated aging with long-term administration of D-gal have been widely used in anti-aging studies, due to the increase of chronic inflammation and decline of cognition that similarity with natural aging in animals. (**Huang et al., 2013;Qian et al., 2021**).

Treadmill exercise plays a significant role in influencing bone health, with positive effects depending on various factors such as exercise intensity, duration, frequency, and individual characteristics. Understanding these effects is crucial for optimizing the benefits and minimizing potential risks (**Santos et al ., 2017**). The primary positive effects of treadmill exercise on bone are the improvement of bone density. Weight-bearing exercises, including walking and running on a treadmill, subject bones to mechanical loading, stimulating bone formation. This is particularly important in the prevention of age-related bone loss and osteoporosis(**Abd El-Kader et al ., 2016**).



Exercising on a treadmill raises metabolic rate because it demands more energy from your muscles, which in turn causes muscle mass to grow and energy expenditure to rise (Poehlman *et al* ., 1991). As an alternative to storing galactose, the body can try to convert it into energy (Tan *et al* ., 2018). Osteoblasts and stromal stem cells express receptor activator of NF- $\kappa$ B ligand (RANKL), which binds to its receptor, RANK, on the surface of osteoclasts and their precursors. This regulates the differentiation of precursors into multinucleated osteoclasts and osteoclast activation and survival both normally and in most pathologic conditions associated with increased bone resorption. Osteoprotegerin (OPG) is secreted by osteoblasts and osteogenic stromal stem cells and protects the skeleton from excessive bone resorption by binding to RANKL and preventing it from interacting with RANK. The RANKL/OPG ratio in bone marrow is thus an important determinant of bone mass in normal and disease states (Boyce and Xing, 2008).

Cathepsin K(CatK) is one of the most potent proteases in lysosomal cysteine proteases family, . Cathepsins are endopeptidase found in the most cells, which takes part in cell autolysis and self-digestion of tissues (Xie *et al* ., 2023). of which main function is to mediate bone resorption, secreted by activated osteoclasts to degrade collagen and other matrix proteins during bone resorption, Cathepsin K is produced and secreted by osteoclasts, which are large multinucleated cells in bone. Cathepsin K breaks down the chemical bonds in proteins, including collagen, leading to the degradation of the bone matrix(Dai *et al.*, 2020).

Runx2 gene represents one of three members of the RUNT domain family of transcription factors (RUNX1,2, and -3) that play central roles in cell fate determination, directing hematopoiesis, skeletogenesis and neurogenesis and play role in osteoclast formation(Cohen, 2009). The Runx2 protein is a transcription factor that binds to specific DNA sequences and regulates the expression of target genes. In particular, it is a key regulator of osteoblast differentiation, which is the process by which precursor cells develop into bone-forming cells. RUNX2 is essential for the formation of bones and skeleton during embryonic development and

is also important for the maintenance and remodeling of bones in adults (**Narayanan et al ., 2019**).

**Aim of study:**

Pathway of RANK, RANK-L ,OPG, Cathepsin-K marker is not clear in the Osteoporosis and the way remodeling without medical treatment ,thus The aims of this research project are to investigate the role of treadmill exercise on the RANK, RANK-L ,OPG, Cathepsin-K pathway by estimate the RANK, RANKL, OPG and cathepsin K proteins and other biomarkers levels with femoral x-ray and histological examination light microscope and electron microscope.

# **Chapter Two**

## **Literature Review**

## ***2.Literature Review***

### **2.1 Bones**

Bones are an alive organ consist of about 70% mineral and 30% organic material. Calcium and phosphorous crystals, hydroxyapatite, and some ions such as sodium, fluoride, and magnesium are constituents of the mineral part. In early life bone size and bone marrow density increase through a process called remodeling (**Rosengren , 2010**), the highest bone mass in life is reached, referred to as peak bone mass , after peak bone mass is attained, bone mass is fairly stable until menopause, when female sex hormone levels drop and result in a subsequent loss of bone marrow density the following 5 or 10 years (**Hardcastle et al ., 2011**).

bone develops to a level called the peak bone mass, it is the maximum mass of bone that the body is going to reach after this stage is reached, the slow phase of bone loss begins, it begins around age 40 for cortical bone and 5-10 years earlier for trabecular bone, The surface to volume ratio in cortical bone is much lower than in trabecular bone (**Utami et al., 2019**).

With aging or disease, the cortex becomes more porous, thus gaining surface area but losing strength, in the long bones, increased porosity near the periosteal surface causes more loss of strength than increased porosity near the endocortical surface(**Ott,2018**). Slow periosteal expansion throughout life partially compensates for this loss of strength, because the bending strength is proportional to the radius to the fourth power ,in the trabecular compartment, 20% of the volume is composed of bone, and the remaining space is filled with marrow and fat, trabecular bone transfers mechanical loads from the articular surface to the cortical bone (**Thieschafer,2010**),the hydraulic properties absorb shock, The material properties of the bone compartments differ: trabecular bone has lower calcium

content and more water content compared to cortical bone, trabecular bone has a large surface exposed to the bone marrow and blood flow, and the turnover is higher than in cortical bone, resorption takes place along bone surfaces in the trabecular bone, whereas in the cortical bone, resorption tunnels through the bone itself (**Abdallah *et al.* , 2020** ).

## **2.2 Bone cells**

### **2.2.1 Osteoblast**

Osteoblasts are the cells that "build" bone, as they are commonly called. Osteoblasts synthesize and deposit organic bone matrix(osteoid) proteins or collagen (type 1) and proteoglycan, that will mineralize in both developing skeletons and during the process of bone remodeling that occurs continuously throughout an individual's life (**Tanaka *et al.*, 2005**).They are derived from pluripotent mesenchymal stem cells. Osteoblasts also indirectly regulate osteoclast formation and bone remodeling by cell-cell contact, paracrine signaling, and cell-bone matrix interaction (**Varela and Samadfam, 2017**). Osteoblasts synthesize and secrete bone matrix to maintain the structural integrity and shape of bone. This process promotes bone formation, remodeling, and healing (**Rosenberg *et al.*,2012; Czekanska *et al.*, 2012**). Osteoblasts majorly perform two varieties of functions, within the bone tissue. Firstly, osteoblasts release multiple proteins essential to the formation of the bony structure matrix. Secondly, osteoblasts help in regulating the mineralization of bone. Some of the primary functions of osteoblasts are mentioned below: Osteoblasts have special receptors for hormones such as estrogen, parathyroid hormone (PTH), and vitamin D.

Osteoblasts secrete important factors that activate osteoclasts, i.e.receptor activator of nuclear factor  $\kappa$  B (RANK) ligand and other associated factors which

communicate with other cells. Osteoblasts also secrete a regulatory protein that is involved in the regulation of phosphate excretion from the kidneys. After osteoblasts have finished the making up of new bone, some of them will differentiate into osteocytes and rest of them will surround the matrix of the bone. Some of them, if remained, will either stay on the surface of the new bone or mature into lining cells. Lining cells are involved in the transport of calcium from inside and outside of the bone (Long, 2011;Blair *et al.*, 2017)

### **2.2.2 Osteocyte**

An osteocyte is a specialized cell found in bone tissue. These cells are responsible for maintaining the mineralized bone matrix (Mohamed, 2008). Osteocytes are derived from osteoblasts, which are bone-forming cells. Once osteoblasts become embedded in the bone matrix, they differentiate into osteocytes (Klein-Nulend *et al.* , 2020).

Osteocytes have long, branch-like processes that form a network within the bone and are connected to each other through tiny channels called canaliculi (Schurman *et al.* , 2021). This network allows them to communicate and exchange nutrients and waste products(Wei *et al.* , 2022) . Osteocytes play a crucial role in regulating bone remodeling by sensing mechanical forces and responding to changes in bone density (Uda *et al.* , 2017).

osteocytes are key players in maintaining bone health and function by monitoring and controlling the bone matrix (Robling *et al.*, 2020) and play a significant role in the development and maintenance of bone tissue, and their dysfunction or imbalance can contribute to conditions like osteoporosis(Metzger *et al.* , 2019). Osteoporosis is a condition characterized by a decrease in bone mass and density, leading to increased bone fragility and a higher risk of

fractures(**Pisani et al ., 2016**).In osteoporosis, the activity of osteoclasts (cells that break down bone) may outpace the activity of osteoblasts (cells that build new bone), resulting in a net loss of bone mass. Osteocytes, being central regulators of bone remodeling, also contribute to this process (**El Miedany et al ., 2022**).

Changes in the communication network between osteocytes, alterations in their response to mechanical loading, and disruptions in the signaling pathways they are involved in can all be factors in the development of osteoporosis (**Yan et al ., 2020**). Osteocytes are sensitive to mechanical stresses, and reduced mechanical loading (such as lack of physical activity) can lead to decreased bone density (**Rolvien et al ., 2022**). Additionally, hormonal changes, especially in postmenopausal women, can affect osteocyte function and contribute to bone loss (**McNamara, 2021**).

The role of osteocytes in osteoporosis is essential for developing effective treatments and interventions to manage and prevent the condition (**Pathak et al ., 2020**). Strategies that promote proper osteocyte function, maintain a balance between bone resorption and formation, and support overall bone health are crucial in addressing osteoporosis (**Cao et al ., 2020**).

### **2.2.3 Osteoclast**

The osteoclast is a highly specialised, multinucleated, tissue-specific macrophage responsible for bone resorption (**Sun et al ., 2021**). Bone resorption by the active osteoclast occurs through the development of an acidic environment in which H<sup>+</sup> ions are transported via proton pumps and lytic enzymes tartrate resistant acid phosphatase (TRAP) and cathepsin K are released into the resorption compartment( **Blair et al ., 1989**). This dissolves hydroxyapatite and allows enzymatic degradation of the bone matrix proteins which are then phagocytosed by

the osteoclasts and excreted (**Zhao ,2012**). Osteoclasts differentiate from monocyte precursors at or near the bone surface. Three molecules: receptor activator of nuclear factor kB ligand (RANKL) and its receptor RANK, and the decoy receptor osteoprotegerin (OPG), form the RANKL/RANK/OPG pathway (Fig. 1) which plays a critical role in the differentiation of osteoclasts from its haematopoietic progenitors (**Liu et al .,2015**).

### **2.3 Osteoporosis**

Osteoporosis is a disease involving the bones characterized by reduced bone mass, deterioration of bone structure, increased bone fragility, and an increased risk of fracture, Osteoporosis can be measured partly through bone mass or bone density (**Ringle, 2009; Kasem et al .,2016; Wu et al ., 2017; Aibar-Almazán et al ., 2022**) .

Osteoporosis affects the normal daily activities and quality of life of patients who suffer from this disease, quality of life is affected through the increased risk of fracture in areas such as the hip vertebrae and wrist (**Lekamwasam et al .,2012**).These complications can ultimately lead to significant morbidity and mortality (**Buckley et al ., 2017**).

It a metabolic bone problem, also recognized as “the silent thief” because there is slow bone loss, generally occurs over the years, and without any symptoms until the bone becomes so brittle that suddenly fracture occurs (**Martinetal , 2010**). Osteoporosis is the most common disorder related to age (**Lippuner et al ., 2005; Abdallah et al ., 2020**). As a result; bones tend to become more fragile and more susceptible to fractures (**Piñar-Gutierrez et al ., 2022**).



### **2.3.1 Classification of osteoporosis**

Two types of osteoporosis can be subdivided into Primary osteoporosis which results from bone depletion due to hypo gonadal function related to aging, and age-related disorder characterized by decreased bone mass and increased susceptibility to fractures in the absence of other recognizable causes of bone loss ,Secondary osteoporosis is also called senile osteoporosis takes place after 70 years of age, involving both trabecular and cortical bone and Secondary osteoporosis it is due to the effect of medications like steroids or certain medical conditions (**Hendrickx et al ., 2015**). Which may be caused by chronic systemic diseases, endocrine and metabolic disorders, medication (glucocorticoids) and nutritional disorders(**El-Haroun et al .,2020**).

### **2.3.2 Causes of osteoporosis**

Known factors that can cause an imbalance in osteoclasts and osteoblasts include estrogen deficiency, testosterone deficiency (**Poirier-Solomon, 2001**), hyperthyroidism malabsorption (**Bonnick and Lewis, 2006**), smoking and Increased alcohol intake (**Henneicke et al ., 2014**),Unbalanced diets and disordered eating (**Utami et al .,2019**), low calorie intake and excessive exercise (**Ringle, 2009** ),calcium and vitamin D deficiency (**Abdallah et al .,2020**),women with type I diabetes (**Abdallah et al., 2020**), inheritable genetic factors as identified by family history, lifestyle factors immobilization, specific conditions such as juvenile or pregnancy-related osteoporosis (**Wu et al., 2017** ),Previous medical disorders such as corticosteroids intake (**El-Haroun et al ., 2020**).

### **2.3.3 Mechanism of osteoporosis**

Under normal physiological conditions, the strength of adult bone is maintained through constant renewal of bone matrix. This process, called bone remodeling, involves two highly coordinated events: resorption of existing bone by osteoclasts, followed by restitution of new bone by osteoblasts. Osteoclast is responsible for bone resorption by proteolytic digestion and bone acidification while osteoblasts responsible for the secretion of osteoid tissue. The regulation of these two processes is organized by osteoprotegerin(OPG), Receptor Activator Of Nuclear Factor Kappa B(RANK), and RANK ligand (RANKL) (**Boyce and Xing, 2008**).

Osteoblasts express RANKL when bone resorption is activated (**Hofbauer and Schoppet, 2004**), which binds and activates the RANK receptor. Activated RANK stimulates complex intracellular biochemical processes which result in osteoclasts activation and thus resorption. OPG acts as RANKL inhibitor; OPG inhibits bone resorption by preventing RANKL from binding to RANK. OPG/RANKL ratio is considered an important factor that predicts bone formation or resorption (**Marques et al .,2011**). In osteoporosis, bone formation becomes insufficient to reconstruct the bone matrix resorbed by the osteoclasts, therefore leading to a reduction in bone mass and predisposing bone to fracture. This negative balance is commonly ascribed to alterations of the osteoclast and osteoblast activities (**Raisz,2005**).

### **2.3.4 Risk of osteoporosis**

Bone loss occurs without symptoms, therefore, osteoporosis is not usually discovered until a patient has a fracture (**Overdorf et al ., 2001**) .Therefore, the following are common symptoms of the disease: back pain caused by vertebral compression, height loss, spinal deformity(kyphosis with a loss of 4-8 inches in height), fractures of vertebrae(about one per year in the beginning of the disease), hips, wrists, and other bones (**Rossini et al .,2016**),geing, ethnicity, diet (low calcium and vitamin D intake), hyperthyroidism, Cushing’s disease, anorexia nervosa, lifestyle (sedentary, cigarette smoking, excessive alcohol intake, certain medication use (glucocorticoids and some anticonvulsants), obesity, and disuse/ microgravity conditions (space flight, bed rest, paralysis) are common risk factors for the development of osteoporosis(**Alexandre et al .,2011;Kim et al .,2019**)

### **2.3.5 Diagnosis of osteoporosis**

Bone loss typically happens gradually and painlessly, the first sign of osteoporosis can be breaking a bone. But it is possible to determine osteoporosis, even before a bone is broken, by getting a bone density test, the test can also detect if bone density is lower than normal. Bone loss that has not reached the stage of an osteoporosis diagnosis is called osteopenia. One of the most common osteoporosis tests is dual X-ray absorptiometry (DXA or DEXA).

The most recent technique used to measure bone mass or bone mineral density(BMD), it has better reproducibility, shorter scan time and is capable of measuring the density of the entire skeleton, It uses two x-ray beams with different levels of energy, After eliminating soft tissue absorption, the absorption of each beam by bone is used to calculate the bone mineral density, It is a portable device

that is easy to use and convenient (Agarwal and Stout, 2003; Johansson *et al* .,2009).

### **2.3.6 Weight loss**

Osteoporosis risk increases significantly when one is underweight. This is because people who are underweight often also have a smaller frame size and therefore have a lower peak bone mass. Maintaining a normal, healthy weight is important and acts as a form of weight-bearing exercise for the skeletal system as a person moves about. Additionally, inadequate nutrition negatively impacts peak bone mass and BMD. The most striking relationship between being underweight and bone health is seen in people with the psychiatric illness anorexia nervosa. Anorexia nervosa is strongly correlated with low peak bone mass and a low BMD (Mehler and Weiner,2003).

## **2.4 Process of Bone Remodeling**

In general, bone remodeling can be separated into 5 phases: (1) Activation phase in which bone remodeling is initiated by either local mechanical or hormonal signal; osteocytes are believed to sense and transduce these signals into a biological response in bone(Komori ,2013 ;Katsimbri ,2017).

In the activation phase, local (*i.e.*, TGF- $\beta$ , macrophage colony-stimulating factor (M-CSF), receptor activator of NF- $\kappa$ B ligand (RANKL) and systemic regulators (*i.e.*, vitamin D, calcium, PTH, estrogen, androgen, and glucocorticoid) will promote osteoclastogenesis and a new round of remodeling is commenced(McHugh *et al* ., 2000). (2) Resorption phase in which mature osteoclasts will secrete matrix metalloproteinases (MMPs) to digest both mineral and organic matrix. In this phase, the Howship's resorption lacunae are formed underneath the canopy cells (Ono *et al* ., 2018) .(3) Reversal phase in which the

mature osteoclasts will undergo apoptosis and osteoblasts are directed to the resorption site (**Raggatt ,2010**). In this phase, local molecules such as TGF- $\beta$  will be released and attract osteoblasts to initiate bone formation (**Martin *et al* ., 2005; Tang *et al* ., 2009**). (4) Formation phase in which osteoblasts will take over the bone remodeling process, this process normally takes 4-6 months (**Katsimbri ,2017**).

In this phase, many local and systemic regulators such as Wnt, Sclerostin, and PTH will induce osteoblastogenesis in bone (**Raggatt ,2010**). Organic bone matrix (osteoid) composed of different proteins such as type I collagen starts to deposit until the entire compensation for bone resorption is achieved. (5) Termination phase in which an equal amount of bone matrix being resorbed and formed, the formation phase will be terminated. In this phase, osteoblasts will either go apoptosis or form the new osteocytes (**Raggatt ,2010; Katsimbri , 2017**) and bone mineralization will start and complete during this phase ( **Pettit ,2008**).

## **2.5 D-galactose (D-gal)**

### **2.5.1 D-gal chemical properties**

D-gal is a monosaccharide sugar that is about same sweet as glucose. The chimerical formation is C<sub>6</sub>H<sub>12</sub>O<sub>6</sub> D galactose is found in many foods such as milk, butter, cheese, yogurt, honey, beets, plums, cherries, figs, and celery (**Azman & Zakaria,2019**)

The term D comes when the hydroxyl group on carbon 5 is located on the right side of the Fischer projection, as show in Figure(2.1)

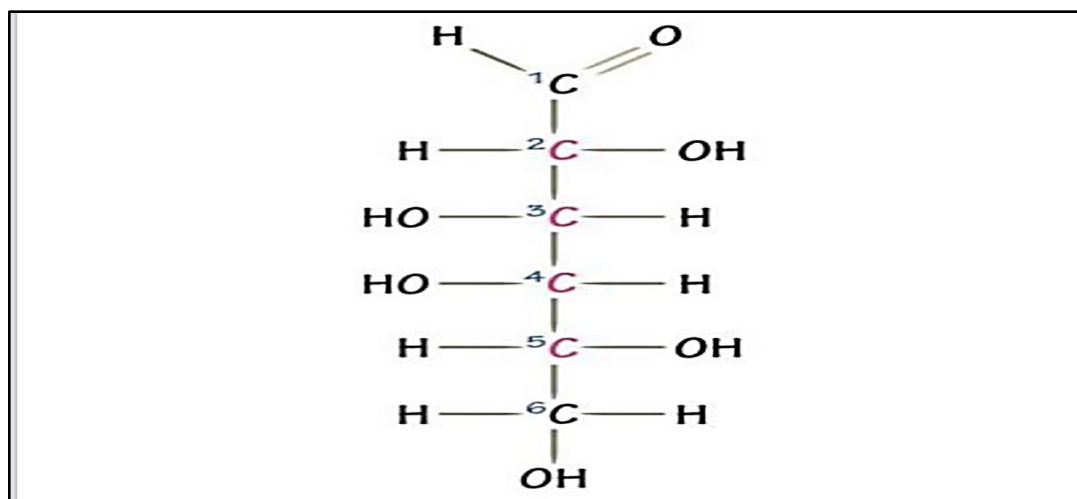


Figure (2-1): Chemical structure of D-gal ( Zaitoun *et al* .,2018)

The maximal recommended daily dose of galactose for healthy adult is 1.5 g/kg/day (maximum 50 g/day). And excreted from the body within about 8 h after ingestion (Morava,2014;Wong *et al* .,2017). At high levels, it can be converted into aldose and hydroperoxide under the catalysis of galactose oxidase, resulting in the generation of reactive oxygen species (ROS) (Wu *et al* .,2008). Galactose is extensively used for modeling aging-related pathophysiological processes in rodents (Azman & Zakaria, 2019). Oxidative stress (OS) has been proposed as the main driver mediating galactose-induced senescence, although exact pathophysiological mechanisms mediating detrimental effects (Azman & Zakaria, 2019).

The biological importance of D-gal goes beyond its importance as a nutrient and a metabolite (Bo-Htay *et al* .,2018). Galactose is an omnipresent epimer of glucose that was first described by Louis Pasteur in (1856) following Erdmann's observation that hydrolysis of the milk sugar lactose yields a substance that is not glucose both in its free form and attached to other molecules forming oligo- or polysaccharides, all living organisms (Coelho *et al* .,2015). Furthermore, together with glucose (in the form of disaccharide lactose) galactose is a cornerstone of

animal milk that provides structural and metabolic support during the most sensitive developmental period (Coelho *et al* ., 2015).Regardless of its importance as a nutrient and pertinent physiological role best reflected in glycolipids, or glycoproteins, galactose is ubiquitous in biological consequences of inherited defects of its metabolism, the biochemistry of galactose and its implications in health and disease remain enigmatic (Conte *et al* ., 2021).

### **2.5.2 D-galactose metabolism**

D-galactose metabolized by The Leloir pathway which named after Luis Federico Leloir, who first described it (Walter & Fridovich Keil, 2014).

In the first step, galactose mutarotase facilitates the conversion of  $\beta$ D-gal to  $\alpha$ -D-gal since this is the active form in the pathway. Next,  $\alpha$ -D-gal is phosphorylated by galactokinase to galactose 1- phosphate. In the third step, D-gal -1-phosphate uridylyltransferase converts galactose 1-phosphate to UDP-galactose using UDP-glucose as the uridine diphosphate source.Finally UDP-galactose 4-epimerase recycles the UDP-galactose to UDP-glucose for the transferase reaction. Additionally, phosphoglucomutase converts the D-glucose 1- phosphate to D-glucose 6-phosphate. ( Walter & Fridovich-Keil, 2014), as show in Figure(2.2)

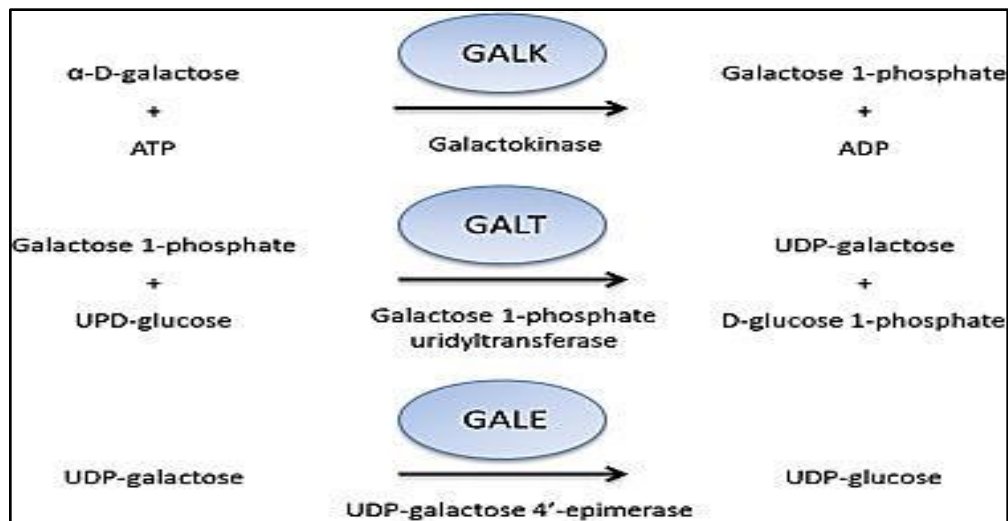


Figure (2-2) :Disorders of galactose metabolism .(Berry, 2015).

### 2.5.3 Role of D-galactose on Aging

Aging is the process of becoming older and it is usually associated with dynamic changes in the biological, psychological, physiological, environmental, behavioural and social processes (Dharmarajan *et al .*, 2021). D-gal causes aging changes related to natural aging processes, such as shorter lifespan, neurodegeneration and cognitive dysfunction, (AGE) formation and oxidative stress, and transcriptional gene changes (Cardoso *et al .*, 2015; Tian *et al .*, 2019).

Accumulating evidence suggests that mitochondrial dysfunction and oxidative stress play major roles in aging Chronic administration of D-gal has been reported to cause deterioration of cognitive and motor skills that are similar to symptoms of aging and, therefore, is regarded as a model of accelerated aging because enhancing endogenous antioxidants is now widely regarded as an attractive therapy for conditions associated with mitochondrial oxidative stress (Parameshwaran *et al .*, 2010; Lian *et al .*, 2017). D-gal is used to hasten the aging process in various tissues in rodent models and it has been shown to



successfully mimic the oxidative alterations that take place in the natural aging process in various tissues (**Yanar *et al.* , 2019**).

#### **2.5.4 Effect of D-galactose on bone**

D-galactose is a monosaccharide sugar that has been used in experimental models to induce accelerated aging and study the effects of oxidative stress on various tissues, including bone (**Umbayev *et al.* , 2020**). The administration of D-gal is known to generate reactive oxygen species (ROS) and induce oxidative stress, which can have implications for bone health (**Xu *et al.* , 2020**), as shown in Figure(2.3).

D-gal -induced oxidative stress can negatively impact bone cells, including osteoblasts (bone-forming cells) and osteoclasts (bone-resorbing cells). Increased ROS levels may lead to cellular damage, affecting the function and viability of these crucial bone cells. Oxidative stress has been associated with impaired osteoblast differentiation and mineralization, potentially compromising bone formation (**Wang *et al.* , 2022**).

Chronic exposure to D-gal may lead to a reduction in bone mineral density (BMD). BMD is a key indicator of bone strength and is essential for maintaining skeletal integrity. The alterations in BMD observed in response to D-gal may contribute to compromised bone structure and increased susceptibility to fractures (**Imerb *et al.* , 2022**).

D-gal induced oxidative stress may interfere with the normal cross-linking of collagen fibers in bone, affecting its mechanical properties. This could result in bones that are more prone to fractures due to reduced elasticity and strength(**Harkema *et al.* , 2016**).

Oxidative stress triggered by D-gal may stimulate inflammatory responses in the bone microenvironment. Increased production of pro-inflammatory cytokines can contribute to an imbalance in bone remodeling, favoring bone resorption over bone formation. This dysregulation may lead to the progression of bone-related disorders (Chandra and Rajawat, 2021).

The oxidative stress generated by D-gal may mimic some aspects of natural aging processes, including the decline in bone mass and strength observed in elderly individuals (Azman and Zakaria, 2019).

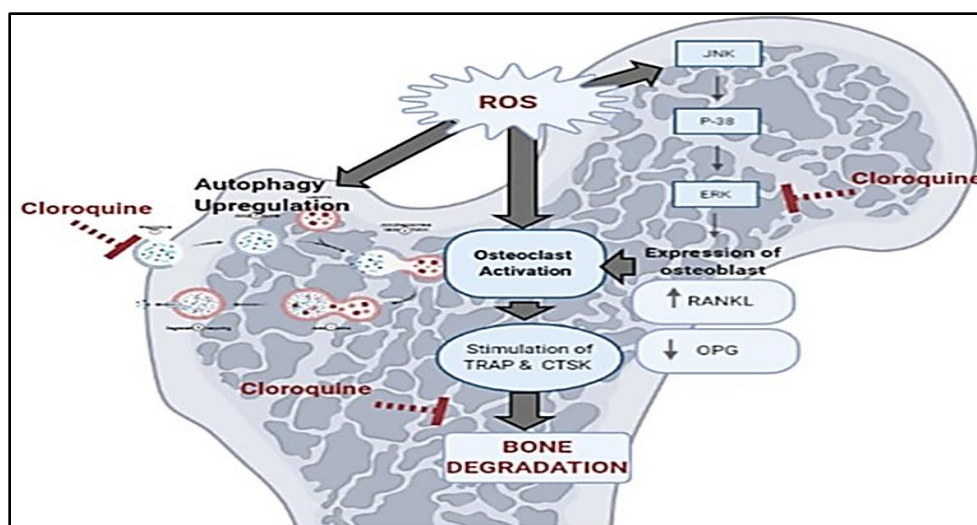


Figure (2-3): different bases upon which CQ inhibits osteoclastogenesis.

(Mahmoud *et al* .,2021).

## 2.6 Treadmill effect on bone health

Treadmill exercise can have several positive effects on bone health, contributing to overall skeletal strength and density. Bone is a dynamic tissue that responds to mechanical loading, and treadmill exercise provides a weight-bearing activity that can stimulate bone remodeling (Friedman & Kohn,2022).

Treadmill such as walking or running, subject bones to mechanical stress. This stress stimulates bone-forming cells (osteoblasts) to lay down new bone tissue, leading to an increase in bone density (**Warden & Fredericson., 2014**). Higher bone density is associated with improved bone strength and reduced risk of fractures (**De Kam *et al.*, 2009**).

Treadmill exercise increase a dynamic process known as bone remodeling, This involves the removal of old or damaged bone by cells called osteoclasts and bone remodeling removal of the old or damaged bone by cells called osteoclasts and the formation of new bone by osteoblasts (**Bellido & Bruzzaniti, 2019**).

## **2.7 Osteoporotic parameters**

### **2.7.1 Receptor Activator of Nuclear Factor kappa-B Ligand (RANKL)**

RANKL is initially produced as an integral membrane bound protein but can be cleaved by proteases into a functional soluble form (**Teitelbaum, 2000**). RANKL binds to its receptor RANK on osteoclast progenitors and stimulates osteoclast differentiation and function (**Dougall *et al.* , 1999**). RANKL is involved in the fusion of osteoclast precursors into multinucleated cells, differentiation into mature osteoclasts and continued survival (**Teitelbaum, 2000**). RANKL relies on macrophage-colony stimulating factor (M-CSF, also known as CSF-1) as a co-factor for osteoclast differentiation (**Takahashi *et al.*, 1991**). RANKL is a type II homotrimeric trans membrane protein that is expressed as a membrane-bound and a secreted protein, which is derived from the membrane form as a result of either proteolytic cleavage or alternative splicing (**Ikeda *et al.* , 2001**).

The proteolytic cleavage of RANKL requires ADAM (a disintegrin and metalloprotease domain) (**Hikita *et al.* , 2006**) and matrix metalloproteases (**Lynch**

*et al ., 2005*). RANKL expression is stimulated in osteoblast/stromal cells by most of the factors that are known to stimulate osteoclast formation and activity. It is highly expressed in lymph nodes, thymus and lung, and at low levels in a variety of other tissues including spleen and bone marrow (**Wada *et al .,2005***). In inflamed joints it is expressed by synovial cells and secreted by activated T cells. These sources of RANKL appear to be responsible, at least in part, for mediating the joint destruction in patients with rheumatoid arthritis (**Komatsu *et al .,2022***).

RANKL is produced by cells of the osteoblast lineage, including matrix-embedded osteocytes. Membrane bound RANKL is cleaved by proteases to form soluble RANKL. OPG is predominantly secreted by osteoblasts to bind to RANKL to suppress its activity and regulate osteoclastic bone resorption.

### **2.7.2 Receptor Activator of Nuclear Factor kappa-B (RANK)**

Receptor Activator of Nuclear Factor kappa-B (RANK) is a protein that plays a crucial role in the regulation of bone metabolism. It is a cell surface receptor that belongs to the tumor necrosis factor (TNF) receptor superfamily. RANK is primarily expressed on the surface of osteoclast precursor cells, which are involved in bone resorption—the process of breaking down and removing old or damaged bone tissue.( **Renema *et al ., 2016***).

When RANK interacts with its ligand, RANKL (Receptor Activator of Nuclear Factor kappa-B Ligand), it activates signaling pathways that lead to the differentiation and activation of osteoclasts. Osteoclasts are responsible for the breakdown of bone tissue, allowing for the continuous remodeling of the skeleton. (**Holliday *et al .,2021***).

### **2.7.3 Osteoprotegerin (OPG)**

OPG is expressed in many tissues apart from osteoblasts, including heart, kidney, liver, spleen, and bone marrow (**Wada *et al* .,2005**). Its expression is regulated by most of the factors that induce RANKL expression by osteoblasts. Although there are contradictory data, in general up regulation of RANKL is associated with down regulation of OPG, or at least lower induction of OPG, such that the ratio of RANKL to OPG changes in favor of osteoclastogenesis. Many reports have supported the assertion that the RANKL/OPG ratio is a major determinant of bone mass (**Hofbauer and Schoppet,2004**), as show in Figure(2.4).

Osteoprotegerin (OPG) is a protein that plays a crucial role in regulating bone density. It's involved in the regulation of bone remodeling, which is the process of breaking down and rebuilding bone tissue. OPG helps to control the activity of osteoclasts, which are cells responsible for bone resorption (breaking down bone tissue) (**Kenkre & Bassett,2018**).

OPG acts as a "decoy receptor" for a protein called RANKL (Receptor Activator of Nuclear Factor Kappa-B Ligand). RANKL is essential for the formation and activation of osteoclasts. By binding to RANKL, OPG prevents it from interacting with its receptor on osteoclasts, ultimately inhibiting bone resorption (**Infante *et al.*, 2019**).

This regulation is crucial for maintaining the balance between bone formation and bone breakdown, helping to ensure the integrity and strength of the skeletal system. Imbalances in this system can lead to conditions such as osteoporosis or excessive bone loss ( **Wawrzyniak& Balawender, 2022**).

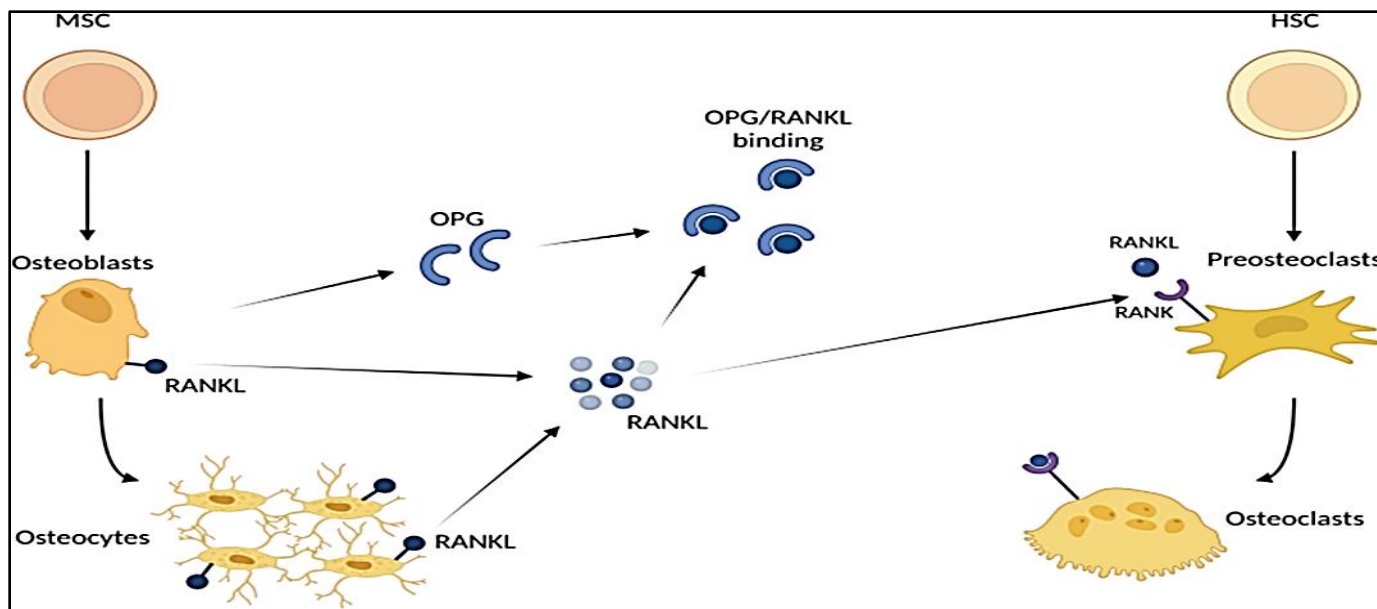


Figure (2.4) :RANKL/RANK/OPG pathway(Kim, A. S *et al.* ,2022).

## 2.7.4 Cathepsin K

Cathepsin K is responsible for the degradation of type I collagen in osteoclast-mediated bone resorption. osteoclast-mediated bone resorption is aided by the cysteine protease cathepsin K, which is involved in the breakdown of proteins that make up the bone matrix (Deaton *et al.*, 2005). Cathepsins are endopeptidase found in most cells, which takes part in cell autolysis and self-digestion of tissues (XIE *et al.*, 2023). In human, there are 11 members of cathepsins (cathepsin B, C, F, H, K, L, O, S, V, W, and Z), which are distinguished by their structures, catalytic mechanisms, and which proteins they cleave (Turk *et al.*, 2001). Cathepsin K (Cat K) is a cysteine protease of the papain family, now considered to be the major enzyme responsible for degradation of the organic bone matrix(Dai *et al.*, 2020). It is highly and selectively expressed in osteoclasts and, under acidic conditions, has the unique ability to degrade type I collagen helical regions(Brömme & Wilson, 2011). Complete deficiency of Cat K activity leads to

pseudosyndostosis, a severe and rare autosomal recessive bone sclerotic disorder, and Cat K null-rat are osteopetrotic (Hershey, 2005), as shown in Figure(2.5).

Cathepsin K is produced and secreted by osteoclasts, which are large multinucleated cells in bone. Cathepsin K binds to the protein components of the bone matrix, including collagen. Cathepsin K breaks down the chemical bonds in proteins, including collagen, leading to the degradation of the bone matrix (Dai *et al.*, 2020).

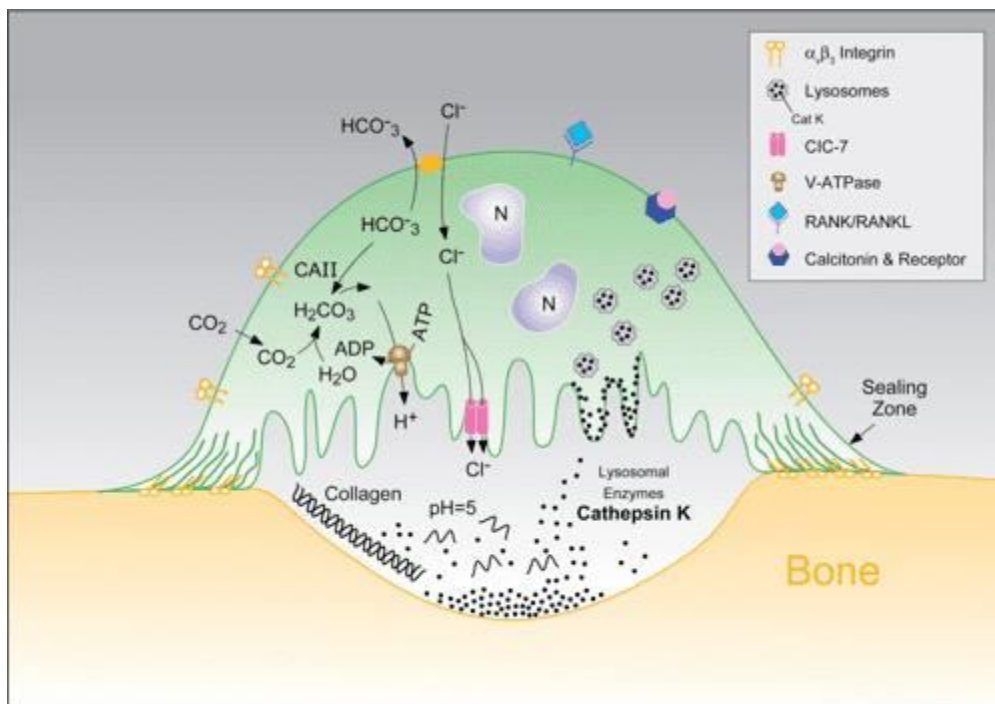


Figure (2.5): Cathepsin K - A new molecular target for osteoporosis (Rodan & Duong.,2008)

## 2.8 RUNX2 gene

The RUNX2 gene, a critical player in the orchestration of skeletal development, belongs to the runt-related transcription factor (RUNX) family. As a transcription factor, the RUNX2 protein governs the intricate processes involved in bone formation and development. This gene is integral to the differentiation of osteoblasts, the specialized cells responsible for bone matrix synthesis and

mineralization (Wildman *et al* .,2019). The intricate regulatory network controlled by RUNX2 is crucial for ensuring the proper formation and maintenance of the skeletal system throughout an individual's life (Di Pietro *et al* .,2021).

The RUNX2 protein is a transcription factor that binds to specific DNA sequences and regulates the expression of target genes. In particular, it is a key regulator of osteoblast differentiation, which is the process by which precursor cells develop into bone-forming cells. RUNX2 is essential for the formation of bones and skeleton during embryonic development and is also important for the maintenance and remodeling of bones in adults (Narayanan *et al* ., 2019).

The significance of RUNX2 in bone development is underscored by its association with Cleido cranial Dysplasia (CCD), a rare genetic disorder. CCD manifests with a spectrum of skeletal abnormalities, such as delayed fontanelle closure, dental anomalies, and craniofacial irregularities (Geister, 2013). The link between mutations in the RUNX2 gene and CCD emphasizes the gene's pivotal role in skeletal morphogenesis. Understanding the intricate molecular mechanisms governed by RUNX2 provides valuable insights into the pathophysiology of skeletal disorders, offering potential avenues for therapeutic interventions and genetic counseling (Gong *et al*., 2022).

The other Runx factors also have roles in skeletal development. *Runx1* and *Runx3* contribute to endochondral bone formation (Lian *et al* .2003; Brenner *et al* ., 2004; Yoshida *et al* ., 2004), their essential functions during embryogenesis are manifested in other tissues. *Runx1* is essential for definitive hematopoiesis, and is frequently mutated in cancer stem cells that give rise to acute leukemias (Miyoshi *et al* .,1991; Okada *et al* ., 1998; Miyamoto *et al* .,2000). *Runx3* is needed for the development of dorsal root ganglia proprioceptive



neurons and proper control of gastric epithelium growth (**Levanon *et al* .,2002; Li *et al* .,2002**).

The important roles of Runx2 in human development are evident in CCD, a rare autosomal dominant disease. Heterozygous loss of function of *Runx2* through a variety of mutations (e.g., deletions, point mutations, insertions, and missense mutations) segregate with abnormal skeletal phenotypes in CCD families (**Otto *et al* .,2002; Yoshida *et al* .,2002**). These alterations affect just one allele of *Runx2* on chromosome 6q21 and would be predicted to decrease wild-type Runx2 levels and activity by one half. *Runx2* haploinsufficiency in mice causes similar phenotypes as observed in CCD families, with a primary defect in intramembranous bone formation (**Komori *et al* .,1997; Otto *et al* .1997**). As one may suspect given the importance of DNA binding to a transcription factor, many mutations in CCD individuals are found in the DNA binding domain of Runx2, other mutations are present in regions proximal and distal to the DNA binding domain. These mutations suggest important roles for other parts of Runx2 in skeletal development. Indeed, CCD mutations in the Runx2 carboxy-terminus impair Smad interaction and transcriptional activation (**Zhang *et al* .,2000**). Moreover, transgenic mice lacking the carboxy-terminus of Runx2 develop a CCD-like phenotype (**Choi *et al* .,2001**).

# **Chapter Three**

## **Methodology**

### 3. Materials and Methods

#### 3.1. Materials

##### 3.1.1. Instruments and Equipment:

All the devices utilized as a part of this study are summarized in Table 3.1.

Table 3.1. Apparatus and equipment with their manufactures.

No.	Apparatus & Equipment	Company	Manufactures
1.	Anatomical set (Scissors, Forceps, Scalpel)	Chemo lab	China
2.	Balance	Denver	Germany
3.	Beakers (100, 250, 500, 1000)	Chemo lab	India
4.	Centrifuge	Hettich	Germany
5.	Colony flask	Chemo lab	India
6.	Cotton	India	Entrepreneur
7.	Digital balance	Denver	Germany
8.	Digital camera	Canon	China
9.	DXA machine	Hologic	USA
10.	ELIZA printer	epson	japan
11.	ELIZA reader	biotek	USA
12.	Eppendorf's tubes	Chemo lab	India
13.	Filter paper	Chemo lab	India
14.	Gel tube	Chemo lab	India
15.	Incubator	Lab tech	Korea
16.	Insulin syringe	eldawlia	Egypt
17.	Light Microscope	Olympus	Japan
18.	Micropipettes (different volumes)	dragonmed	China
19.	Microscope with camera	Olympus	Japan
20.	Microtome	Leica RM	USA
21.	Pipette tips (10 – 1000) $\mu$ l volume	Chemo lab	China
22.	Real-Time RT- qPCR	Chemo lab	USA
23.	Sensitive balance	Sartorius	Germany
24.	Slide & cover slip	Chemo lab	China
25.	Spectrophotometer	EMCLAB	Germany
26.	Surgical gloves	Chemo lab	China
27.	Syringe (1 ml, 5 ml)	Chemo lab	China
28.	Scanning Electron microscope (SEM)	ZEISS	Germany
29.	Test tubes	Chemo lab	China
30.	Treadmill machine	local	
31.	Vortex	Sturat	United

32.	Water bath	labtech	Korea
-----	------------	---------	-------

### 3. 1.2. Chemicals and Kits

All the chemicals and the standard kits used in this study are shown in Table 3.2.

**Table 3.2: Chemicals and Kits with their suppliers.**

No.	Chemicals & Kits	Company	Suppliers
1.	Absolute ethanol	haymankimia	Uk
2.	Calcitonin kit	ELK biotecnology	China
3.	Calcium kit	ELK biotecnology	China
4.	Cathepsin K	ELK biotecnology	China
5.	Concentrated phosphor kit	ELK biotecnology	China
6.	D-gal	Thomas Baker	India
7.	Eosin Stain	Himedia Lab	India
8.	Formalin 37 %	chemanol	SA
9.	Hematoxylin Stain	Himedia Lab	India
10.	Osteoprotegerin	ELK biotecnology	China
11.	Parathyroid hormone Kit	ELK biotecnology	China
12.	Potassium kit	ELK biotecnology	China
13.	Rat RANk (Receptor Activator Of Nuclear Factor Kappa B)	ELK biotecnology	China

14.	Rat RANKL(SolubleReceptor Activator of Nuclear factor-kB Ligand)	ELK biotecnology	China
15.	Sodium kit	ELK biotecnology	China
16.	Vitamin D kit	ELK biotecnology	China

### 3.2. Examination methods

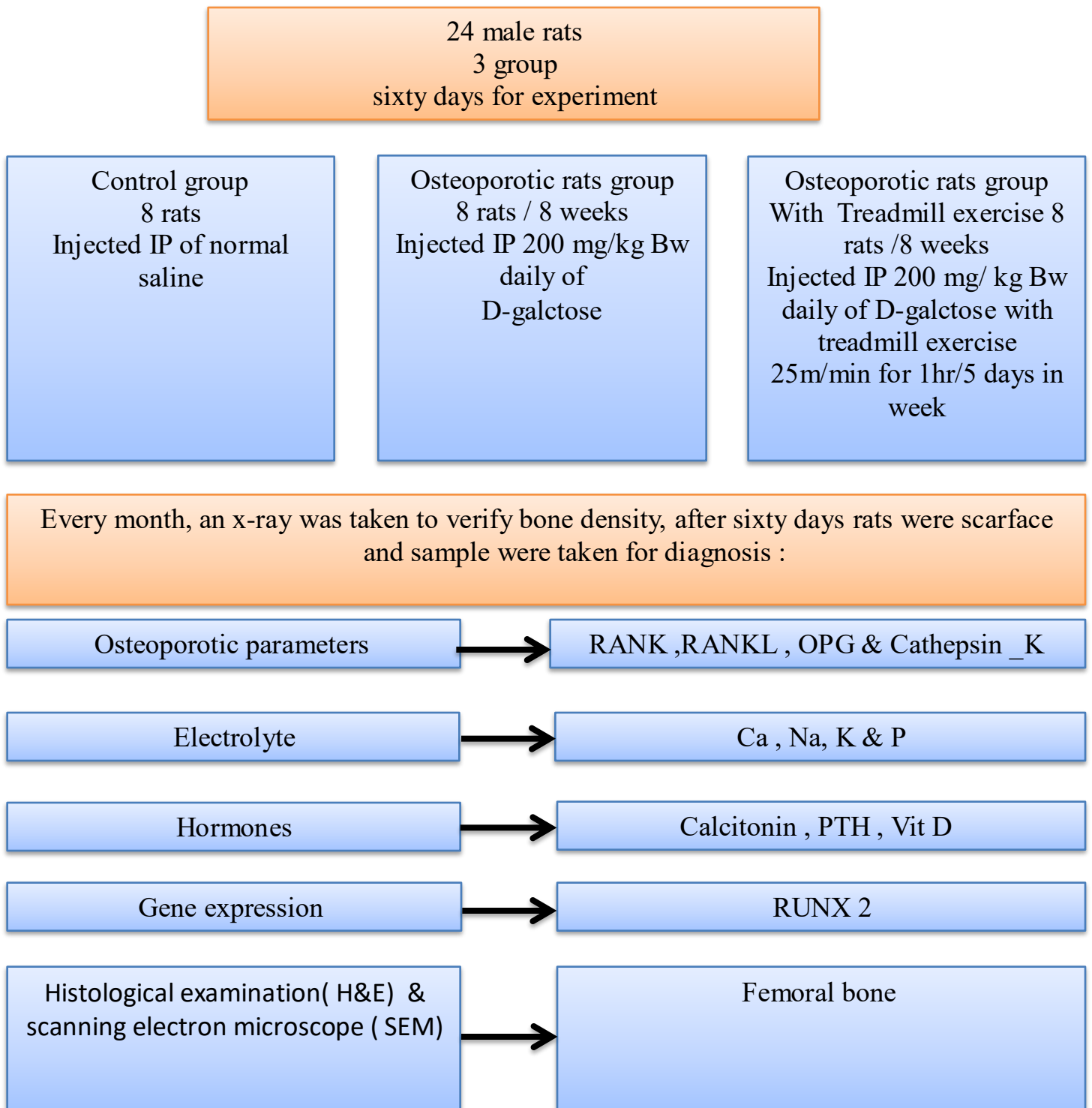
#### 3.2.1. Experimental protocol

Twenty-four male rats, each weighing between (190 - 210) g, were employed in this investigation. The rats were kept in clean, comfortable cages with free access to food and water (ad libitum), a 12-hour cycle of light and darkness, 50±5% relative humidity, and a constant temperature (18 ±2°C). They were kept for two weeks in order to acclimate them to the usual experimental setting.

##### 3.2.1.1. Experimental Design

Twenty four (24) white rat for sixty days, was classified in to three groups and each group divided at random (8/group):

1. control group: rats received 0.2 ml of normal saline, which was injected intraperitoneally for sixty days.
2. D-gal group: rats in the D-gal group received 200 mg/kg B.W. of D-gal injected intraperitoneally for sixty days (**Mahmoud *et al* .,2021**)
3. D-gal+ treadmill group: rats in the D-gal+ tread mill group received the same injections plus the added benefit of running on a treadmill for 25 m/min, five days a week, for an hour, for sixty days(**Iwamoto *et al* .,2004**), experimental design was shown in figure(3.1)



Figure(3.1) :Experimental Design

### 3.2.1.2. Treadmill

Treadmill is a popular exercise machine designed for indoor walking, jogging, or running. It consists of a moving belt that allows users to simulate the experience of walking or running while staying in one place (Yuen., *et al* 2018). Treadmills offer a convenient and efficient way to engage in cardiovascular exercise, enhance physical fitness, and achieve various health benefits (Kenney., *et al* 2022) .

In designing a treadmill for rats it's crucial to accurately measure and understand the speed at which the treadmill operates. This ensures that experiments or training sessions we conducted consistently and effectively. Here's a detailed breakdown of how we calculated the conversion from treadmill rotations per minute (RPM) to meters per second (m/s): Firstly, we started by determining the length of the treadmill. Measurement revealed that the length of the treadmill was 70 centimeters. This measurement provides a fundamental parameter for our subsequent calculations. Next, we examined the treadmill's RPM, which was recorded at 36 rotations per minute. This RPM value indicates how many times the treadmill belt rotates within a minute under the specified conditions. To find out the total distance covered by the treadmill belt in one minute, we multiplied the length of the treadmill (70 cm) by the RPM (36 rotations per minute), resulting in a total distance of 2520 centimeters per minute. Since the standard unit for speed is meters per second (m/s), we needed to convert the total distance covered per minute from centimeters to meters. To do this, we divided the total distance (2520 cm/min) by 100 cm, yielding a distance of 25.20 meters per minute. Finally, to express the speed in meters per second, converted the speed from meters per minute to meters per second. By dividing the speed (25.20 meters per minute) by 60 seconds (the number of seconds in a minute), we obtained a final speed of

approximately 0.42 meters per second.( (Iwamoto *et al* .,2004),as shown in Figure (3.2)



Figure (3.2): The treadmill machine (25m/min ) that was used in the experiment, and the machine was designed by the researcher.

The treadmill:  $=70L=70$  cm

Rotations per minute:  $=36RPM=36$

Distance covered per minute:  $distance/minute=Ddistance/minute=L \times RPM$

$distance/minute=70 \times 36=2520Ddistance/minute=70 \times 36=2520$  cm/minute

Converting speed to meters per minute: $distance/minute=25.20Ddistance/minute$   
 $=25.20$  meters/minute

Distance covered per second: $distance/second=distance/minute60Ddistance/second$   
 $=60Ddistance/minute$

$distance/second=25.2060 \approx 0.42Ddistance/second=6025.20 \approx 0.42$  meters/second



### **3.2.1.3. Collect of the blood samples**

Blood samples were drawn after starving the animals overnight, After sixty day of the experiment, the animals anesthetized by ketamine & xylazine in order to control and calm the animal before the blood draw. Five ml blood was drawn sby heart puncture directly and the animal was lying on its back, and sterile medical syringes of 5 ml were used, then the blood was placed In special gel tube not containing an anticoagulant, the serum was separated by a centrifuge at a speed of 5000 r / min for 5 minutes, the separated serum put in a eppendorf's tubes and kept in freeze at -20 ° C until the completion of the measurements

### **3.3. Ethical approve**

Under the reference number UOK.VET. PH.2023.075 the study was conducted at the Kerbala University/ College of Veterinary Medicines in Iraq's anatomical facility.

### **3.4. Detection of serum Biomarkers of Bone:**

#### **3.4.1. Detection of serum RANK:**

**Serum RANK** was detected by use a special ELISA kit according to method of (Crisafulli *et al* .,2005) as shown in appendix I.

#### **3.4.2. Detection of serum RANKL:**

**Serum RANKL** was detected by use a special ELISA kit according to method of (Crisafulli *et al* ., 2005) as shown in appendix II

#### **3.4.3. Detection of serum Cathepsin K:**

**Serum Cathepsin K** was detected by use a special ELISA kit according to method of (Sun *et al* ., 2013) as shown in appendix III

#### **3.4.4 .Detection of serum osteoprotegerin:**

**Serum osteoprotegerin** was detected by use a special ELISA kit according to method of (Szalay *et al .*, 2003) as shown in appendix IV.

### **3.5. Detection of serum Hormones that effect on bone:**

#### **3.5.1. Detection of serum Calcitonin:**

**Serum Calcitonin** was detected by use a special ELISA kit according to method of (Gür *et al .*, 2003) as shown in appendix V.

#### **3.5.2 .Detection of serum parathyroid (PTH):**

**Serum parathyroid** was detected by use a special ELISA kit according to method of (Chiang *et al .*, 2011) as shown in appendix VI

#### **3.5.3. Detection of serum Vit D:**

**Serum Vit D** was detected by use a special ELISA kit according to method of (Sadat-Ali *et al .*,2011) as shown in appendixVII

### **3.6 .Detection of serum Electrolytes:**

#### **3.6.1. Detection of serum Calcium (Ca):**

**Serum Calcium** was measured according to method of (Burtis *et al.*, 2005) by the use of a special kit as shown in appendix VIII

#### **3.6.2. Detection of serum phosphorus (P):**

**Serum phosphorus** was measured according to method of (Burtis *et al.*, 2005) by the use of a special kit as shown in appendix IX

#### **3.6.3. Detection of serum sodium (Na):**

**Serum sodium** was detected by use a special kit according to method of (Tang *et al .*, 2020) as shown in appendix X

### 3.6.4. Detection of serum potassium (K):

**Serum sodium** was detected by use a special kit according to method of (Xiong *et al* .,2018) as shown in appendix XI

### 3.7. Bone parameters:

#### 3.7.1 Examination of bone mineral density by X-ray :

Rats were anaesthetized using mixture of I/M ketamine (100mg/kg) xylazine (10 mg/kg) (Saha *et al* .,2005). The anesthetized rat was positioned in ventral recumbence on the scan Figure(3.3). All scans were performed using DXA(Hologic QDR-1000 System, Hologic Inc., Waltham, USA) at the first day of the experiment ,after one month and the end of the experiment the high- resolution scan was performed to evaluate the bone mineral density (BMD) at the femur of rats,as shown in Figure (3-3).



Figure (3-3):Hologic dual-energy X-ray absorptiometry scan machine.

### **3.7.2. Histopathological study:**

The bone was decalcified by use special acidic formalin then the tissue proceeded according to method mentioned in (**Suvarna *et al* .,2018**). Slides were then stained with hematoxylin and eosin ( H&E) and examined by use light microscope .as shown in appendix**XII**

### **3.7.3. Scanning Electron Microscope(ESM) :**

Bone samples from the femoral of the rat fixed with formaldehyde. the fixed bone samples dehydrate using a series of ethanol solutions with increasing concentrations. This removes water from the samples and prepares them for the subsequent steps. critical point drying may be employed to avoid structural damage caused by surface tension during the drying process. Once dehydrated, mount the bone samples onto SEM stubs using a suitable adhesive. Ensure that the samples are securely attached to the stubs to prevent movement during imaging. To enhance conductivity and minimize charging effects during SEM imaging, coat the bone samples with a thin layer of conductive material palladium. This can be achieved using a sputter coater or a carbon evaporator. Place the mounted and coated bone samples into the SEM chamber and adjust the imaging parameters as needed. Capture high-resolution images of the bone structure at various magnifications and orientations. Once the imaging is complete the SEM images show the microstructure and morphology of the bone samples (**Shah *et al* .,2019**).

## **3.8. Gene expression:**

### **3.8.1 RUNX2 gene expression:**

This approach was carried out according to the comparative Ct approach ( $\Delta\Delta Ct$ ) with normalization to the level of the control group in the presence of the transcript levels to those of GAPDH mRNA. This was achieved according to the recommendation of (**Schroeder *et al* .,2005**).

### 3.8.2 Quantitative Reverse Transcriptase Real-Time RT- qPCR:

Animals were anesthetized and dissected so samples could be obtained (the head of the femur bone). TRIzol™ Reagent/thermofisher scientific was used to preserve the organs in clean dark containers. The first strand of cDNA is synthesized ,first strand cDNA synthesis kit. The primer mixture consists of an anchored oligo(dT)18 primer and a random hexamer primer. Delivery the extracted total RNA were treated with DNase enzyme to remove the trace amounts of genomic DNA from the eluted total RNA by using samples (DNase enzyme) and done according to method described by promega company, USA instructions as follow according to (Schroeder *et al.*, 2005). Following synthesis of cDNA, gene specific primers can be used to determine the level of gene ,20µl reactions Prepare GoTaqR 1-Step RT-qPCR Reaction Mix as a single batch that includes the common components, such as Go TaqR 1-Step RT-qPCR Master Mix, CXR dye, nuclease-free water and Go Script RT Mix. Divide the batch into individual volumes then add the remaining components; o quantify the mRNA expression level of RUNX2 bone resorption cytokines, the relative amounts of glyceraldehyde 3-phosphate dehydrogenase (GAPDH) mRNA were analyzed. RNA extraction, cDNA synthesis, and real-time PCR were performed as described by (Yang *et al* ., 2012). This study used primer sequences shown in **Table (3.3)**.

**Table (3.3): Nucleotides sequences for RUNX2 gene and Housekeeping gene**

Gene of interest		Primers	PCR
<b>RUNX2</b>	F	5- GACTGTGGTTACCGTCATGGC-3	100 bp
	R	5- ACTTGGTTTTTCATAACAGCGGA	
Housekeeping gene		Primers	
<b>GADPH</b>	F	5-AGCCCAAGATGCCCTTCAGT-3	88 bp
	R	5-CCGTGTTCTACCCCAATG-3	

### 3.9.Statistical analysis:

Statistical analysis of data for experiments in the present study was performed by prism V8.0 on the basis of one way and two way analysis of variance (ANOVA) using significant level of (P<0.05) (Kwiatkowska *et al* ., 2006 )

# **Chapter Four**

## **Result and Discussion**

### 4-1Effect of D-gal and treadmill on femoral bone X-Ray:

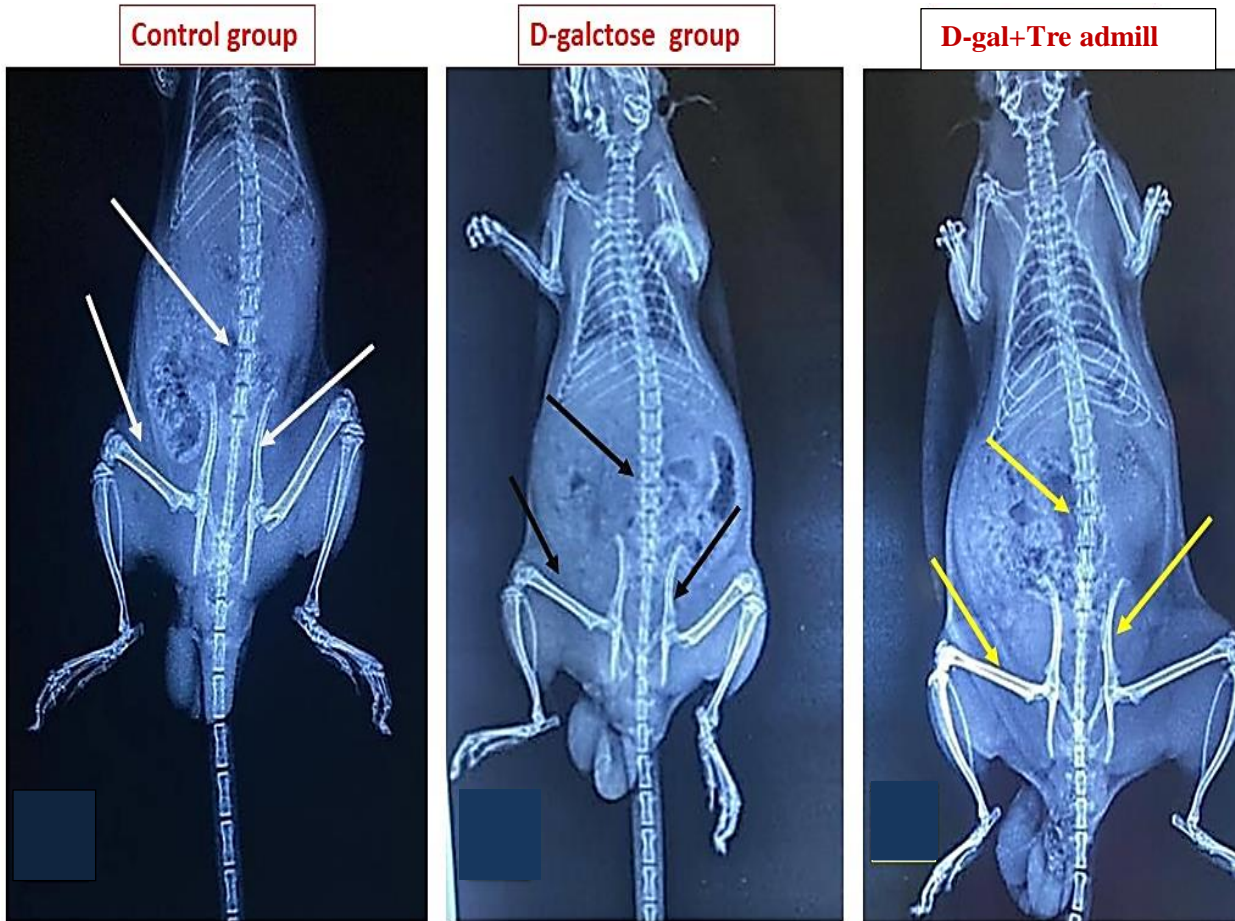


Figure (4-1): Radiographic image of the bones with white arrow of control group showing normal bone density .Radiographic image of the bones with black arrow of D-galctose group and treadmill group with yellow and black arrow showing normal bone density (At zero time).



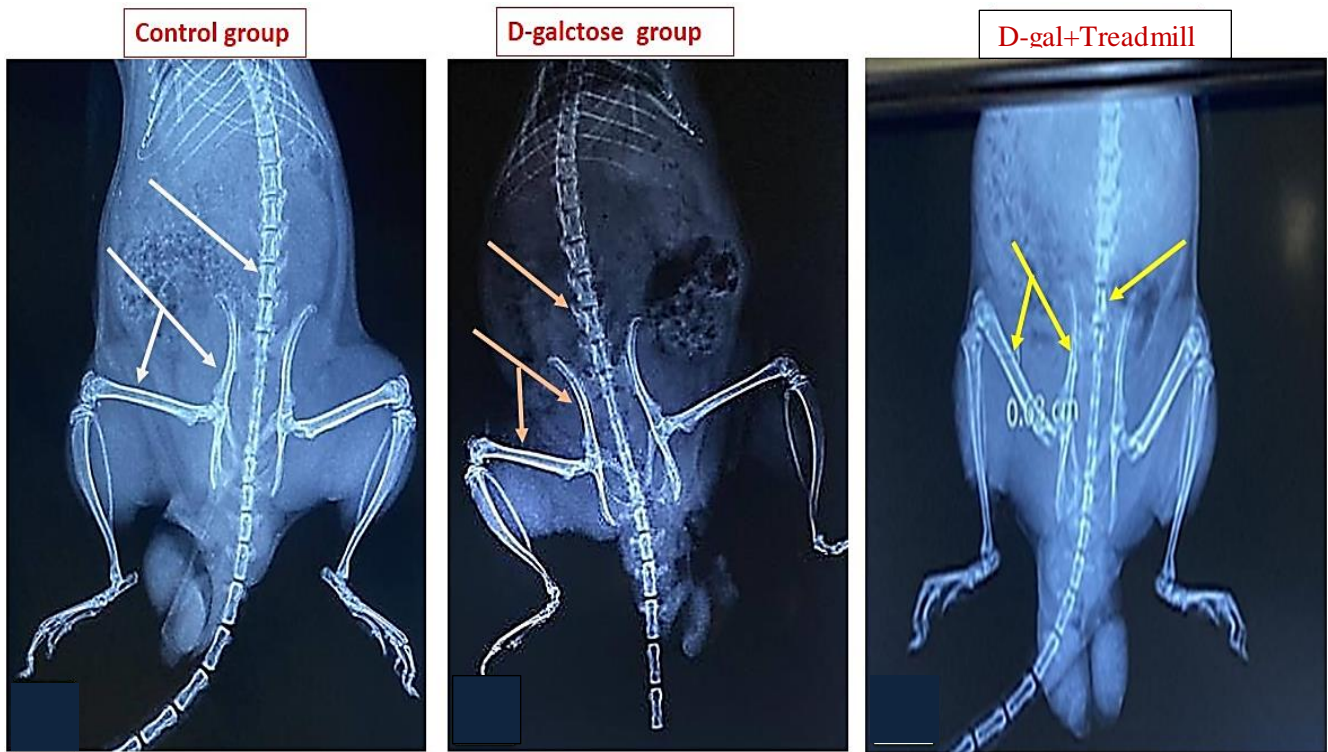


Figure (4-2): Radiographic image of the bones at day 30 of the experiment with white arrow of control group showing normal bone density. While Radiographic image of the bones with treadmill group with yellow arrow showing significantly improved more than D-galctose group with brown arrow, abnormal bone density, decrease osteoporosis with increase in bones mineral density around the vertebral ,femoral and pelvic bones especially at the middle and epiphysis of bones ( after one month).

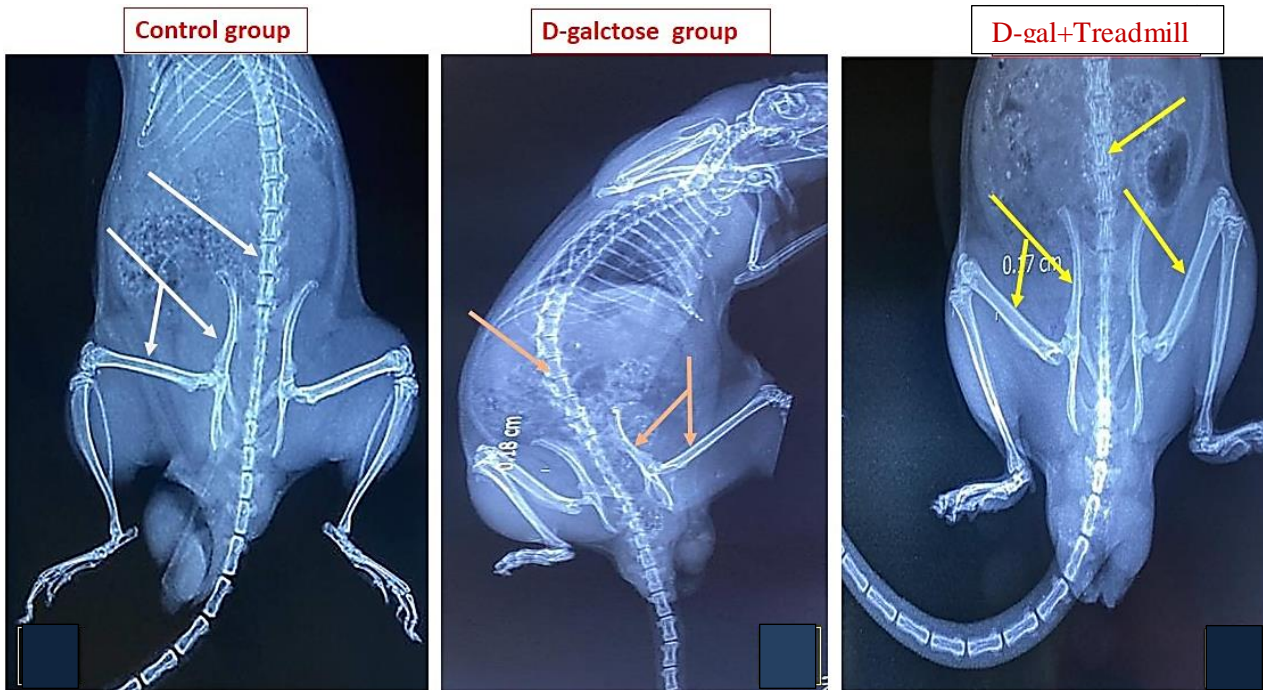


Figure (4-3): Radiographic image of the bones with white arrow of control group showing normal bone density .While Radiographic image of the bones with treadmill group show a lees bone density as comper with control the D-gal group showing a significant sclerosis with reduce in bones mineral density around the vertebral ,femoral and pelvic bones with a high radiopaque area brown arrow ( after two month).

Table (4-1 ) Effect of 200 mg/kg of D-gal daily for 1st , 30 and 60 days days and 25m/min days treadmill sport in the bone density g/cm on the male rats

Groups days	Control	D-gal	D-gal treadmill
First day	0.368±0.031 A a	0.358±0.024 A a	0.354±0.061 A a
30days	0.354±0.051 A a	0.266±0.032 B b	0.304±0.042 A b
60days	0.372±0.043 A a	0.186±0.025 B c	0.285±0.032 C c

Values are expressed as mean ± SE n=5/ group .Capital letter denote between groups difference (p<0.001)vs. control. Small letter denote within group difference (p<0.01) vs. first day . D-gal animal received200mg/kg D-gal tread animals received200mg/kg 25m/min days treadmill sport

The images presented in (Figure 4-1,4-2 and 4-3) show important findings about the effect of D-gal on bone density and the potential impact of the Treadmill device in its treatment, the control group has normal bones with an appropriate density, and this is expected in the group that was not exposed to any intervention. As for the D-gal group ,bones appear less dense compared to the control group, and this indicates the development of osteoporosis due to mineral deficiency in the vertebrae, thigh, and pelvis, as is evident in the x-rays.

Table(4.1) and Figure (4-1) showed there is non significant differences in the D-gal group and (Treadmill +D-gal) group with control group( $0.368\pm 0.031$ ), ( $0.354\pm 0.051$ ) and( $0.372\pm 0.043$ ),while the same table and figure showed a significant( $P<0.01$ ) decrease in the D-gal group( $0.266\pm 0.032$ ) compare with control group and (Treadmill +D-gal) groups of 30 days of the experiment.

Figure (4-2) the control group show a normal bone density at 30 day of the experiment while the D-gal group show a significant decrease in the bone density and decrease osteoporosis with increase in bones mineral density around the vertebral ,femoral and pelvic bones especially at the middle and epiphysis of bones, while the d-gal and treadmill show a significantly improved more than D-gal group.

Also the result investigate of the 60 days of the experiment a significant( $P<0.01$ ) decrease(  $0.186\pm 0.025$ ) compare with control ( $0.372\pm 0.043$ ) and (Treadmill +D-gal) group ( $0.285\pm 0.032$ ). on the other hand at the 60 day of the experiment the radiographic image of the control group showed normal bone density , the D-gal group showed a sclerosis with reduce in bones mineral density around the vertebral ,femoral and pelvic bones with a high radiopaque area ,while treadmill group showed a less radiographic change as compare with the control group as shown in figure (4-3). The role of the(Treadmill +D-gal) group of 30 and 60 days ranged to significant( $P<0.01$ )

In the (Treadmill +D-gal) group, less dense bones were also observed compared to the control group, but to a lesser extent than in the D-gal group. This suggests that D-gal may have weakened the bones initially, but there is no clear effect of Treadmill in improving bone density yet. After a month of the experiment, it was noted there was significant change observed with in bone density, as for the (Treadmill +D-gal) group there was a noticeable improvement in bone density compared to the D-gal group. This improvement can be explained by the mechanism of the Trimil device stimulating bone formation. The D-gal group showed continued reduction in bone density, and this supports the idea that D-gal weakens bones. In Figure 3, after two months of conducting the experiment, it was observed that there was no change in the control group as expected, but the group (Treadmill+ D-gal) showed a whiter area in the bones compared to the D-gal group ,which is showed by the brown arrow. This could indicate The result is excessive stimulation of bone formation from the Treadmill device. In the D-gal group ,it was observed that bone density continued to decrease, as an evident in the examination results.

From the process of regeneration. Chronic inflammation stimulated by the presence of D-gal affects the secretion of inflammatory cytokines, which are molecules that lead to the activation of bone-destroying cells (osteocytes) and increased bone destruction(**Imerb et al., 2023**) . There is also a hormonal imbalance, as D-gal affects the levels of the main hormones that regulate bone building, such as calistinin and PTH which leads to an imbalance in the bone building process(**Dowhan & Dharmarajan, 2020**).

The results of the current research showed that the use of the Treadmill device led to a significant improvement in bone density and reduced osteoporosis in rats that were injected with D-gal . These benefits are due to several mechanisms, the most important of which is stimulating bone formation, as the treadmill stimulates the secretion of

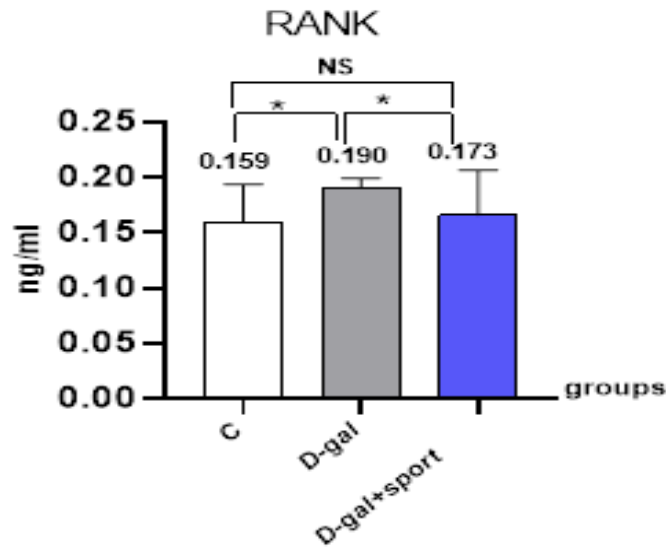
factors that stimulate bone formation (osteoblasts) and increases the synthesis of extracellular matrix proteins, which leads to increased bone density(Liu *et al .*, 2018) . The treadmill also helps reduce the secretion of inflammatory cytokines, which leads to the inhibition of bone-destroying cells (bone-eating cells) and reduces bone fracture (Pranoto *et al .*, 2003 ). The mechanical loading experienced during treadmill exercise stimulates osteoblasts to produce bone matrix. This process is crucial for the repair of micro damage within the bone and contributes to the overall adaptive response of bone to physical activity (Qin & Hu., 2020).

## **4-2 Effect of D-gal and treadmill on serum biomarkers:**

### **4-2-1Effect of D-gal and treadmill on serum RANK/RANKL:**

The current study show an increase in the RANK in the D-gal group as compare with the control group .the D-gal group was significant ( $P < 0.0022$ ) at  $(0.190 \pm 0.015)$  compared to the control group  $(0.159 \pm 0.0013)$ , while the (treadmill+D-gal) group showed a significant decrease in the serum RANK compare with D-gal group $(0.173 \pm 0.09)$ , as shown in figure (4-4).

The study show that there was a significant increase in the RANKL as  $(0.195 \pm 0.01)$  in the D-gal group compared to the control group  $(0.155 \pm 0.01)$ , while the (treadmill+D-gal) group showed a significant decrease in the serum RANKL compare with D-gal group $(0.159 \pm 0.09)$ ,as shown in figure (4-5).



Figure(4.4): Effect of 200 mg/kg of D-gal and 25m/min for 1hr/5 days treadmill sport for 8 weeks in the serum RANK concentration on male rats. Values are expressed as mean  $\pm$  SE.

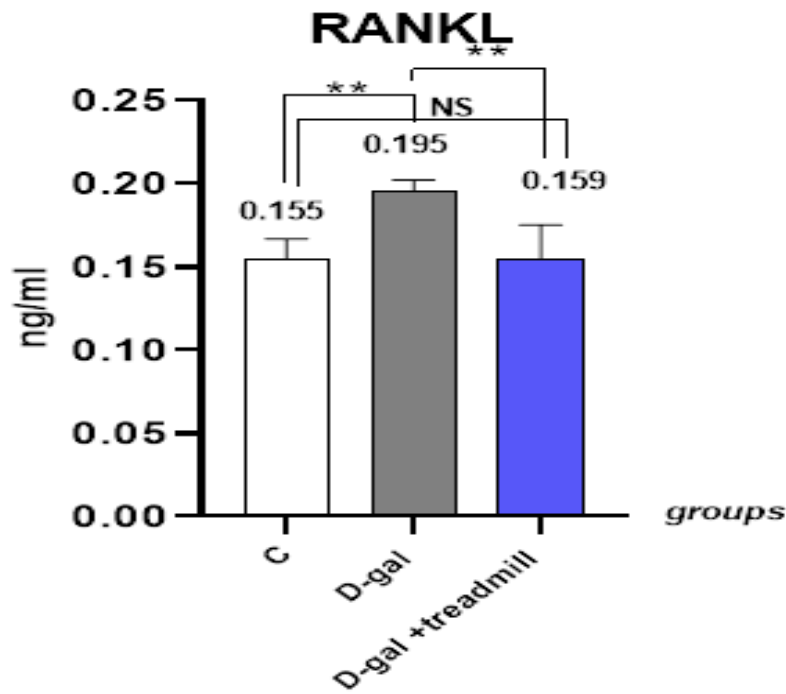


Figure (4-5) Effect of 200 mg/kg of D-gal and 25m/min for 1hr/5 days treadmill sport in the serum RANKL concentration on male rats.

Chronic exposure to D-gal has been shown to induce oxidative stress and inflammation in various tissues including bone (Xu *et al* ., 2020). These oxidative cellular stress responses can trigger signaling cascades that culminate in increased RANKL gene expression thereby promoting osteoclast genesis and bone reabsorption(Wang *et al* ., 2020). D-gal exposure has been shown to alter DNA methylation patterns within the RANKL gene promoter region leading to enhanced transcriptional activity(Tardito *et al* ., 2019).

(Zhao & Ivashkiv .,2011) found that RANK signaling pathway activation triggers a cascade of events leading to transcriptional upregulation of target genes involved in osteoclast differentiation, bone resorption, and immune cell activation. Dysregulation of serum RANK gene expression is implicated in the pathogenesis of osteoporosis, inflammatory bone diseases, and cancer metastasis.

Studies have demonstrated alterations in serum RANK mRNA levels following D-gal administration accompanied by changes in bone turnover markers and bone mineral density(Hor *et al* ., 2019 ; Xu *et al* ., 2020). Studies also shown that ROS generated during D-gal metabolism can activate transcription factors, such as nuclear factor-kappa B (NF-κB) and activator protein-1 (AP-1) which regulate serum RANK gene transcription ,oxidative stress induced DNA damage and histone modifications may alter chromatin structure leading to changes in serum RANK gene accessibility and expression(Tornatore *et al* ., 2012 ; Brzóška & Rogalska., 2013 ; Thakur *et al* ., 2014).

D-gal may also exert indirect effects on RANKL expression through modulation of inflammatory and oxidative stress pathways(Wu *et al* ., 2020). Immune cells including T cells, B cells, and macrophages, contribute to the production of RANKL during inflammation. Activated T cells especially T-helper 17 (Th17) cells are potent

producers of RANKL B cells and macrophages also secrete RANKL in response to inflammatory stimuli(**Adamopoulos & Bowman., 2008 ;Li et al ., 2022**)

Some studies found that Oxidative stress may influences RANKL expression is the nuclear factor kappa B (NF- $\kappa$ B) signaling pathway. ROS generated by D-gal can activate NF- $\kappa$ B signaling leading to the translocation of NF- $\kappa$ B transcription factors into the nucleus, once in the nucleus NF- $\kappa$ B binds to specific regulatory elements within the RANKL gene promoter region thereby enhancing RANKL transcription(**Zhang et al ., 2021 ;Wang et al ., 2022**). This process represents a direct link between oxidative stress induced by D-gal and the up regulation of RANKL expression.

Studies also found that Oxidative stress has been shown to activate the mitogen-activated protein kinase (MAPK) pathway including extracellular signal-regulated kinase (ERK), c-Jun N-terminal kinase (JNK) and p38 MAPK(**Runchel et al ., 2011 ;Liu et al., 2011**),These kinases can phosphorylate transcription factors such as activator protein 1 (AP-1) which in turn can bind to the RANKL gene promoter and stimulate its transcription(**Malik et al ., 2023** ).

Metabolism of D-gal leads to the production of ROS through various pathways including autoxidation of D-gal generation of advanced glycation end-products (AGEs) and activation of NADPH oxidase and mitochondrial electron transport chain (**Song et al., 2021**), (**Winter&Bickford., 2019**) found that excessive ROS accumulation can over when cellular antioxidant defenses, resulting in oxidative damage to lipids, proteins, and nucleic acids. Experimental models utilizing D-gal administration have consistently demonstrated increased oxidative stress markers and cellular dysfunction, mirroring aging-related change (**Atef et al., 2022**).



The primary positive effects of treadmill exercise on bone are the improvement of bone density. Weight-bearing exercises, including walking and running on a treadmill, subject bones to mechanical loading, stimulating bone formation. This is particularly important in the prevention of age-related bone loss and osteoporosis (**Abd El-Kader et al .,2016**). Studies find that Treadmill exercise influences the secretion of hormones, such as parathyroid hormone (PTH), estrogen, and insulin-like growth factor 1 (IGF-1) which modulate RANK gene expression. PTH and IGF-1 promote osteoblast activity while suppressing osteoclast formation(**Qi et al ., 2019;Zhang et al .,2023**), also treadmill exercise reduces systemic inflammation which can indirectly suppress RANK gene expression by decreasing the production of pro-inflammatory cytokines, such as interleukin-1 (IL-1) and tumor necrosis factor-alpha (TNF- $\alpha$ )( **Hill et al ., 2020**). (**Santos et al ., 2017 ;Xu et al ., 2021**) found that Treadmill exercise may induce epigenetic changes such as DNA methylation and histone modifications that affect RANK gene expression (**Santos et al ., 2017 ;Xu, et al ., 2021**).

Studies found that treadmill has been demonstrated to suppress the production of inflammatory cytokines such as tumor necrosis factor-alpha (TNF- $\alpha$ ) and interleukin-1 beta (IL-1 $\beta$ )( **Al-Jarrah & Erekat.,2018**) ,which are known inducers of RANKL expression. By reducing inflammation, exercise can indirectly decrease RANKL levels and mitigate its osteoclast genic effects(**Luo et al ., 2018**).

Exercise-induced mechanical strain during treadmill on bone tissue can stimulate the production of anti-inflammatory cytokines and growth factors such as interleukin-10 (IL-10) and transforming growth factor-beta (TGF- $\beta$ )(**smith et al ., 2016**). These factors have been shown to inhibit RANKL expression and promote osteoblast differentiation and bone formation(**Yi et al ., 2018;Amarasekara et al ., 2021**). the mechanical loading associated with treadmill running may contribute to the suppression of RANKL and the maintenance of bone homeostasis.

### 4-2-2 Effect of D-gal and treadmill on serum OPG:

In the current study demonstrated that the D-gal group serum OPG concentration( $4.32 \pm 0.20$ ) was significantly lower ( $P < 0.0003$ ) than the control groups ( $7.94 \pm 0.01$ ), and (treadmill+D-gal) group ( $6.92 \pm 0.05$ ) showed a significant decrease compare with control and (treadmill+D-gal) groups, as shown in figure(4-6).

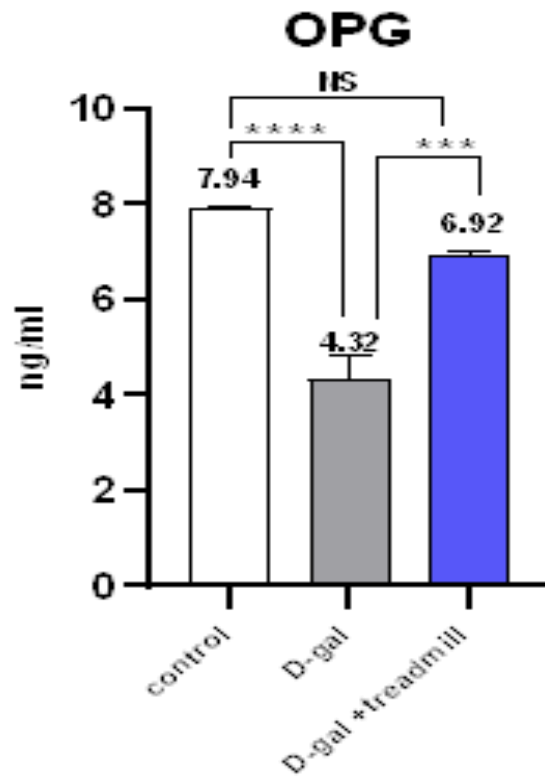


Figure (4-6) :Effect of 200 mg/kg of D-gal daily for 8weeks and 25m/min days treadmill sport in the serum OPG concentration on the male rats

Oxidative stress resulting from D-gal metabolism activates signaling pathways involved in osteoclast differentiation and bone resorption (Xu *et al* ., 2020). ROS-mediated modifications of OPG and RANKL may alter their binding affinity affecting the balance between bone formation and resorption. Furthermore inflammation

induced by D-gal may up regulate RANKL expression further exacerbating bone loss (Wang *et al.*, 2022 ; Carletti *et al.* , 2024).

D-gal metabolism leads to the generation of ROS and oxidative stress which have been implicated in the downregulation of OPG expression. Oxidative stress activates various signaling pathways including nuclear factor-kappa B (NF- $\kappa$ B) and mitogen-activated protein kinase (MAPK) which can suppress OPG gene transcription and promote RANKL-induced osteoclast genesis(Wang *et al.* , 2022;Li *et al.* , 2023 )

D-gal -induced aging is associated with chronic low-grade inflammation characterized by elevated levels of pro-inflammatory cytokines such as tumor necrosis factor-alpha (TNF- $\alpha$ ) and interleukin-6 (IL-6)( Permpoonputtana *et al.* , 2018; Weitzmann, 2013). found that inflammatory mediators can stimulate osteoclast formation and activity directly and indirectly by promoting RANKL expression and inhibiting OPG production. Thus, the inflammatory milieu induced by D-gal may contribute to the dysregulation of the OPG/RANKL ratio and exacerbate bone loss.

Also D-gal -induced mitochondrial dysfunction may also play a role in the regulation of OPG expression ,mitochondrial dysfunction impairs cellular energy metabolism and induces oxidative stress leading to alterations in gene expression and cellular signaling pathways(Imerb, 2023). Emerging evidence suggests that mitochondrial dysfunction may contribute to the pathogenesis of age-related bone disorders by modulating osteoblast and osteoclast function Mitochondrial dysfunction in osteoclasts impairs their ability to generate ATP leading to reduced bone resorption capacity and decreased bone turnover. (Liu *et al.* , 2024)

Treadmill exercise may modulate OPG expression through its effects on systemic factors and cellular signaling pathways. Studies found that Treadmill -induced alterations in hormonal milieu, such as increased secretion of growth factors like

insulin-like growth factor 1 (IGF-1) and testosterone may stimulate OPG production by osteoblasts. Moreover, exercise exerts anti-inflammatory effects and reduces circulating levels of pro-inflammatory cytokine which can suppress OPG expression and promote bone resorption (Mohamad *et al.* , 2016 ; Qi *et al.* , 2019).

On the other hand, IGF-1 stimulates OPG production by activating phosphoinositide 3-kinase (PI3K)/Akt and MAPK pathways, while testosterone upregulates OPG gene transcription through androgen receptor-mediated signaling (Massicotte *et al.* , 2006). Treadmill exercise imposes mechanical forces on bones leading to microdamage and deformation. Osteoblasts, the bone-forming cells, sense these mechanical signals and respond by increasing OPG gene expression (Birch *et al.* , 2013).

(Yavropoulou & Yovos, 2016) found that mechanotransduction pathways including integrin-mediated signaling and cytoskeletal remodeling play a crucial role in translating mechanical stimuli into cellular responses. Activation of focal adhesion kinase (FAK), mitogen-activated protein kinase (MAPK), and Wnt/ $\beta$ -catenin signaling pathways stimulates OPG gene transcription and promoting bone formation and inhibiting osteoclastogenesis.

#### **4-2-3 Effect of D-gal and Treadmill on serum cathepsin K (Cat-K):**

In the current study, the D-gal groups' Cathepsin K concentration was significantly higher ( $P < 0.0001$ ) at  $(260.08 \pm 11.05)$  than the control groups  $(163.07 \pm 15.09)$ , while the (treadmill+D-gal) group showed a significant decrease in the serum Cat-K compared with the D-gal group  $(0.168.30 \pm 12.22)$ , and showed no significant difference with the control group, as shown in figure (4-7).

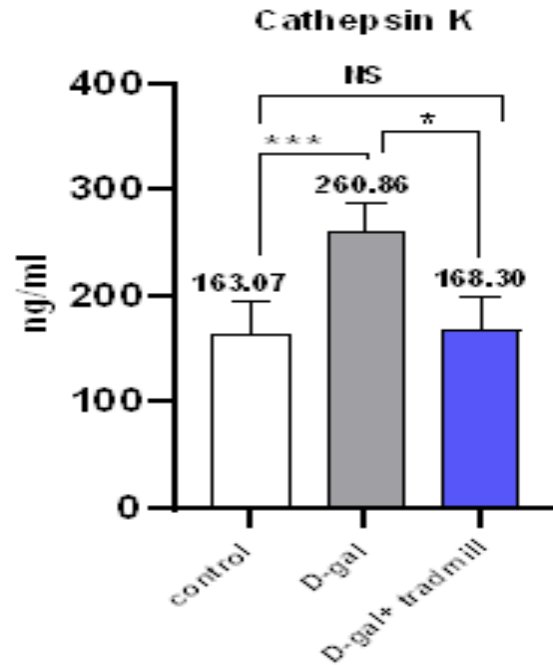


Figure (4-7): Effect of 200 mg/kg of D-gal daily for 8weeks and 25m/min days treadmill sport in the serum Cathepsin k concentration on the male rats

The level of cathepsin K rises with high D-gal consumption, and this is thought to be a sign of worsened bone loss (Li *et al* ., 2019). But disagreement studies by (Teno ,2008; Soung ,2013) found the potential of cathepsin K inhibitors in reducing bone resorption and enhancing bone repair .Cellular stress-inducing intrinsic damage, such as DNA damage or increased ROS, eventually converges at the mitochondria where the fate of the cell is decided. Under pathological conditions, not only the expression and activity of Cathepsin are increased, but also lysosomal membrane permeabilization leads to the release of Cathepsin into the cytoplasm, initiating various types of PCD (Zamyatnin *et al* ., 2022). Cystatins a superfamily of tight-binding inhibitors of papain-like cysteine peptidases, are widely applied to inhibit Cathepsin (Watanabe *et al* ., 2014).

Studies found that the consumption of D-gal exacerbates age- and obesity-related bone loss, leading to an elevation in the serum level of cathepsin K(Imerb *et al* ., 2014).

2023). Cathepsin K is responsible for the degradation of type I collagen in osteoclast-mediated bone resorption (Garnero *et al* ., 1989). Cathepsin K (Cat K) is a cysteine protease of the papain family, now considered to be the major enzyme responsible for degradation of the organic bone matrix. It is highly and selectively expressed in osteoclasts and, under acidic conditions, has the unique ability to degrade type I collagen helical regions (Bromme *et al* ., 1995 ; Garnero *et al* ., 1989).

The abundant expression of Cat K instead of the other cathepsins was previously identified in osteoclasts (Drake *et al* ., 1996) . Furthermore, a study has shown elevation in the serum RANK, RANK-L OPG in the D-gal group compare with other groups and increase in the serum Cat K expression which is regulated by the receptor activator of nuclear factor  $\kappa$ B ligand (RANKL)-RANK signaling (Troen, 2006), the critical signaling pathway of osteoclastogenesis. The activation of RANKL-RANK signaling pathway in osteoclast precursors stimulates the pro-osteoclastogenic transcriptional factor NFATc1 (nuclear factor of activated T cells) to initiate the transcription of Cat K (Balkan *et al* ., 2009). In the process of bone resorption, Cat K are secreted from mature osteoclast into the “sealing zone,” a dynamic actin- rich cell–matrix adhesion structure that defines the resorption area of bone (Takito *et al* ., 2018) It is known that Cat K could efficiently degrade type I collagen (Garnero *et al* ., 2018).

The current study agreement with (Lotinun *et al* ., 2013) found that the CatK-deficient osteoclasts would secrete more sphingosine-1-phosphate (S1P) to enhance osteoblastic bone formation. The excess mechanical stress loading could stimulate the Cat K expression in human chondrocytes (Suzuki *et al* ., 2020) inhibition of Cat K by mechanical stress for 8 weeks and 25m/min days treadmill sport could suppress the cartilage degradation as well as the systemic and local bone loss (Asagiri *et al* ., 2008; Svelander *et al* ., 2009 ; Yamashita *et al* ., 2018 ; Yamada 2019) and Since

suppression of CatK activity could prevent bone resorption without perturbing bone formation (Costa *et al* ., 2011), it has become an attractive target for anti-resorptive drug development. Activation of Cathepsin K can be activated by transitioning from its inactive form to its active form. Possible activators may involve changes in acidity and the presence of other enzymes (Boon, 2020).The proteolytic activity of Cathepsin K on the bone matrix results in weakened bone structure and loss of bone density, contributing to the development of osteoporosis. This increases the risk of fractures and bone deterioration (Sharma *et al* ., 2021).

#### **4-3 Effect of D-gal and Treadmill on serum electrolyte (Na ,Ca,P & K) :**

Figure (4-8) showed a significant decrease ( $P < 0.05$ ) in the serum calcium concentration at ( $15.42 \pm 0.38$ ) in the D-gal group compared to the control group ( $21.66 \pm 1.20$ ),while (treadmill+D-gal) group showed a significant the lower concentration at( $10.72 \pm 0.52$ ) compared to other groups. The lower concentration in the serum Na in the D-gal group was significant ( $P < 0.05$ ) at ( $81.05 \pm 5.46$ ) compared to the control group( $100.10 \pm 7.806$ ), while (treadmill+D-gal) group showed a significant the lower concentration at( $59.82 \pm 4.40$ ) compared to other groups. In the serum P concentration not significantly between D-gal group and other groups , the current study demonstrated that the D-gal groups serum K concentration was significantly lower ( $P < 0.05$ ) than the control groups ( $4.77 \pm 0.31$ ), while control group ( $6.17 \pm 0.26$ ),and not significantly differences between (treadmill+D-gal) group and other groups ,as shown in figure (4-8).

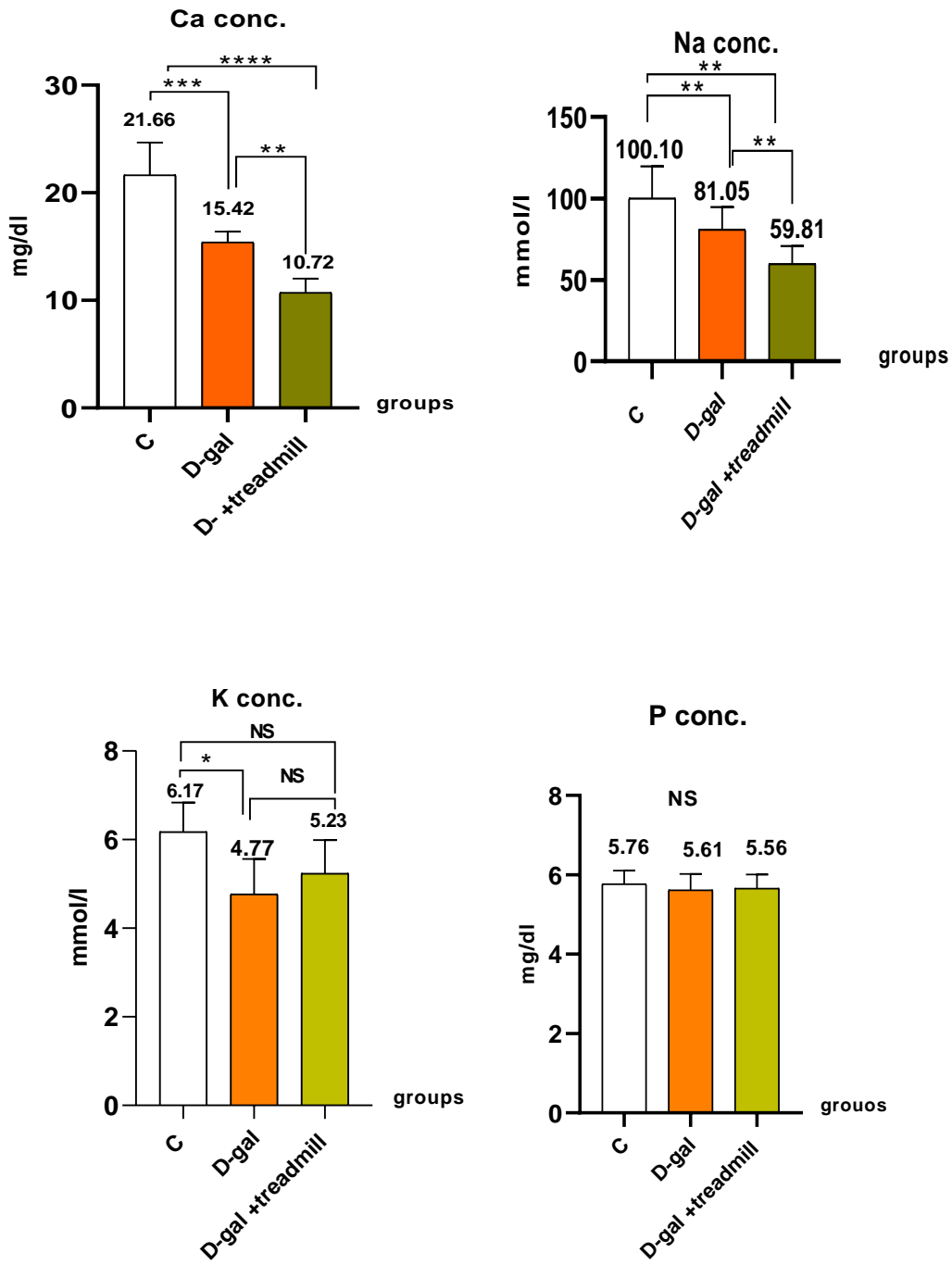


Figure (4-8 ) Effect of 200mg/kg of D-gal and 25m/min for 1hr/5 days treadmill sport for 8weeks on the serum Na ,Ca,P & K concentration on male rats .



serum Ca level of D-gal group showed a decrease as compare with the other group this result may occur due to the imbalance of the Ca hormones in the body (PTH & calcitonin) and this lead to increase Ca imbalance between the bone and the body which lead to increase serum Ca, also the calcitonin hormone increase the activity of the osteoclast cells which lead to destruction of the osteocyte and this increase serum Ca level inflammation due to increase the oxidative stress also case necrosis in the osteocyte that lead to release the Ca into the blood stream which play a role in the increase the serum Ca consecration in the D-gal treated rats. In addition due to the loss of calcium from the bones, this may have happened because D-galactose leads to bone cell (osteocyte) apoptosis and death in bone tissue, which leads to activity in the osteoclast, while the control group did not change and was similar to normal bone tissue. and this result is in agreement with (McDERMOTT & Kidd, 1987 ; Cerqueni *et al* ., 2022).

Also the current study show a significant decrease in serum Na concentration in the treadmill group as compare with the other groups and this result is in agreement with (Muhammad *et al* ., 2022), how found that this decrease occur due to the effect of treadmill to increase sweating in the rats and the sweat is contain an amount of Na in it and this lead to decrease the amount of Na in the body .On the other hand the D-gal group show a significant decrease in the Na as compared with the control group this result is in agreement with (Dong *et al* ., 2022) how found this may occur due to the ability of D-gal to increase of the oxidative stress in the kidney blood vessels that lead to decrease the Na reabsorption from the kidney which will case a decrease in the body sodium that lead to decrease of serum Na . Also Mitochondrial dysfunction due to high oxidative stress in renal cells may impact sodium transport mechanisms. Oxidative stress can influence the redox state of proteins, including ion transporters in

the kidney. Some sodium transporters are sensitive to changes in redox status, and alterations in their activity may affect sodium reabsorption (Amabebe *et al* ., 2013 ; Aranda-Rivera *et al* ., 2021; Jo *et al* ., 2023 ).

on the other hand serum concentration of K<sup>+</sup> in the D-gal group shows a significant decrease as compare with the other group. The K<sup>+</sup> concentration inosculated with the Na so when there is decrease in the Na in the body due to disorder the K level will also decrease, Since D-gal leads to damage to the blood vessels in the kidney, this leads to the excretion of minerals from the body, such as sodium and potassium, and this explains the reason for their deficiency in the process of complete reabsorption of the excreted materials (Jang *et al* ., 2017 ; Wang *et al* ., 2022).

#### **4-4 Effect of D-gal and Tread mill on serum bone related hormones:**

In the current study there was a significant increase in the PTH at (201.55± 7.02) in the D-gal group compared to the control (treadmill+D-gal) groups (109.81 ± 6.79) ,while (treadmill+D-gal)group showed a not significant compared to control groups. However, there was a a significant increase in the Calcitonin in the D-gal group was significant (P < 0.05) at( 739.58 ± 20.24) compared to the control and (treadmill+D-gal) groups (200.76 ± 3.33),while (treadmill+D-gal)group showed not significant compared to control groups , as shown in figure (4-9).

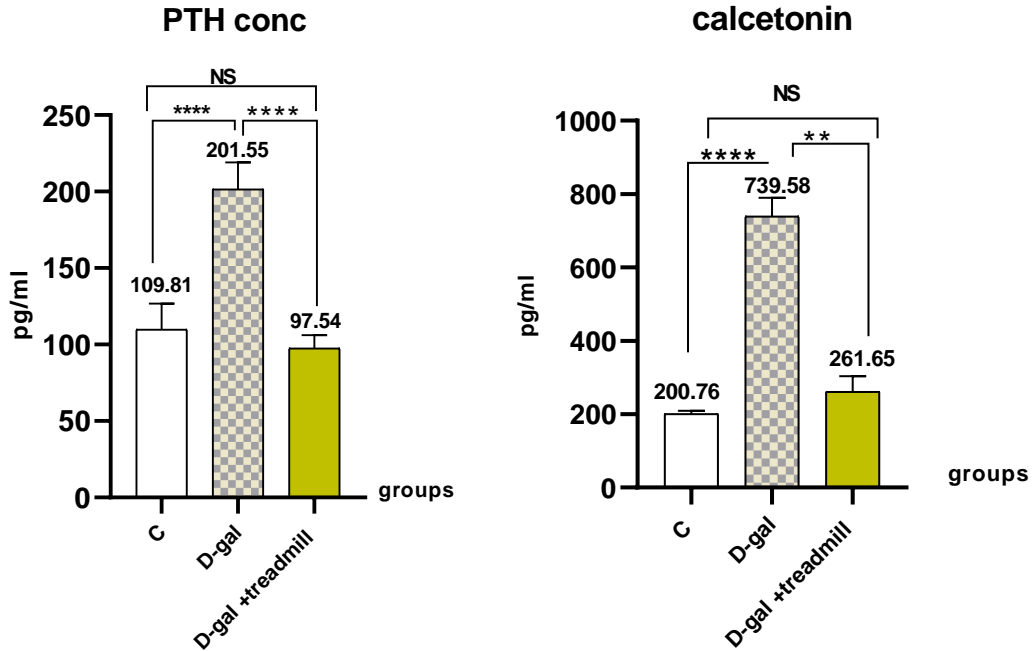


Figure (4-9 ) Effect of 200mg/kg of D-gal and 25m/min for 1hr/5 days treadmill sport for 8weeks on the serum calcitonin and PTH concentration on male rats .

The current study demonstrated that the D-gal group serum Vit D concentration was significantly higher ( $P < 0.05$ ) than the control group ( $303.48 \pm 4.12$ ), while control ( $140.5 \pm 3.96$ ), and (treadmill+D-gal)groups ( $201.21 \pm 6.67$ ) showed not significant compared to control groups, as shown in figure (4-10).

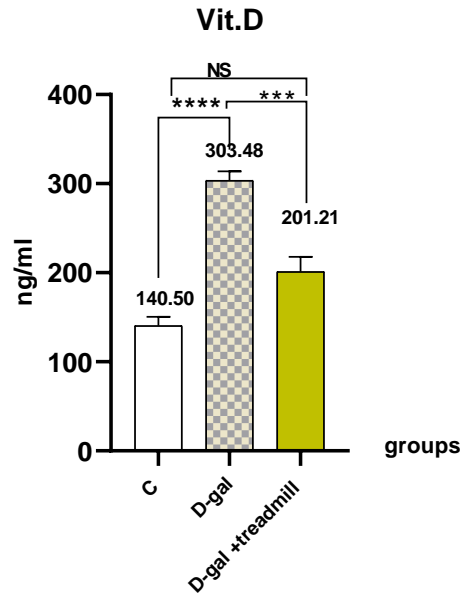


Figure (4-10) Effect of 200mg/kg of D-gal and 25m/min for 1hr/5 days treadmill sport for 8weeks on the serum Vit.D concentration on male rats .

In the current study there was a significant increase in the (PTH, Vit D & calcitonin) level in the serum of the D-gal rats group as compared with the other groups . This result may occur due to the Oxidative Stress-Induced DNA Damage, ROS generated during oxidative stress can inflict damage on cellular DNA. Parathyroid gland cells may be vulnerable to such genetic alterations, potentially impacting the expression of genes involved in PTH synthesis and release. Oxidative stress-induced changes in DNA integrity could lead to long-term consequences for PTH regulation, adding another layer to the complex relationship between oxidative stress and the endocrine system (Vono *et al* ., 2018 ;Souliotis *et al* ., 2019 ; Jacquillet *et al* ., 2019).

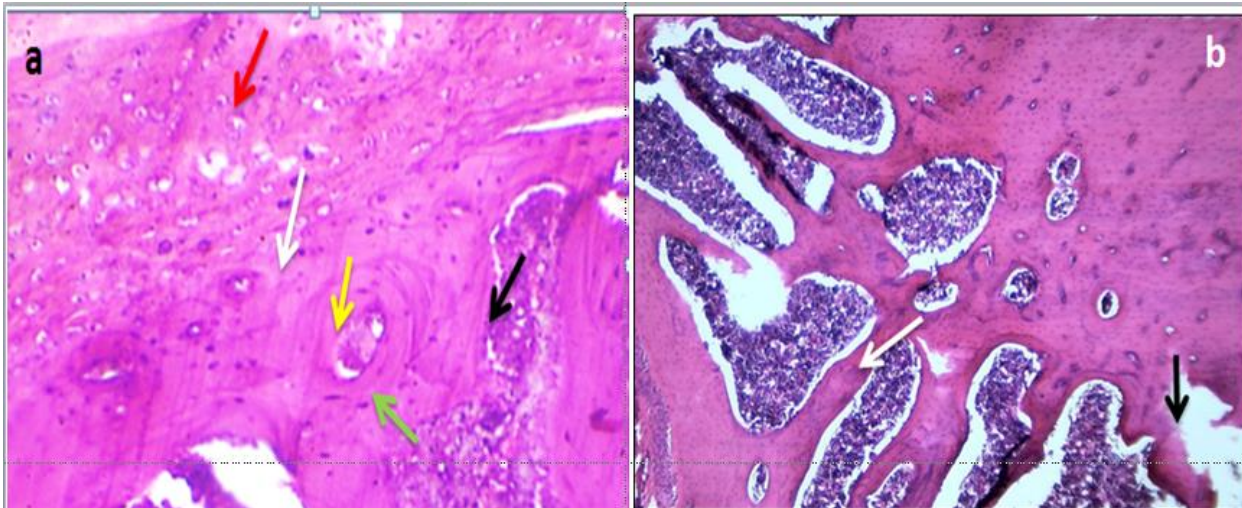
Calcium-sensing receptors (CaSR) play a crucial role in regulating PTH secretion by sensing changes in extracellular calcium levels. Oxidative stress has been linked to alterations in CaSR function. D-gal -induced oxidative stress may modulate the sensitivity of CaSR in the parathyroid glands, affecting their ability to respond appropriately to changes in calcium concentrations. This, in turn, could impact the

finely tuned regulation of PTH release in response to calcium homeostasis (**Brown 2013; Manayi *et al* ., 2014 ; Kosiba *et al* ., 2020**)

Prolonged exposure to oxidative stress may contribute to parathyroid hyperplasia, a condition characterized by the enlargement of the parathyroid glands. This enlargement could be a compensatory response to oxidative damage, aiming to maintain adequate PTH production. However, the hypertrophic changes may lead to dysregulation of PTH secretion, further complicating the relationship between oxidative stress and the endocrine function of the parathyroid glands (**Deska *et al* ., 2019; Rendina & Rosen, 2022**).

#### **4-5 Effect of D-gal and treadmill on femoral bone histology :**

The control group of the current study showed a normal bone structure with compact bone plat and remarkable canals bone trabeculae ,surrounding cavities of normal bone marrow as shown in figure (4-11 a) . The D-gal treated animal, revealing the significant histological alterations manifested by marked thinning of trabeculae with irregular borders sever resorption and perforation of compact bone with irregular atrophied osteocytes and marked cavities formations with numerous typical large multinucleated osteoclasts released from surface of bony trabeculae with numerous typical large multinucleated osteoclasts released from surface of bony trabeculae and typical large multinucleated osteoclasts in bone plate with irregular plates edges (4-11 b , 4-12 C&D and 4-13 E&F )



Figure(4-11) Photomicrograph of bone tissue section for a control animal, showing the normal histology of cortical bone, compact bone plate (white arrow), remarkable canals (yellow arrow) with significant osteocyte lei into their lacunae (red arrow), bone trabeculae( green arrow) surrounding cavities of bone marrow (black arrow). (b) Photomicrograph of bone tissue section for D-gal treated animal, revealing the significant histological alterations manifested by marked thinning of trabeculae (white arrow) with irregular eroded borders (black arrow) (H and E,4X)\

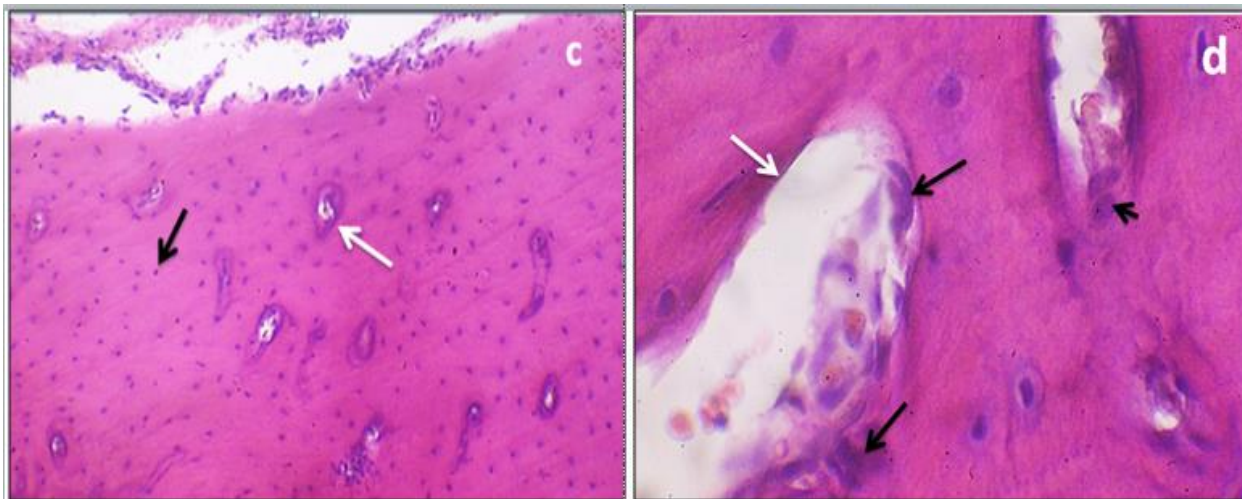
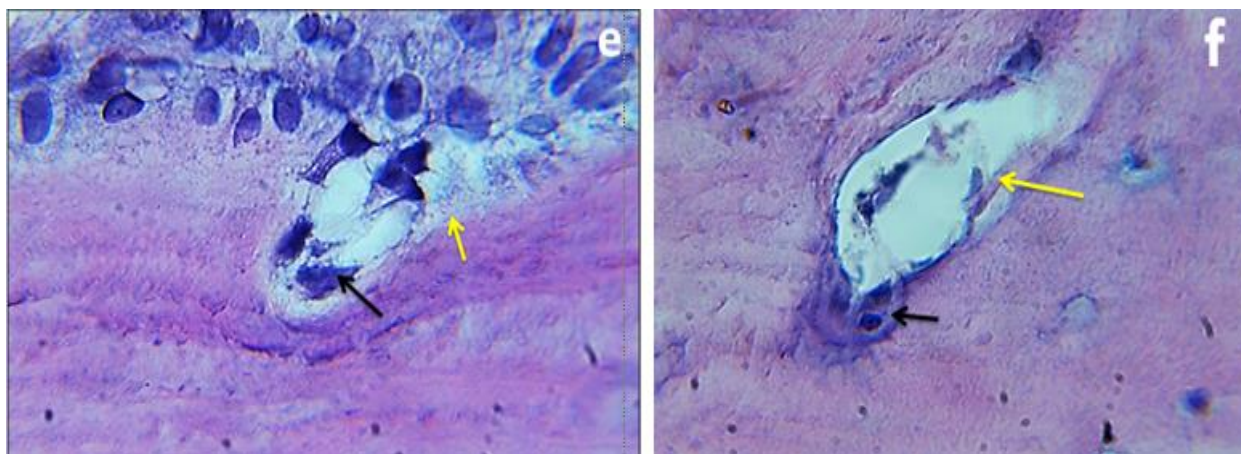


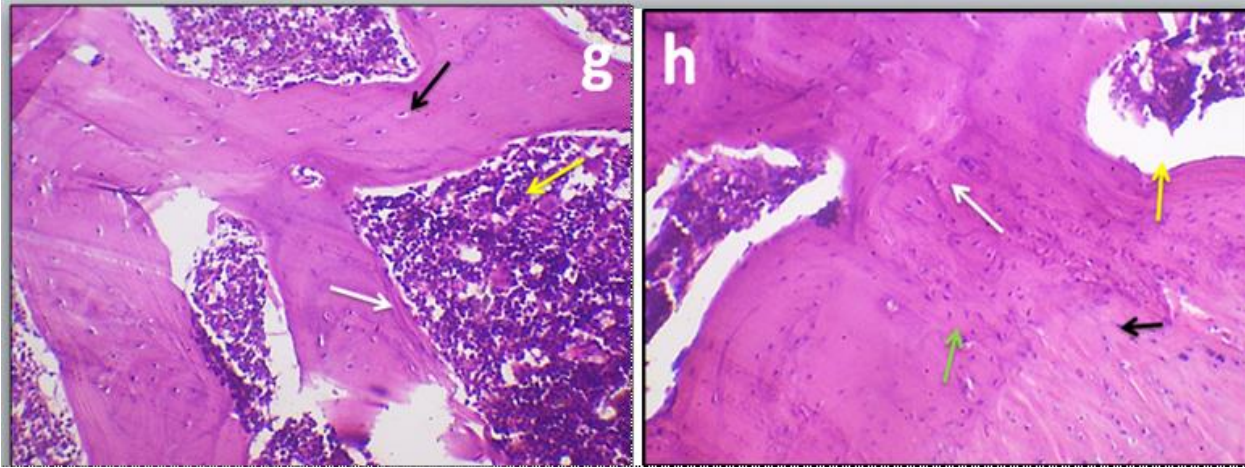
Figure (4-12) Photomicrograph of bone tissue section for D-gal treated animal , revealing the significant histological alterations manifested by sever resorption and perforation of compact bone (white arrow) with irregular atrophied osteocytes (black arrow) , (2d) Photomicrograph of bone tissue section for D-gal treated animal , revealing remarkable histological alterations represented by marked cavities formations (white arrow) with numerous typical large multinucleated osteoclasts released from surface of bony trabeculae (black arrow) .(H and E,40X)



Figure(4-13) Photomicrograph of bone tissue section for D-gal treated animal , revealing remarkable histological alterations manifested by typical large multinucleated osteoclasts in bone plate (black arrow) with irregular plates edges(yellow arrow) (3f) Photomicrograph of bone tissue section for D-gal treated animal , revealing remarkable histological alterations manifested by marked lack of typical large multinucleated osteoclasts in bone plate (black arrow) with irregular plates edges(yellow arrow) . (H and E,100X)

The presented photomicrographs reveal histological alterations in bone tissue sections from D-gal treated animals. These findings align with previous research by (Moser *et al* .,2019; Rikkonen *et al* .,2021) that demonstrating the detrimental effects of D-gal on bone health. Figure (4-12 d) show cases resorption and perforation of compact bone .This indicates loss of bone mass, potentially due to increased osteoclast activity.Also, displays irregular, atrophied osteocytes.

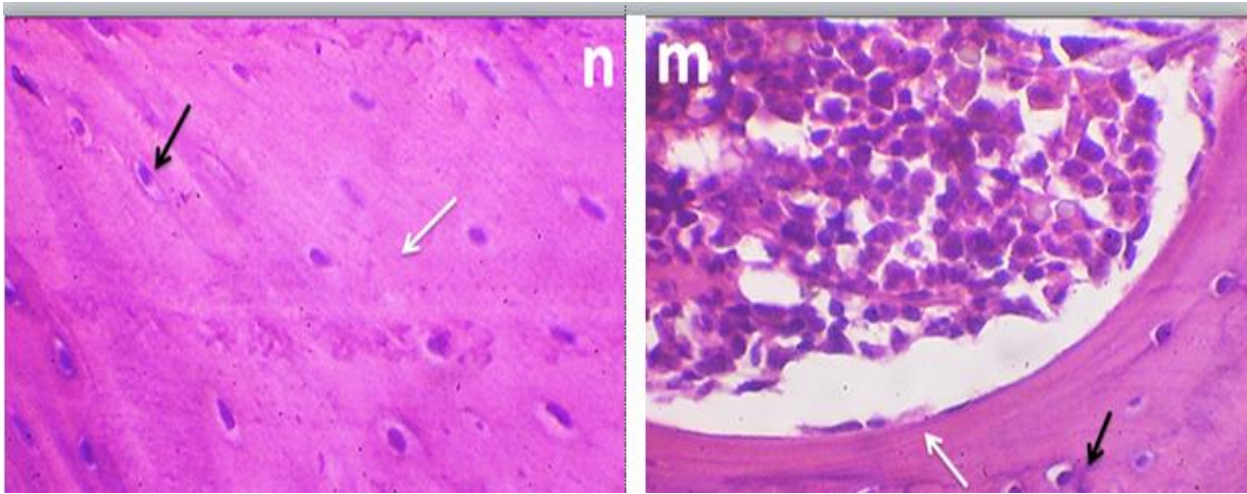
The observed resorption, osteocyte atrophy, and cavity formations suggest a net loss of bone mass. The presence of osteoclasts further supports this notion. While the absence of osteoclasts in one figure warrants further investigation, the overall findings align with previous research and highlight the potential detrimental effects of D-gal on bone health. A study conducted by researcher (Moser *et al* .,2019) aligns with the findings of our current study.



Figure(4-14) Photomicrograph of bone tissue section for D-gal treated animal with exercise, showing reversible histological changes characterized by marked thickness in bone trabeculae with newly added lamellar structure (white arrow), numerous healthy osteocytes in trabeculae (black arrow) with abundant cellularity red marrow (yellow arrow),(4 h) Photomicrograph of bone tissue section for D-gal treated animal with exercise, showing reversible histological changes characterized by marked thickness in bone trabecular with regular lamination (white arrow), moderate to severe increase on osteocytes (black arrow) with less cavities in bony plate (yellow arrow)and reduction in microfissures (green arrow) . (H and E,4X)

Building upon the observations of D-gal induced bone damage (4-13) showcases the remarkable reversal of these histological alterations in animals treated with D-gal alongside treadmill . This compelling evidence highlights the potential protective effects of exercise against D-gal mediated bone deterioration. This Figure provides compelling evidence that exercise can effectively counteract D-gal induced bone damage. The increased trabecular thickness, new lamellar bone structure, healthy osteocytes, and cellular red marrow observed in the exercise group highlight the potential of exercise as a therapeutic strategy to compact bone loss associated with D-gal exposure. A study of (Yu *et al* .,2020 ) demonstrated that exercise prevented bone loss and increased bone mineral density in rats treated with D-gal .





Figure(4-15) Photomicrograph of bone tissue section for D-gal treated animal with exercise, showing marked reversible histological changes, compact bone matrix (white arrow), and numerous well-differentiated osteocytes settled in their lacunae (black arrow). (5m) Photomicrograph of bone tissue section for D-gal treated animal with exercise, showing reversible histological changes, elongated osteoblasts at the border of the trabeculae (white arrow) with reversed osteocytes normal histology(black arrow). (H and E,40X).

The photomicrographs Figures (4-14 and 4-15) offer a compelling visual representation of exercise-mediated bone restoration in D-gal treated animals. The restored bone structure, healthy osteocyte population, and active osteoblast presence highlight the potential of exercise as a therapeutic strategy to compact bone loss associated with D-gal exposure. Further research is warranted to fully elucidate the underlying mechanisms and optimize exercise protocols for maximizing bone health benefits. These findings align with previous studies demonstrating the protective effects of exercise against bone loss. As mentioned earlier, reported similar observations of exercise preventing bone loss and promoting bone formation in D-gal or other bone-deteriorating models.

**4-6 Effect of D-gal and treadmill on femoral bone examined by scanning electron microscope:**

The control group showed a reversible of the histological alterations manifested by marked thickness of trabeculae and lamellars with emularte in the space of the Haversian canal (cavities in bony plate) and improve in the bone matrix as shown in figure (4-16).

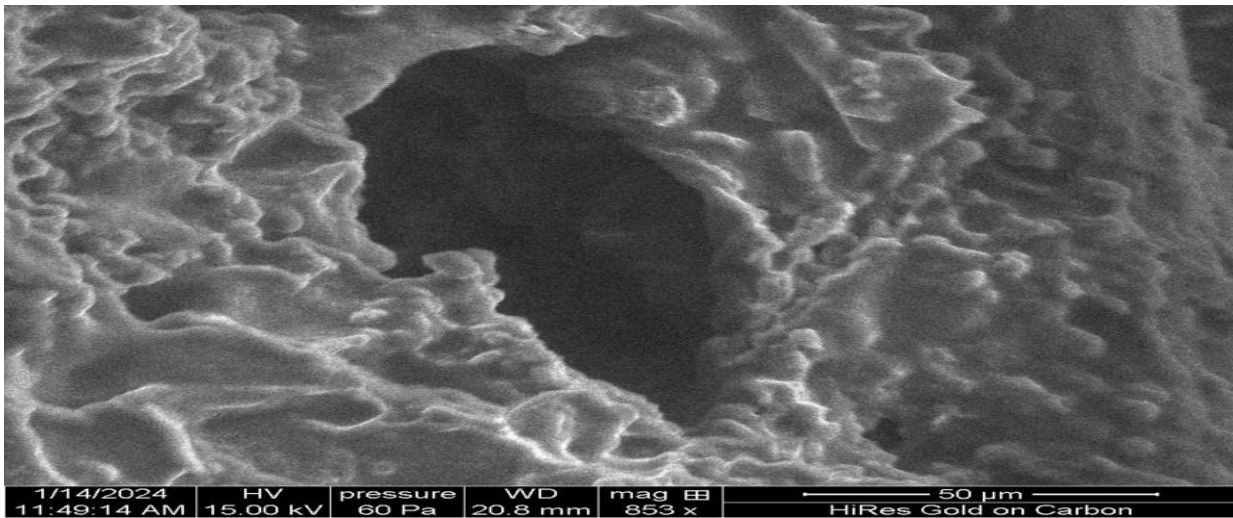


**Figure (4-16)** Electron microscope photograph of the control group showed a reversible of the histological alterations manifested by marked thickness of trabeculae and lamellars with emularte in the space of the Haversian canal (cavities in bony plate) and improve in the bone matrix

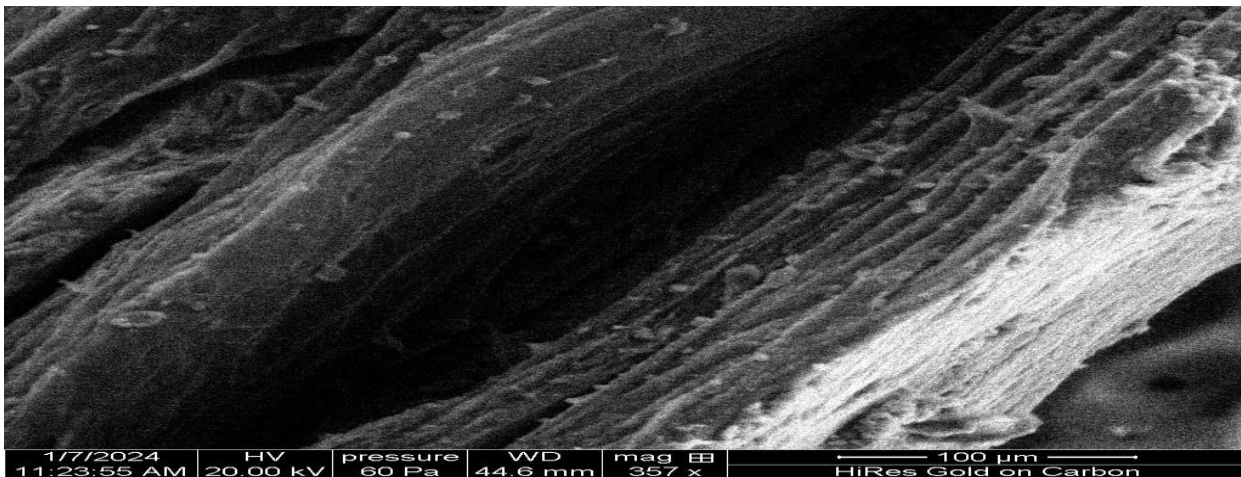


**Figure (4-17)** Electron microscope photograph of the D-gal group showed a significant histological alteration manifested by marked thinning and irregular of trabeculae and lamellar with enlarged in the space of the Haversian canal (cavities in bony plate) resorption in the bone matrix

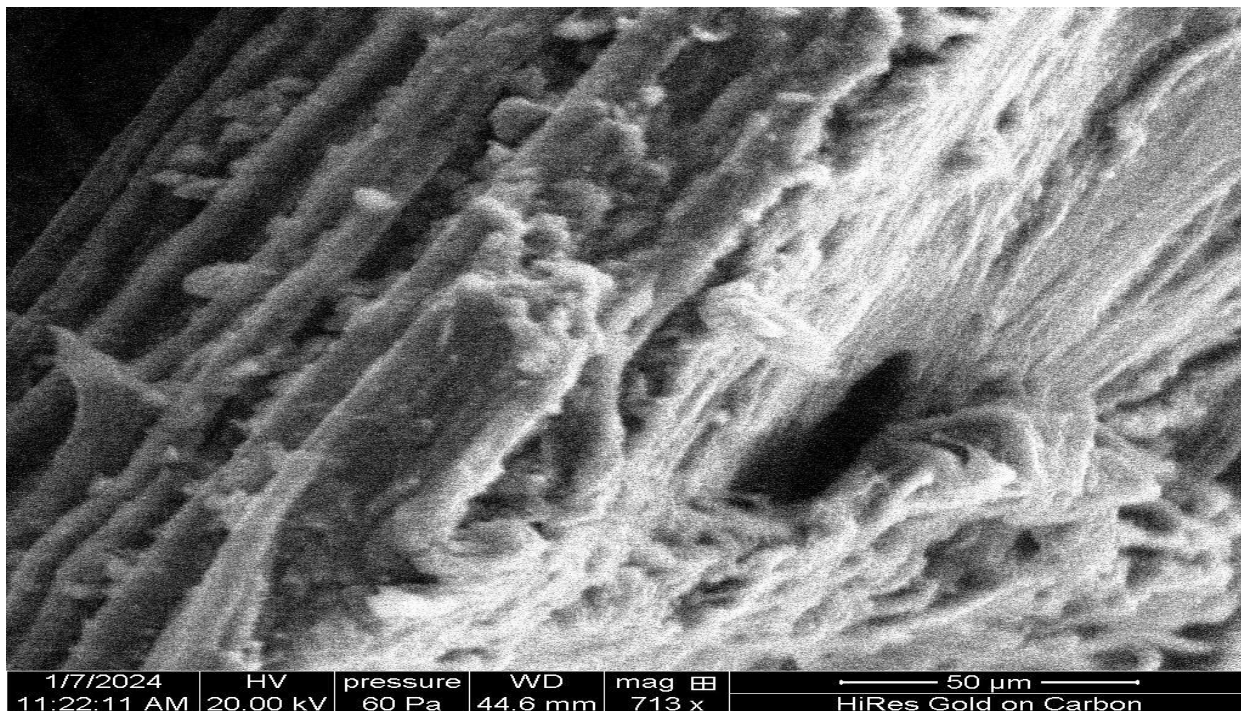


Figure (4-18) Electron microscope photograph of the D-gal + treadmill group showed a reversible of the histological alterations manifested by marked thickness of trabeculae and bone lamellar in the space of the Haversian canal (cavities in bony plate) in the bone matrix

Electron microscopy of bone tissue from rats fed D-gal revealed significant changes in bone structure. Wide spaces between the bones were observed, indicating bone thinning. Additionally, cracks were present in the bones, suggesting damage to the bone matrix. Findings of fig.(4-17 ) provide clear evidence that D-gal can cause substantial bone changes in rats. These changes, including bone thinning and bone matrix damage, could lead to bone weakness and an increased risk of fractures. There are Several mechanisms could explain the detrimental effects of D-gal on bone health for example Interference with Mineral Absorption: D-gal may interfere with the absorption of calcium and phosphorus from the intestines. These minerals are essential for bone building and maintenance. A study by (Imerb *et al .*, 2022)confirmed this effect, finding that rats fed D-gal exhibited significantly reduced calcium and phosphorus absorption, leading to bone thinning and decreased bone density. Additionally ,D-gal may induce oxidative stress in bone cells, leading to cellular

damage and bone matrix breakdown. At study by (**García *et al.*,2024**) supported this effect, demonstrating that bone cells exposed to D-gal *in vitro* experienced increased levels of free radicals, resulting in DNA and protein damage in the cells and bone matrix damage. (**Mhd *et al.*,2022**) conducted a study on mice, comparing the effects of a D-gal -rich diet to a normal diet, and concluded that the D-gal diet resulted in significant bone loss and impaired bone formation.

The electron microscope unveils a reversal of bone damage in the D-gal plus treadmill group compared to the D-gal only group shown in figure (4-18) .This translates to thicker trabecular and denser bone lamellae within the haversian canals (cavities within the bone) of the treadmill exercising rates . This remarkable shift in bone structure signifies that treadmill exercise can effectively counteract the detrimental effects of D-gal on bone health.

Several mechanisms underpin this protective effect of treadmill exercise against D-gal induced bone damage.( **Partadiredja *et al* ,2019**) support the recent study that Treadmill exercise can stimulate the production of osteoblasts, the bone-building cells, leading to enhanced bone formation. This increased bone formation compensates for the bone loss induced by D-gal . Additionally,( **Yu *et al* ,2020**)other researcher agree that treadmill exercise has been shown to reduce oxidative stress in various tissues, including bone. Since oxidative stress is a major culprit in D-gal induced bone damage, reducing it through exercise protects bone cells and promotes overall bone health.

Finally, treadmill exercise may improve the absorption of calcium and phosphorus from the intestines, essential minerals for bone formation, this enhanced absorption counteracts the interference with mineral absorption. In essence, treadmill exercise emerges as a powerful strategy to prevent or reverse D-gal bone damage, highlighting

its potential role in maintaining bone health and preventing osteoporosis, especially for those exposed to higher levels of D-gal .

#### 4-7 Effect of D-gal and Treadmill on Runx-2 gene expression:

In the current study there was a significant increase in the runx-2 gene expression in the D-gal group as compare with the other groups , also there was a significant decrease in the treadmill group as compare with the control group as shown in the figure (4-19) and this result is in agremant with (**Jing *et al* ., 2023**).

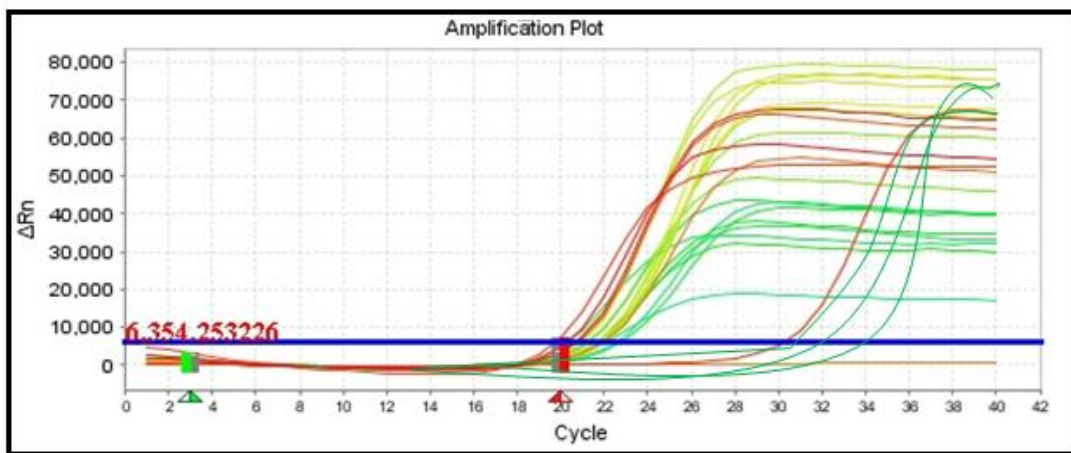


Figure (4-19): Amplification curve of the tested samples represented the runx-2 gene. this indicate a successful RNA extraction and cDNA synthesis

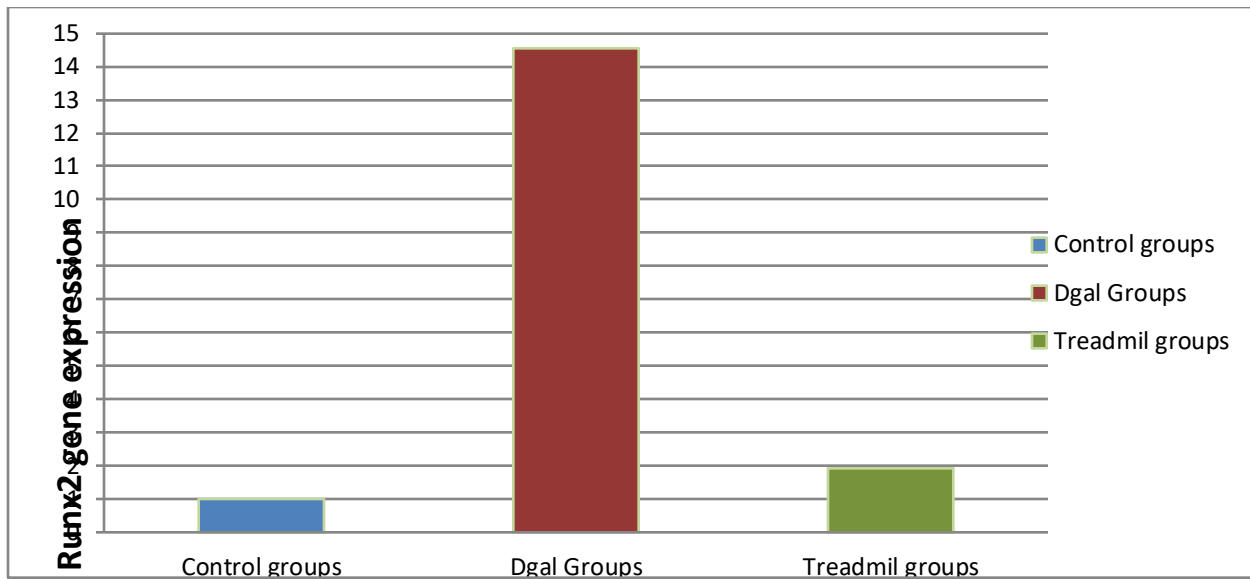


Figure (4-20): Fold change comparison between the group expressed runx-2 gene . and show a significant increase in the D-gal group as compare with the control group and treadmill group.

Inflammatory cytokines such as tumor necrosis factor-alpha (TNF- $\alpha$ ) and interleukin-1 (IL-1) can activate pathways that stimulate Runx-2 expression. MPs are potent inducers of osteoblast differentiation and bone formation. Severe damage may upregulate the expression of BMPs, which in turn activate Runx-2 expression and activity.

The inflammation due to D-gal administration may significantly influence the transcriptional activity of Runx-2 tumor necrosis factor-alpha (TNF- $\alpha$ ) a pro-inflammatory cytokine abundantly produced at the site of injury has been shown to stimulate Runx-2 expression in osteoblasts. TNF- $\alpha$  activates downstream signaling pathways, including the NF- $\kappa$ B pathway, which can directly interact with Runx-2 regulatory elements to enhance its transcriptional activity(**Gandhi *et al* ., 2021**).

Interleukin-1 (IL-1) is another potent inflammatory cytokine which increase in case of d-gal administration has been linked to the up regulation of Runx-2 expression. IL-1 promotes osteoblast differentiation and bone formation by modulating various signaling cascades including the MAPK pathway which can converge on Runx-2 to

promote its transcriptional activity(Alexander .,2006; Griffin *et al* ., 2006 ). The Wnt/ $\beta$ -catenin pathway which plays a fundamental role in bone development and repair. Wnt ligands released during the inflammatory response stabilize cytoplasmic  $\beta$ -catenin, allowing its translocation into the nucleus where it interacts with transcription factors such as T-cell factor/lymphoid enhancer factor (TCF/LEF) and Runx-2 to promote osteoblast differentiation and bone formation. Treadmill activity is considered a possible moderator, which uses a robust experimental design that incorporates D-Gal induction to mimic accelerated aging and osteoporosis (He *et al* .,2020). Understanding the molecular mechanisms of treadmill exercise's effects on osteoclast activity will shed light on bone homeostasis and provide new avenues for the research and development of treatments to prevent and treat osteoporosis and improve bone health(McDonald *et al* ., 2021).

**Chapter five**

**Conclusion**

**&**

**Recommendation**



## **5. Conclusions & Recommendations**

### **5.1 Conclusions:**

After 60 days of the animal receives 200 mg/kg BW D-gal with use of a treadmill at 25 m/min for 5 days weekly for sixty days conclusions are the following:

**1-** The X-Ray examination show a decrease in density and inflammation in the D-gal group while there is ameliorate the density to the control level in the D-gal plus treadmill group.

**2-**D-gal can effect on bone biomarker (increase in RANK , RANKL ,Cathepsin K) and decrease in serum OPG while treadmill show a significant decrease compared with D-gal group.

**3-**Revealed significant variations in parathyroid hormone, Calcitonin and Vitamin D levels, increased in the serum of calcium in the D-gal group compared to the control and treadmill group. In contrast, no a significant in the serum of sodium, potassium and phosphorus in the treadmill plus D-gal group compared to the control group.

**4-** Treadmill has emerged as an effective treatment option as a modulator of bone remodeling which uses a robust experimental design that incorporates D-gal induction to mimic accelerated aging and osteoporosis

**5-** Histological examination of the bone tissue in our study showed thinning trabeculae of numerous an large multinucleated osteoclast marked cavity in the D-gal group ,while the group that was under treadmill showed an increase in the number of osteoblast cells with fewer cavities in the bony plates and reduction in micro-fissure in femur compact bone by using scanning electron microscope..

**6-** Fold change comparison between the groups expressed group show an increase in the Runx2 gene expression in the D-gal group as compare with the treadmill and control group .

## **5.2 Recommendations :**

**1-**Study on effect of treadmill on the high cholestrol diet (HCD) .

**2-**Study the effect of treadmill on the cardiovascular system.

**3-**It is recommended to exercise for periods of no less than five hours per week in order to get rid of the negative effects of harmful substances in the body.

**4-** Investigate the dynamic regulation of osterix and Runx2 by RANK/RANKL signaling over the course of osteoporosis development.

**5-**Using another animal model in the experiment to study the physiological changes that occur in the body.

**6-**Measure glucocorticoids and thyroid hormone.

# **Chapter Six**

## **References**

**Abd El-Kader, S. M., Al-Jiffri, O. H., Ashmawy, E. M., & Gaowgzeh, R. A. M. (2016).** Treadmill walking exercise modulates bone mineral status and inflammatory cytokines in obese asthmatic patients with long term intake of corticosteroids. *African health sciences*, 16(3), 798-808.

**Abdallah, H. M., Farag, M. A., Algandaby, M. M., Nasrullah, M. Z., Abdel-Naim, A. B., Eid, B. G., ... & Malebari, A. M. (2020).** Osteoprotective activity and metabolite fingerprint via UPLC/MS and GC/MS of *Lepidium sativum* in ovariectomized Rats. *Nutrients*, 12(7), 2075

**Adamopoulos, I. E., & Bowman, E. P. (2008).** Immune regulation of bone loss by Th17 cells. *Arthritis research & therapy*, 10, 1-9.

**Agarwal, S. C., & Stout, S. D. (Eds.). (2003).** Bone loss and osteoporosis: an anthropological perspective. Kluwer Academic /Plenum Publishers

**Aibar-Almazán, A., Voltés-Martínez, A., Castellote-Caballero, Y., Afanador-Restrepo, D. F., Carcelén-Fraile, M. D. C., & López-Ruiz, E. (2022).** Current status of the diagnosis and management of osteoporosis. *International journal of molecular sciences*, 23(16), 9465

**Alexandre C; Vico L Pathophysiology of bone loss in disuse osteoporosis. Joint Bone Spine, (2011), 78(6), 572–576. 10.1016/j.jbspin.2011.04.007 PMID: 21664854**

**Al-Jarrah, M. D., & Erekat, N. S. (2018).** Treadmill exercise training could attenuate the upregulation of interleukin-1 beta and tumor necrosis factor alpha in the skeletal muscle of mouse model of chronic/progressive Parkinson disease. *NeuroRehabilitation*, 43(4), 501-507.

**Amabebe, E., Omorodion, S. I., Ozoene, J. O., Ugwu, A. C., & Obika, L. F. (2013).** Sweating and thirst perception in premenopausal, perimenopausal and postmenopausal women during moderate exercise. *Journal of Experimental & Integrative Medicine*, 3(4).

**Amarasekara, D. S., Kim, S., & Rho, J. (2021).** Regulation of osteoblast differentiation by cytokine networks. *International journal of molecular sciences*, 22(6), 2851.

- Aranda-Rivera, A. K., Cruz-Gregorio, A., Aparicio-Trejo, O. E., & Pedraza-Chaverri, J. (2021).** Mitochondrial redox signaling and oxidative stress in kidney diseases. *Biomolecules*, 11(8), 1144.
- Asagiri, M., Hirai, T., Kunigami, T., Kamano, S., Gober, H. J., Okamoto, K., ... & Takayanagi, H.(2008)**Cathepsin K-dependent toll-like receptor 9 signaling revealed in experimental arthritis. *Science*, 319(5863), 624-627. DOI: 10.1126/science.1150110
- Azman, K. F., & Zakaria, R. (2019).** D-gal -induced accelerated aging model: an overview. *Biogerontology*, 20(6), 763-782
- Azman, K. F., Safdar, A., & Zakaria, R. (2021).** D-gal -induced liver aging model: Its underlying mechanisms and potential therapeutic interventions. *Experimental gerontology*, 150, 111372.
- Atef, M. M., Emam, M. N., Abo El Gheit, R. E., Elbeltagi, E. M., Alshenawy, H. A., Radwan, D. A., ... & Abd-Ellatif, R. N. (2022).** Mechanistic insights into ameliorating effect of geraniol on D-galactose induced memory impairment in rats. *Neurochemical Research*, 47(6), 1664-1678.
- Baig, M., Tariq, S., & Tariq, S. (2015).** Homocysteine and leptin in the pathogenesis of osteoporosis—evidences, conflicts and expectations. *Advances in Osteoporosis*, 37
- Balkan, W., Martinez, A. F., Fernandez, I., Rodriguez, M. A., Pang, M., and Troen, B. R(2009).** Identification of NFAT binding sites that mediate stimulation of cathepsin K promoter activity by RANK ligand. *Gene* 2009; 446, 90–98. DOI: 10.1016/j.gene.2009.06.013
- Bellido, T., Plotkin, L. I., & Bruzzaniti, A. (2019).** Bone cells. In *Basic and applied bone biology* (pp. 37-55). Academic Press.
- Birch, H. L., Sinclair, C., Smith, R. K., & Goodship, A. E. (2013).** Skeletal physiology: responses to exercise and training. *Equine Sports Medicine and Surgery E-Book: Equine Sports Medicine and Surgery E-Book*, 145.
- Blair HC, Teitelbaum SL, Ghiselli R, Gluck S.(1989).** Osteoclastic bone resorption by a polarized vacuolar proton pump. *245(4920):855–7.*

- Bo-Htay, C., Palee, S., Apaijai, N., Chattipakorn, S. C., & Chattipakorn, N. (2018).** Effects of d-galactose-induced ageing on the heart and its potential interventions. *Journal of Cellular and Molecular Medicine*, 22(3), 1392-1410
- Bonnick, S.L. and Lewis, L.A. (2006).** *Bone Densitometry for Technologists*. Toronto, Canada: Humana Press. pp 8-9, 221- 44, 258-265, 289-312.
- Boon, L., Ugarte-Berzal, E., Vandooren, J., & Opdenakker, G. (2020).** Protease propeptide structures, mechanisms of activation, and functions. *Critical Reviews in Biochemistry and Molecular Biology*, 55(2), 111-165.
- Boyce, B.F. and Xing, L.(2008).** Functions of RANKL/ RANK/OPG in bone modeling and remodeling. *Archives of biochemistry and biophysics*, 473(2):139-146.
- Brenner O, Levanon D, Negreanu V, et al. 2004.** Loss of Runx3 function in leukocytes is associated with spontaneously developed colitis and gastric mucosal hyperplasia. *Proc Natl Acad Sci USA* 101: 16016–16021.
- Briot K, Roux C (2015)** Glucocorticoid-induced osteoporosis. *RMD Open* 1:e000014
- Brömme, D., & Wilson, S. (2011).** Role of cysteine cathepsins in extracellular proteolysis. In *Extracellular matrix degradation* (pp. 23-51). Berlin, Heidelberg: Springer Berlin Heidelberg.
- Bromme, D., and Okamoto, K. (1995).** Human cathepsin O2, a novel cysteine protease highly expressed in osteoclastomas and ovary molecular cloning, sequencing and tissue distribution. *Biol. Chem. Hoppe Seyler* 1995; 376, 379–384. DOI: 10.1515/bchm3.1995.376.6.379
- Brzóška, M. M., & Rogalska, J. (2013).** Protective effect of zinc supplementation against cadmium-induced oxidative stress and the RANK/RANKL/OPG system imbalance in the bone tissue of rats. *Toxicology and applied pharmacology*, 272(1), 208-220.
- Cardoso, A., Magano, S., Marrana, F. and Andrade, J. P. (2015).** Dgalactose high-dose administration failed to induce accelerated aging changes in neurogenesis, anxiety, and spatial memory on young male Wistar rats.

Rejuvenation research., 18(6): 497-507

**Carletti, A., Gavaia, P. J., Cancela, M. L., & Laizé, V. (2024).** Metabolic bone disorders and the promise of marine osteoactive compounds. *Cellular and Molecular Life Sciences*, 81(1), 11.

**Cohen Jr, M. M. (2009).** Perspectives on RUNX genes: an update. *American journal of medical genetics Part A*, 149(12), 2629-2646.

**Chandra, A., & Rajawat, J. (2021).** Skeletal aging and osteoporosis: mechanisms and therapeutics. *International journal of molecular sciences*, 22(7), 3553.

**Chiang, T. I., Chang, I. C., Lee, H. S., Lee, H., Huang, C. H., & Cheng, Y. W. (2011).** Osteopontin regulates anabolic effect in human menopausal osteoporosis with intermittent parathyroid hormone treatment. *Osteoporosis international*, 22, 577-585.

**Choi JY, Pratap J, Javed A, et al. 2001.** Subnuclear targeting of Runx/Cbfa/AML factors is essential for tissue-specific differentiation during embryonic development. *Proc Natl Acad Sci USA* 98: 8650–865.

**Costa, A. G., Cusano, N. E., Silva, B. C., Cremers, S., & Bilezikian, J. P. Cathepsin K(2011).**its skeletal actions and role as a therapeutic target in osteoporosis; *Nature Reviews Rheumatology*,; 7(8), 447-456.

**Crisafulli, A., Micari, A., Altavilla, D., Saporito, F., Sardella, A., Passaniti, M., ... & Squadrito, F. (2005).** Serum levels of osteoprotegerin and RANKL in patients with ST elevation acute myocardial infarction. *Clinical Science*, 109(4), 389-395.

**Dai, R., Wu, Z., Chu, H. Y., Lu, J., Lyu, A., Liu, J., & Zhang, G. (2020).** Cathepsin K: the action in and beyond bone. *Frontiers in cell and developmental biology*, 8, 433.

**De Kam, D., Smulders, E., Weerdesteyn, V., & Smits-Engelsman, B. C. M. (2009).** Exercise interventions to reduce fall-related fractures and their risk factors

**Deaton, D. N., & Tavares, F. X. (2005).**Design of cathepsin K inhibitors for osteoporosis. *Current Topics in Medicinal Chemistry*. 5[16]: 1639-1675

**Dharmarajan, T. S. (2021).** Physiology of aging. *Geriatric gastroenterology*, 101-153.

**Di Pietro, L., Barba, M., Palacios, D., Tiberio, F., Prampolini, C., Baranzini, M., ... & Lattanzi, W. (2021).** Shaping modern human skull through epigenetic, transcriptional and post-transcriptional regulation of the RUNX2 master bone gene. *Scientific Reports*, 11(1), 21316

**Docherty, S., Harley, R., McAuley, J. J., Crowe, L. A., Pedret, C., Kirwan, P. D., ... & Millar, N. L. (2022).** The effect of exercise on cytokines: implications for musculoskeletal health: a narrative review. *BMC Sports Science, Medicine and Rehabilitation*, 14(1), 1-14.

**Dong, Y., Wu, X., Han, L., Bian, J., He, C., El-Omar, E., ... & Wang, M. (2022).** The potential roles of dietary anthocyanins in inhibiting vascular endothelial cell senescence and preventing cardiovascular diseases. *Nutrients*, 14(14), 2836.

**Dowhan Hoag, L., & Dharmarajan, T. S. (2020).** Calcium and phosphorus. *Geriatric Gastroenterology*, 1-29

**Dougall, W. C., Glaccum, M., Charrier, K., Rohrbach, K., Brasel, K., De Smedt, T., ... & Schuh, J. (1999).** RANK is essential for osteoclast and lymph node development. *Genes & development*, 13(18), 2412-2424.

**Drake, F. H., Dodds, R. A., James, I. E., Connor, J. R., Debouck, C., Richardson, S., ... & Gowen, M. (1996).** Cathepsin K, but Not Cathepsins B, L, or S, is abundantly expressed in human osteoclasts (\*). *Journal of Biological Chemistry*, 271(21), 12511-12516.

**Duff, W. R., & Chilibeck, P. D. (2020).** Hormonal Regulation of the Positive and Negative Effects of Exercise on Bone. *Endocrinology of Physical Activity and Sport*, 229-247.

**El-Haroun, H., Soliman, M., & El-Gawad, A. (2020).** Comparative Study on the Possible Protective Effect of *Lepidium Sativum* versus Teriparatide in Induced Osteoporosis in Adult Male Guinea Pigs. *Egyptian Journal of Histology*, 43(3), 931-947

**El-Shishtawy, S.H., Mosbah, O., Sherif, N., Metwaly, A., Hanafy, A. and Kamel, L. (2016).** Association between serum visfatin and carotid atherosclerosis in diabetic and non-diabetic patients on maintenance



Hemodialysis. *Electronic physician.*, 8(2)

**Föger-Samwald, U., Dovjak, P., Azizi-Semrad, U., Kersch-Schindl, K., & Pietschmann, P. (2020).** Osteoporosis: Pathophysiology and therapeutic options. *EXCLI journal*, 19, 1017.

**Friedman, M. A., & Kohn, D. H. (2022).** Calcium and phosphorus supplemented diet increases bone volume after thirty days of high speed treadmill exercise in adult mice. *Scientific Reports*, 12(1), 14616.

**Frost, H.M. (2003).** Bone's mechanostat: A 2003 update. *Anat. Rec. Part A*, 275A, 1081-1101

**García-Trejo, S. S., Gómez-Sierra, T., Eugenio-Pérez, D., Medina-Campos, O. N., & Pedraza-Chaverri, J. (2024).** Protective Effect of Curcumin on D-gal -Induced Senescence and Oxidative Stress in LLC-PK1 and HK-2 Cells. *Antioxidants (Basel, Switzerland)*, 13(4), 415.

**Garnero, P., Borel, O., Byrjalsen, I., Ferreras, M., Drake, F. H., McQueney, M. S. (1989).** The collagenolytic activity of cathepsin K is unique among mammalian proteinases. *J. Biol. Chem* 273, 32347–32352.

**Geister, K. A. (2013).** The Genetic and Molecular Etiologies of Two Spontaneous Mouse Models of Skeletal Dysplasia and Infertility (Doctoral dissertation).

**Gong, L., Odilov, B., Han, F., Liu, F., Sun, Y., Zhang, N., ... & Ren, J. (2022).** Identification a novel de novo RUNX2 frameshift mutation associated with cleidocranial dysplasia. *Genes & Genomics*, 44(6), 683-690.

**González, L. A., Vásquez, G. M., & Molina, J. F. (2009).** Epidemiología de la osteoporosis. *Revista Colombiana de Reumatología*, 16(1), 61-75

**Grimaud, E., Soubigou, L., Couillaud, S., Coipeau, P., Moreau, A., Passuti, N., ... & Heymann, D. (2003).** Receptor activator of nuclear factor  $\kappa$ B ligand (RANKL)/osteoprotegerin (OPG) ratio is increased in severe osteolysis. *The American journal of pathology*, 163(5), 2021-2031.

- Gür, A., Denli, A., Çevik, R., Nas, K., Karakoç, M., & Saraç, A. J. (2003).** The effects of alendronate and calcitonin on cytokines in postmenopausal osteoporosis: a 6-month randomized and controlled study. *Yonsei Medical Journal*, 44(1), 99-109.
- Hardcastle, A. C., Aucott, L., Fraser, W. D., Reid, D. M., & Macdonald, H. M. (2011).** Dietary patterns, bone resorption and bone mineral density in early post-menopausal Scottish women. *European journal of clinical nutrition*, 65(3), 378-385
- Harkema, L., Youssef, S. A., & de Bruin, A. (2016).** Pathology of mouse models of accelerated aging. *Veterinary pathology*, 53(2), 366-389.
- He, Z., Chen, P., Li, X., Wang, Y., Yu, G., Chen, C., ... & Zheng, Z. (2020).** A spatiotemporal deep learning approach for unsupervised anomaly detection in cloud systems. *IEEE Transactions on Neural Networks and Learning Systems*, 34(4), 1705-1719.
- Hendrickx, G., Boudin, E., & Van Hul, W. (2015).** A look behind the scenes: the risk and pathogenesis of primary osteoporosis. *Nature Reviews Rheumatology*, 11(8), 462-474.
- Henneicke H, Gasparini S, Brennan-Speranza T, Zhou H and Seibel M. 2014.** Glucocorticoids and bone: local effects and systemic implications. *Trends in Endocr and Metab*, 25: 197–211.
- Hershey, C. L. (2005).** The role of the microphthalmia transcription factor in osteoclast differentiation and bone development. Harvard University.
- Hikita, A., Yana, I., Wakeyama, H., Nakamura, M., Kadono, Y., Oshima, Y., ... & Tanaka, S. (2006).** Negative regulation of osteoclastogenesis by ectodomain shedding of receptor activator of NF- $\kappa$ B ligand. *Journal of Biological Chemistry*, 281(48), 36846-36855.
- Hill, G. W., Gillum, T. L., Lee, B. J., Romano, P. A., Schall, Z. J., Hamilton, A. M., & Kuennen, M. R. (2020).** Prolonged treadmill running in normobaric hypoxia causes gastrointestinal barrier permeability and elevates circulating levels of pro-and anti-inflammatory cytokines. *Applied Physiology, Nutrition, and Metabolism*, 45(4), 376-386.
- Hofbauer, L. C., & Schoppet, M. (2004).** Clinical implications of the

osteoprotegerin/RANKL/RANK system for bone and vascular diseases. *Jama*, 292(4), 490-495.

**Holliday, L. S., Patel, S. S., & Rody Jr, W. J. (2021).** RANKL and RANK in extracellular vesicles: Surprising new players in bone remodeling. *Extracellular vesicles and circulating nucleic acids*, 2, 18.

**Hor, Y. Y., Ooi, C. H., Lew, L. C., Jaafar, M. H., Lau, A. Y., Lee, B. K., ... & Liong, M. T. (2021).** The molecular mechanisms of probiotic strains in improving ageing bone and muscle of d-galactose-induced ageing rats. *Journal of applied microbiology*, 130(4), 1307-1322.

**Horsburgh, S., Robson-Ansley, P., Adams, R., & Smith, C. (2015).** Exercise and inflammation-related epigenetic modifications: focus on DNA methylation. *Exercise immunology review*, 21.

**Huang, C. C., Chiang, W. D., Huang, W. C., Huang, C. Y., Hsu, M. C., & Lin, W. T. (2013).** Hepatoprotective Effects of Swimming Exercise against D-gal -Induced Senescence Rat Model. *Evidence-based complementary and alternative medicine : eCAM*, 2013, 275431.

**Ikeda, T., Kasai, M., Utsuyama, M., & Hirokawa, K. (2001).** Determination of three isoforms of the receptor activator of nuclear factor- $\kappa$ B ligand and their differential expression in bone and thymus. *Endocrinology*, 142(4), 1419-1426.

**Imam, M.U., Zhang, S., Ma, J., Wang, H. and Wang, F. (2017).** Antioxidants mediate both iron homeostasis and oxidative stress. *Nutrients*, 9(7): 671.

**Imerb, N., Thonusin, C., Pratchayasakul, W., Chanpaisaeng, K., Aeimlapa, R., Charoenphandhu, N., ... & Chattipakorn, S. C. (2023).** Hyperbaric oxygen therapy exerts anti-osteoporotic effects in obese and lean D-galactose-induced aged rats. *The FASEB Journal*, 37(11), e23262.

**Imerb, N., Thonusin, C., Pratchayasakul, W., Arunsak, B., Nawara, W., Ongnok, B., Aeimlapa, R., Charoenphandhu, N., Chattipakorn, N., & Chattipakorn, S. C. (2022).** D-gal -induced aging aggravates obesity-induced bone dyshomeostasis. *Scientific reports*, 12(1), 8580.

**Infante, M., Fabi, A., Cognetti, F., Gorini, S., Caprio, M., & Fabbri, A. (2019).** RANKL/RANK/OPG system beyond bone remodeling:

involvement in breast cancer and clinical perspectives. *Journal of Experimental & Clinical Cancer Research*, 38, 1-18.

**Iwamoto, J., Shimamura, C., Takeda, T., Abe, H., Ichimura, S., Sato, Y., & Toyama, Y. (2004).** Effects of treadmill exercise on bone mass, bone metabolism, and calciotropic hormones in young growing rats. *Journal of bone and mineral metabolism*, 22, 26-31.

**Jang, J., Park, H. J., Kim, S. W., Kim, H., Park, J. Y., Na, S. J., ... & Cho, D. W. (2017).** 3D printed complex tissue construct using stem cell-laden decellularized extracellular matrix bioinks for cardiac repair. *Biomaterials*, 112, 264-274.

**Jo, M. J., Lee, J. K., Kim, J. E., & Ko, G. J. (2023).** Molecular mechanisms associated with aging kidneys and future perspectives. *International Journal of Molecular Sciences*, 24(23), 16912.

**Johansson, H., Kanis, J.A., Oden, A., Johnell, O. and McCloskey, E.(2009).**BMD, clinical risk factors and their combination for hip fracture prevention. *Osteoporosis Int.*,20(10):1675-82.

**Kasem, M. A., Abdel-Aleem, A. M., Said, A. S., & Khedr, E. S. G. (2016).**Histological effect of bisphosphonate, vitamin D and olive oil on glucocorticoid induced osteoporosis (Gio) in Albino Rat. *The Egyptian Journal of Hospital Medicine*, 65(1), 699-708

Katsimbri P The biology of normal bone remodelling. *Eur. J. Cancer Care (Engl.)*, 2017, 26(6) 10.1111/ecc.12740 PMID: 28786518

**Kenkre, J. S., & Bassett, J. H. D. (2018).** The bone remodelling cycle. *Annals of clinical biochemistry*, 55(3), 308-327.

**Kenney, W. L., Wilmore, J. H., & Costill, D. L. (2021).** Physiology of sport and exercise. *Human kinetics*.

**Kim, H. Y., & Kim, Y. (2019).** Associations of obesity with osteoporosis and metabolic syndrome in Korean postmenopausal women: a cross-sectional study using national survey data. *Archives of Osteoporosis*, 14, 1-9.

**Kim, A. S., Girgis, C. M., & McDonald, M. M. (2022).** Osteoclast recycling

and the rebound phenomenon following denosumab discontinuation. *Current Osteoporosis Reports*, 20(6), 505-515.

**Komatsu, N., & Takayanagi, H. (2022).** Mechanisms of joint destruction in rheumatoid arthritis—immune cell–fibroblast–bone interactions. *Nature Reviews Rheumatology*, 18(7), 415-429

**Komori, T. (2013).** Functions of the osteocyte network in the regulation of bone mass. *Cell and tissue research*, 352, 191-198.

**Kwiatkowska, M., Norman, G., & Parker, D. (2006).** Quantitative analysis with the probabilistic model checker PRISM. *Electronic Notes in Theoretical Computer Science*, 153(2), 5-31.

**Lekamwasam, S., Adachi, J. D., Agnusdei, D., Bilezikian, J., Boonen, S., Borgström, F., ... & Compston, J. E. (2012).** A framework for the development of guidelines for the management of glucocorticoid-induced osteoporosis. *Osteoporosis International*, 23(9), 2257-2276.

**Levanon, D., Bettoun, D., Harris-Cerruti, C., Woolf, E., Negreanu, V., Eilam, R., ... & Groner, Y. (2002).** The Runx3 transcription factor regulates development and survival of TrkC dorsal root ganglia neurons. *The EMBO journal*.

**Letarouilly, J. G., Broux, O., & Clabaut, A. (2019).** New insights into the epigenetics of osteoporosis. *Genomics*, 111(4), 793-798

**Li, L., Chen, B., Zhu, R., Li, R., Tian, Y., Liu, C., ... & Gao, S. (2019).** *Fructus Ligustri Lucidi* preserves bone quality through the regulation of gut microbiota diversity, oxidative stress, TMAO and Sirt6 levels in aging mice. *Aging (Albany NY)*, 11(21), 9348.

**Li, Q. L., Ito, K., Sakakura, C., Fukamachi, H., Inoue, K. I., Chi, X. Z., ... & Ito, Y. (2002).** Causal relationship between the loss of RUNX3 expression and gastric cancer. *Cell*, 109(1), 113-124.

**Li, B., Wang, P., Jiao, J., Wei, H., Xu, W., & Zhou, P. (2022).** Roles of the RANKL–RANK Axis in Immunity—Implications for Pathogenesis and Treatment of Bone Metastasis. *Frontiers in immunology*, 13, 824117.

**Li, Q., Tian, C., Liu, X., Li, D., & Liu, H. (2023).** Anti-inflammatory and

antioxidant traditional Chinese Medicine in treatment and prevention of osteoporosis. *Frontiers in Pharmacology*, 14, 1203767.

**Lian, J. B., Balint, E., Javed, A., Drissi, H., Vitti, R., Quinlan, E. J., ... & Stein, G. S. (2003).** Runx1/AML1 hematopoietic transcription factor contributes to skeletal development in vivo. *Journal of cellular physiology*, 196(2), 301-311

**Lian, W., Jia, H., Xu, L., Zhou, W., Kang, D., Liu, A., & Du, G. (2017).** Multi-protection of DL0410 in ameliorating cognitive defects in Dgalactose induced aging mice. *Frontiers in aging neuroscience*, 9, 409.

**Lippuner, K., Golder, M., & Greiner, R. (2005).** Epidemiology and direct medical costs of osteoporotic fractures in men and women in Switzerland. *Osteoporosis International*, 16(2), S8-S17

**Liu, J., Gao, Z., & Liu, X. (2024).** Mitochondrial dysfunction and therapeutic perspectives in osteoporosis. *Frontiers in Endocrinology*, 15, 1325317.

**Liu, W., & Zhang, X. (2015).** Receptor activator of nuclear factor- $\kappa$ B ligand (RANKL)/RANK/osteoprotegerin system in bone and other tissues. *Molecular Medicine Reports*, 11(5), 3212-3218

**Liu, Y., Wang, Z., Xie, W., Gu, Z., Xu, Q., & Su, L. (2017).** Oxidative stress regulates mitogen activated protein kinases and c Jun activation involved in heat stress and lipopolysaccharide induced intestinal epithelial cell apoptosis. *Molecular medicine reports*, 16(3), 2579-2587.

**Lotinun, S., Kiviranta, R., Matsubara, T., Alzate, J. A., Neff, L., Lüth, A., ... & Baron, R. (2013).** Osteoclast-specific cathepsin K deletion stimulates S1P-dependent bone formation. *The Journal of clinical investigation*, 123(2).

**Luo, G., Li, F., Li, X., Wang, Z. G., & Zhang, B. (2018).** TNF  $\alpha$  and RANKL promote osteoclastogenesis by upregulating RANK via the NF  $\kappa$ B pathway. *Molecular medicine reports*, 17(5), 6605-6611.

**Lynch, C. C., Hikosaka, A., Acuff, H. B., Martin, M. D., Kawai, N., Singh, R. K., ... & Futakuchi, M. (2005).** MMP-7 promotes prostate cancer-induced osteolysis via the solubilization of RANKL. *Cancer cell*, 7(5), 485-

- MacKelvie, K.J., McKay, H.A., Petit, M.A., Moran, O. and Khan, K.M. (2002).** Bone mineral response to a 7-month randomized controlled, school-based jumping intervention in 121 prepubertal boys: Associations with ethnicity and body mass index. *J. Bone Miner. Res.*, 17: 834-844.
- Mahmoud, M. A. A., Saleh, D. O., Safar, M. M., Agha, A. M., & Khattab, M. M. (2021).** Chloroquine ameliorates bone loss induced by D-gal in male rats via inhibition of ERK associated osteoclastogenesis and antioxidant effect. *Toxicology Reports*, 8, 366-375.
- Malik, D., Narayanasamy, N., Pratyusha, V. A., Thakur, J., & Sinha, N. (2023).** Fat-Soluble Vitamins. In *Textbook of Nutritional Biochemistry* (pp. 229-290). Singapore: Springer Nature Singapore.
- Marques, E.A., Wanderley, F., Machado, L., Sousa, F., Viana, J.L., Moreira-Gonçalves, D., Moreira, P., Mota, J. and Carvalho, J. (2011).** Effects of resistance and aerobic exercise on physical function, bone mineral density, OPG and RANKL in older women. *Experimental gerontology*, 46(7): 524-532.
- Martin, T. J., & Sims, N. A. (2005).** Osteoclast-derived activity in the coupling of bone formation to resorption. *Trends in molecular medicine*, 11(2), 76-81.
- Massicotte, F., Aubry, I., Martel-Pelletier, J., Pelletier, J. P., Fernandes, J., & Lajeunesse, D. (2006).** Abnormal insulin-like growth factor 1 signaling in human osteoarthritic subchondral bone osteoblasts. *Arthritis research & therapy*, 8, 1-12.
- McDonald, M. M., Kim, A. S., Mulholland, B. S., & Rauner, M. (2021).** New insights into osteoclast biology. *Journal of Bone and Mineral Research Plus*, 5(9), e10539.
- McHugh, K. P., Hodivala-Dilke, K., Zheng, M. H., Namba, N., Lam, J., Novack, D., ... & Teitelbaum, S. L. (2000).** Mice lacking  $\beta 3$  integrins are osteosclerotic because of dysfunctional osteoclasts. *The Journal of clinical investigation*, 105(4), 433-440.

**Mehler, P. S. and Weiner, K. (2003).**The Risk of Osteoporosis in Anorexia Nervosa. Reprinted from Eating Disorders Recovery Today, 1:5.

**Mhd Omar, N. A., Dicksved, J., Kruger, J., Zamaratskaia, G., Michaëlsson, K., Wolk, A., ... & Landberg, R. (2022).** Effect of a diet rich in galactose or fructose, with or without fructooligosaccharides, on gut microbiota composition in rats. *Frontiers in Nutrition*, 9, 922336.

**Miyamoto T, Weissman IL, Akashi K. (2000).** AML1/ETO-expressing nonleukemic stem cells in acute myelogenous leukemia with 8;21 chromosomal translocation. *Proc Natl Acad Sci USA* 97: 7521–7526.

**Miyoshi, H., Shimizu, K., Kozu, T., Maseki, N., Kaneko, Y., & Ohki, M. (1991).** t (8; 21) breakpoints on chromosome 21 in acute myeloid leukemia are clustered within a limited region of a single gene, AML1. *Proceedings of the National Academy of Sciences*, 88(23), 10431-10434..

**Mohamad, N. V., Soelaiman, I. N., & Chin, K. Y. (2016).** A concise review of testosterone and bone health. *Clinical interventions in aging*, 1317-1324.

**Moser, S. C., & van der Eerden, B. C. (2019).** Osteocalcin—A versatile bone-derived hormone. *Frontiers in endocrinology*, 9, 424282.

**Muhammad, R., Mughal, A. W., Khan, W., Shah, A., Roman, S., & Shah, I. (2022).** Analysis of Serum Electrolyte Concentration by Exercising on Treadmill Ergometer at different MET Levels. *Webology*, 19(2).

**Narayanan, A., Srinaath, N., Rohini, M., & Selvamurugan, N. (2019).** Regulation of Runx2 by MicroRNAs in osteoblast differentiation. *Life sciences*, 232, 116676.

**Nordstrom, A., Olsson, T. and Nordstrom, P. (2005).**Bone gained from physical activity and lost through detraining: a longitudinal study in young males. *Osteoporos Int.*,16(7):835-41.

**Nordstrom, A., Olsson, T. and Nordstrom, P. (2006).**Sustained benefits from previous physical activity on bone mineral density in males. *J Clin Endocrinol Metab.*,91(7):2600-4.

**Okada, H., Watanabe, T., Niki, M., Takano, H., Chiba, N., Yanai, N., ... &**



- Satake, M. (1998).** AML1 (-/-) embryos do not express certain hematopoiesis-related gene transcripts including those of the PU. 1 gene. *Oncogene*, 17(18), 2287-2293.
- Ono, T., & Nakashima, T. (2018).** Recent advances in osteoclast biology. *Histochemistry and cell biology*, 149, 325-341.
- ossini, M., Adami, S., Bertoldo, F., Diacinti, D., Gatti, D., Giannini, S., ... & Isaia, G. C. Ott, S. M. (2018).** Cortical or trabecular bone: what's the difference. *American journal of nephrology*, 47(6), 373-376
- Otto F, Kanegane H, Mundlos S. (2002).** Mutations in the RUNX2 gene in patients with cleidocranial dysplasia. *Hum Mutat* 19: 209–216
- Overdorf, J., Pachuki-Hyde, L., & Kressenich, C. (2001).** Osteoporosis: There's so much. *RN*, 64(12), 30-35.
- Parameshwaran, K., Irwin, M. H., Steliou, K., & Pinkert, C. A. (2010).** D-gal effectiveness in modeling aging and therapeutic antioxidant treatment in mice. *Rejuvenation research*, 13(6), 729-735
- Park, J.H. and Choi, T.S. (2016).** Splenocyte proliferation and anaphylaxis induced by BSA challenge in a D-gal -induced aging mouse model. *Central-European journal of immunology.*, 41(3): 324–327.
- Partadiredja, G., Karima, N., Utami, K. P., Agustiningsih, D., & Sofro, Z. M. (2019).** The effects of light and moderate intensity exercise on the femoral bone and cerebellum of D-gal -exposed rats. *Rejuvenation research*, 22(1), 20-30.
- Permpoonputtana, K., Tangweerasing, P., Mukda, S., Boontem, P., Nopparat, C., & Govitrapong, P. (2018).** Long-term administration of melatonin attenuates neuroinflammation in the aged mouse brain. *EXCLI journal*, 17, 634.
- Pranoto, A., Rejeki, P. S., Miftahussurur, M., Setiawan, H. K., Yosika, G. F., Munir, M., ... & Yamaoka, Y. (2023).** Single 30 min treadmill exercise session suppresses the production of pro-inflammatory cytokines and oxidative stress in obese female adolescents. *Journal of basic and clinical physiology and pharmacology*, 34(2), 235-242.

- Pettit, A. R., Chang, M. K., Hume, D. A., & Raggatt, L. J. (2008).** Osteal macrophages: a new twist on coupling during bone dynamics. *Bone*, 43(6), 976-982.
- Piñar-Gutierrez, A., García-Fontana, C., García-Fontana, B., & Muñoz-Torres, M. (2022).** Obesity and bone health: a complex relationship. *International journal of molecular sciences*, 23(15), 8303
- Poehlman, E. T., Melby, C. L., & Goran, M. I. (1991).** The impact of exercise and diet restriction on daily energy expenditure. *Sports medicine*, 11, 78-101.
- Poirier-Solomon, L. (2001).** Preventing Osteoporosis: Bone Up On Health. *Diabetes Forecast*, 54(4), 33-35.
- Qian, J., Wang, X., Cao, J., Zhang, W., Lu, C., & Chen, X. (2021).** Dihydromyricetin attenuates D-galactose-induced brain aging of mice via inhibiting oxidative stress and neuroinflammation. *Neuroscience Letters*, 756, 135963
- Qi, Z., Liu, W., & Lu, J. (2016).** The mechanisms underlying the beneficial effects of exercise on bone remodeling: roles of bone-derived cytokines and microRNAs. *Progress in Biophysics and Molecular biology*, 122(2), 131-139.
- Qin, Y. X., & Hu, M. (2020).** In Vivo Models of Muscle Stimulation and Mechanical Loading in Bone Mechanobiology. In *Mechanobiology* (pp. 117-136). Elsevier.
- Qu, L. E., Ding, J., Chen, C., Wu, Z. J., Liu, B., Gao, Y., ... & Wang, L. H. (2016).** Exosome-transmitted lncARSR promotes sunitinib resistance in renal cancer by acting as a competing endogenous RNA. *Cancer cell*, 29(5), 653-668.
- Raggatt, L. J., & Partridge, N. C. (2010).** Cellular and molecular mechanisms of bone remodeling. *Journal of biological chemistry*, 285(33), 25103-25108.
- Raisz, L.G. (2005).** Pathogenesis of osteoporosis: concepts, conflicts, and prospects. *J Clin Invest*, 115: 3318-3325.
- Rehman, S. U., Shah, S.A., Ali, T., Chung, J.I. And Kim, M.O. (2016).** Anthocyanins Reversed D-gal -Induced Oxidative Stress and

Neuroinflammation Mediated Cognitive Impairment in Adult Rats.  
*Molecular neurobiology*, 54(1): 255–271

**Renema, N., Navet, B., Heymann, M. F., Lezot, F., & Heymann, D. (2016).** RANK–RANKL signalling in cancer. *Bioscience reports*, 36(4), e00366.

**Rikkonen, T., Sund, R., Sirola, J., Honkanen, R., Poole, K. E. S., & Kröger, H. (2021).** Obesity is associated with early hip fracture risk in postmenopausal women: a 25-year follow-up. *Osteoporosis International*, 32, 769-777.

**Ringle, K. A. (2009).** An investigation of bone mineral density and bone mineral content among hispanic women by lifestyle factors (Doctoral dissertation, The Ohio State University).

**Rodan, S. B., & Duong, L. T. (2008).** Cathepsin K-A new molecular target for osteoporosis. *IBMS BoneKEy*, 5, 16.

**Rosengren, B. (2010).** Hip fracture incidence and prevalence of osteoporosis in Sweden in recent decades. Lund University

**Rossini, M., Adami, S., Bertoldo, F., Diacinti, D., Gatti, D., Giannini, S., ... & Isaia, G. C. (2016).** Linee guida per la diagnosi, la prevenzione ed il trattamento dell'osteoporosi. *Reumatismo*, 68(1), 1-42.

**Runchel, C., Matsuzawa, A., & Ichijo, H. (2011).** Mitogen-activated protein kinases in mammalian oxidative stress responses. *Antioxidants & redox signaling*, 15(1), 205-218.

**Sadat-Ali, M., Al Elq, A. H., Al-Turki, H. A., Al-Mulhim, F. A., & Al-Ali, A. K. (2011).** Influence of vitamin D levels on bone mineral density and osteoporosis. *Annals of Saudi medicine*, 31(6), 602-608

**Saha, J. K., Xia, J., Grondin, J. M., Engle, S. K., & Jakubowski, J. A. (2005).** Acute hyperglycemia induced by ketamine/xylazine anesthesia in rats: mechanisms and implications for preclinical models. *Experimental Biology and Medicine*, 230(10), 777-784.

**Santos, L., Elliott-Sale, K. J., & Sale, C. (2017).** Exercise and bone health across the lifespan. *Biogerontology*, 18, 931-946.

- Schroeder, T. M., Jensen, E. D., & Westendorf, J. J. (2005).** Runx2: a master organizer of gene transcription in developing and maturing osteoblasts. *Birth Defects Research Part C: Embryo Today: Reviews*, 75(3), 213-225.
- Shah, F. A., Ruscsák, K., & Palmquist, A. (2019).** 50 years of scanning electron microscopy of bone—a comprehensive overview of the important discoveries made and insights gained into bone material properties in health, disease, and taphonomy. *Bone research*, 7(1), 15.
- Sharma, A., Sharma, L., & Goyal, R. (2021).** Molecular signaling pathways and essential metabolic elements in bone remodeling: An implication of therapeutic targets for bone diseases. *Current Drug Targets*, 22(1), 77-104.
- Shahroudi, M. J., Mehri, S., & Hosseinzadeh, H. (2017).** Anti-aging effect of *Nigella sativa* fixed oil on D-galactose-induced aging in mice. *Journal of pharmacopuncture*, 20(1), 29.
- Shwe, T., Bo-Htay, C., Leech, T., Ongnok, B., Jaiwongkum, T., Kerdphoo, S., ... & Chattipakorn, S. C. (2020).** D-gal -induced aging does not cause further deterioration in brain pathologies and cognitive decline in the obese condition. *Experimental Gerontology*, 138, 111001.
- Smith, J. K., Dykes, R., & Chi, D. S. (2016).** The effect of long-term exercise on the production of osteoclastogenic and antiosteoclastogenic cytokines by peripheral blood mononuclear cells and on serum markers of bone metabolism. *Journal of Osteoporosis*
- Song, Q., Liu, J., Dong, L., Wang, X., & Zhang, X. (2021).** Novel advances in inhibiting advanced glycation end product formation using natural compounds. *Biomedicine & Pharmacotherapy*, 140, 111750.
- Su, W., Lv, C., Huang, L., Zheng, X., & Yang, S. (2022).** Glucosamine delays the progression of osteoporosis in senile mice by promoting osteoblast autophagy. *Nutrition & Metabolism*, 19(1), 75.
- Sun, S., Karsdal, M. A., Bay-Jensen, A. C., Sørensen, M. G., Zheng, Q., Dziegiel, M. H., ... & Henriksen, K. (2013).** The development and characterization of an ELISA specifically detecting the active form of cathepsin K. *Clinical biochemistry*, 46(15), 1601-1606.

- Sun, Y., Li, J., Xie, X., Gu, F., Sui, Z., Zhang, K., & Yu, T. (2021).** Macrophage-osteoclast associations: origin, polarization, and subgroups. *Frontiers in Immunology*, 12, 778078.
- Suvarna, K. S., Layton, C., & Bancroft, J. D. (2018).** Bancroft's theory and practice of histological techniques E-Book. Elsevier health sciences.
- Suzuki, M., Takahashi, N., Sobue, Y., Ohashi, Y., Kishimoto, K., Hattori, K., ... & Kojima, T. (2020).** Hyaluronan suppresses enhanced cathepsin K expression via activation of NF- $\kappa$ B with mechanical stress loading in a human chondrocytic HCS-2/8 cells. *Scientific Reports*, 10(1), 216.
- Svelander, L., Erlandsson-Harris, H., Astner, L., Grabowska, U., Klareskog, L., Lindstrom, E., & Hewitt, E. (2009).** Inhibition of cathepsin K reduces bone erosion, cartilage degradation and inflammation evoked by collagen-induced arthritis in mice. *European journal of pharmacology*, 613(1-3), 155-162.
- Szalay, F., Hegedus, D., Lakatos, P. L., Tornai, I., Bajnok, E., Dunkel, K., & Lakatos, P. (2003).** High serum osteoprotegerin and low RANKL in primary biliary cirrhosis. *Journal of hepatology*, 38(4), 395-400.
- Takahashi, N., Udagawa, N., Akatsu, T., Tanaka, H., Shionome, M., & Dr. Suda, T. (1991).** Role of colony-stimulating factors in osteoclast development. *Journal of Bone and Mineral Research*, 6(9), 977-985..
- Takito, J., Inoue, S., & Nakamura, M. (2018).** The sealing zone in osteoclasts: a self-organized structure on the bone. *International journal of molecular sciences*, 19(4), 984.
- Tan, B. L., Norhaizan, M. E., Liew, W. P. P., & Sulaiman Rahman, H. (2018).** Antioxidant and oxidative stress: a mutual interplay in age-related diseases. *Frontiers in pharmacology*, 9, 402374.
- Tang, Y., Wu, X., Lei, W., Pang, L., Wan, C., Shi, Z., ... & Cao, X. (2009).** TGF- $\beta$ 1-induced migration of bone mesenchymal stem cells couples bone resorption with formation. *Nature medicine*, 15(7), 757-765.
- Tang, X., Ma, S., Li, Y., Sun, Y., Zhang, K., Zhou, Q., & Yu, R. (2020).** Evaluating the activity of sodium butyrate to prevent osteoporosis in rats by

promoting osteal GSK-3 $\beta$ /Nrf2 signaling and mitochondrial function. *Journal of agricultural and food chemistry*, 68(24), 6588-6603.

- Tardito, S., Martinelli, G., Soldano, S., Paolino, S., Pacini, G., Patane, M., ... & Cutolo, M. (2019).** Macrophage M1/M2 polarization and rheumatoid arthritis: a systematic review. *Autoimmunity reviews*, 18(11), 102397.
- Teitelbaum, S. L. (2000).** Bone resorption by osteoclasts. *Science*, 289(5484), 1504-1508.
- Thakur, S., Sarkar, B., Cholia, R. P., Gautam, N., Dhiman, M., & Mantha, A. K. (2014).** APE1/Ref-1 as an emerging therapeutic target for various human diseases: phytochemical modulation of its functions. *Experimental & molecular medicine*, 46(7), e106-e106.
- Thieschafer, A. J. (2010).** Bone volumetric density, geometry and strength in young adults (Doctoral dissertation, University of Minnesota).
- Tian, Z., Shen, C., Chen, H., & He, T. (2019).** Fcos: Fully convolutional one-stage object detection. In *Proceedings of the IEEE/CVF international conference on computer vision* (pp. 9627-9636).
- Tong, X., Chen, X., Zhang, S., Huang, M., Shen, X., Xu, J., & Zou, J. (2019).** The Effect of Exercise on the Prevention of Osteoporosis and Bone Angiogenesis. *BioMed research international*, 2019, 8171897.
- Tornatore, L., Thotakura, A. K., Bennett, J., Moretti, M., & Franzoso, G. (2012).** The nuclear factor kappa B signaling pathway: integrating metabolism with inflammation. *Trends in cell biology*, 22(11), 557-566.
- Troen, B. R. (2006).** The regulation of cathepsin K gene expression. *Annals of the New York Academy of Sciences*, 1068(1), 165-172.
- Turk, V., Turk, B., & Turk, D. (2001).** Lysosomal cysteine proteases: facts and opportunities. *The EMBO journal*.
- Umbayev, B., Askarova, S., Almabayeva, A., Saliev, T., Masoud, A. R., & Bulanin, D. (2020).** Galactose-induced skin aging: the role of oxidative stress. *Oxidative Medicine and Cellular Longevity*, 2020.

- Utami, S. L., Ishartadiati, K., Hidayat, M., Enggar, L., & Fitri, D. L. (2019).** Osteoporosis and Risk Factors among Postmenopausal Women in Integrated Health Post for Elderly.
- Ullah, F., Ali, T., Ullah, N., & Kim, M. O. (2015).** Caffeine prevents d-galactose-induced cognitive deficits, oxidative stress, neuroinflammation and neurodegeneration in the adult rat brain. *Neurochemistry international*, 90, 114-124.
- Wada, T., Nakashima, T., Hiroshi, N., & Penninger, J. M. (2006).** RANKL–RANK signaling in osteoclastogenesis and bone disease. *Trends in molecular medicine*, 12(1), 17-25.
- Walter, J. H., & Fridovich-Keil, J. L. (2014).** Galactosemia. Online metabolic and molecular basis of inherited disease (OMMBID). McGraw-Hill, New York
- Wang, D., Bu, T., Li, Y., He, Y., Yang, F., & Zou, L. (2022).** Pharmacological activity, pharmacokinetics, and clinical research progress of puerarin. *Antioxidants*, 11(11), 2121.
- Wang, S., Feng, W., Liu, J., Wang, X., Zhong, L., Lv, C., ... & Mao, Y. (2022).** Alginate oligosaccharide alleviates senile osteoporosis via the RANKL–RANK pathway in D-galactose-induced C57BL/6J mice. *Chemical Biology & Drug Design*, 99(1), 46-55.
- Wang, Y. F., Chang, Y. Y., Zhang, X. M., Gao, M. T., Zhang, Q. L., Li, X., ... & Yao, W. F. (2022).** Salidroside protects against osteoporosis in ovariectomized rats by inhibiting oxidative stress and promoting osteogenesis via Nrf2 activation. *Phytomedicine*, 99, 154020.
- Warden, S. J., Davis, I. S., & Fredericson, M. (2014).** Management and prevention of bone stress injuries in long-distance runners. *Journal of Orthopaedic & Sports Physical Therapy*, 44(10), 749-765.
- Watanabe, S., Hayakawa, T., Wakasugi, K., & Yamanaka, K. (2014).** Cystatin C protects neuronal cells against mutant copper-zinc superoxide dismutase-mediated toxicity. *Cell death & disease*, 5(10), e1497-e1497.
- Wawrzyniak, A., & Balawender, K. (2022).** Structural and metabolic changes in bone. *Animals*, 12(15), 1946.

- Weeks, B.K. and Beck, B.R. (2008).**The BPAQ: A bone-specific physical activity assessment instrument. *Osteoporos. Int.*, 19:1567-1577.
- Weitzmann, M. N. (2013).** The role of inflammatory cytokines, the RANKL/OPG axis, and the immunoskeletal interface in physiological bone turnover and osteoporosis. *Scientifica*, 2013.
- Wildman, B. J., Godfrey, T. C., Rehan, M., Chen, Y., Afreen, L. H., & Hassan, Q. (2019).** MICROmanagement of Runx2 function in skeletal cells. *Current molecular biology reports*, 5, 55-64.
- Winter, A. N., & Bickford, P. C. (2019).** Anthocyanins and their metabolites as therapeutic agents for neurodegenerative disease. *Antioxidants*, 8(9), 333.
- Wong, S. Y. W., Gadomski, T., Van Scherpenzeel, M., Honzik, T., Hansikova, H., Holmefjord, K. S. B., ... & Morava, E. (2017).** Oral D-gal supplementation in PGM1-CDG. *Genetics in Medicine*, 19(11), 1226-1235
- Woo, J. E., Seong, H. J., Lee, S. Y., & Jang, Y. S. (2019).** Metabolic engineering of *Escherichia coli* for the production of hyaluronic acid from glucose and galactose. *Frontiers in bioengineering and biotechnology*, 7, 351
- Wu, L., Ling, Z., Feng, X., Mao, C., & Xu, Z. (2017).** Herb medicines against osteoporosis: active compounds & relevant biological mechanisms. *Current topics in medicinal chemistry*, 17(15), 1670-1691
- Wu, S., Mickley, L. J., Jacob, D. J., Rind, D., & Streets, D. G. (2008).** Effects of 2000–2050 changes in climate and emissions on global tropospheric ozone and the policy-relevant back-ground surface ozone in the United States. *Journal of Geophysical Research: Atmospheres*, 113(D18).
- Wu, Y., Hu, Y., Zhao, Z., Xu, L., Chen, Y., Liu, T., & Li, Q. (2021).** Protective effects of water extract of *Fructus Ligustri Lucidi* against oxidative stress-related osteoporosis in vivo and in vitro. *Veterinary Sciences*, 8(9), 198.
- Wickens, A. P. (2001).** Ageing and the free radical theory. *Respiration physiology*, 128(3), 379-391.
- Xiao, W., Wang, Y., Pacios, S., Li, S., & Graves, D. T. (2016).** Cellular and



molecular aspects of bone remodeling. *Tooth movement*, 18, 9-16.

**Xie, Z., Zhao, M., Yan, C., Kong, W., Lan, F., Narengaowa, ... & Ni, J. (2023).** Cathepsin B in programmed cell death machinery: mechanisms of execution and regulatory pathways. *Cell Death & Disease*, 14(4), 255.

**Xiong, S., Yang, X., Yan, X., Hua, F., Zhu, M., Guo, L., ... & Bian, J. S. (2018).** Immunization with Na<sup>+</sup>/K<sup>+</sup> ATPase DR peptide prevents bone loss in an ovariectomized rat osteoporosis model. *Biochemical Pharmacology*, 156, 281-290.

**Xu, F., Li, W., Yang, X., Na, L., Chen, L., & Liu, G. (2021).** The roles of epigenetics regulation in bone metabolism and osteoporosis. *Frontiers in cell and developmental biology*, 8, 619301.

**Xu, P., Lin, B., Deng, X., Huang, K., Zhang, Y., & Wang, N. (2022).** VDR activation attenuates osteoblastic ferroptosis and senescence by stimulating the Nrf2/GPX4 pathway in age-related osteoporosis. *Free Radical Biology and Medicine*, 193, 720-735.

**Xu, W., Liu, X., He, X., Jiang, Y., Zhang, J., Zhang, Q., ... & Xin, H. (2020).** Bajitianwan attenuates D-gal -induced memory impairment and bone loss through suppression of oxidative stress in aging rat model. *Journal of Ethnopharmacology*, 261, 112992.

**Yahata, T., & Hamaoka, K. (2017).** Oxidative stress and Kawasaki disease: how is oxidative stress involved from the acute stage to the chronic stage?. *Rheumatology*, 56(1), 6-13

**Yamada, H., Mori, H., Nakanishi, Y., Nishikawa, S., Hashimoto, Y., Ochi, Y., ... & Kawabata, K. (2019).** Effects of the cathepsin K inhibitor ONO-5334 and concomitant use of ONO-5334 with methotrexate on collagen-induced arthritis in cynomolgus monkeys. *International journal of rheumatology*, 2019.

**Yamashita, T., Hagino, H., Hayashi, I., Hayashibara, M., Tanida, A., Nagira, K., ... & Nagashima, H. (2018).** Effect of a cathepsin K inhibitor on arthritis and bone mineral density in ovariectomized rats with collagen-induced arthritis. *Bone Reports*, 9, 1-10.

- Yanar, K., Simsek, B., Atukeren, P., Aydin, S., & Cakatay, U. (2019).** Is Dgalactose a useful agent for accelerated aging model of gastrocnemius and soleus muscle of sprague-dawley rats?. *Rejuvenation research*, 22(6), 521-528
- Yang DK, Shin EK, Oh YI, Lee KW, Lee CS, Kim SY, Lee JA, Song JY. Comparison of four diagnostic methods for detecting rabies viruses circulating in Korea. *Journal of Veterinary Science*. 2012;13(1):43-8
- Yavropoulou, M. P., & Yovos, J. G. (2016).** The molecular basis of bone mechanotransduction. *Journal of musculoskeletal & neuronal interactions*, 16(3), 221.
- Yi, L., Li, Z., Jiang, H., Cao, Z., Liu, J., & Zhang, X. (2018).** Gene modification of transforming growth factor  $\beta$  (TGF- $\beta$ ) and interleukin 10 (IL-10) in suppressing Mt Sonicate induced osteoclast formation and bone absorption. *Medical Science Monitor: International Medical Journal of Experimental and Clinical Research*, 24, 5200.
- Yoshida, C. A., Yamamoto, H., Fujita, T., Furuichi, T., Ito, K., Inoue, K. I., ... & Komori, T. (2004).** Runx2 and Runx3 are essential for chondrocyte maturation, and Runx2 regulates limb growth through induction of Indian hedgehog. *Genes & development*, 18(8), 952-963.
- Yu, Y., Wu, J., Li, J., Liu, Y., Zheng, X., Du, M., ... & Liu, Y. (2020).** Cycloastragenol prevents age-related bone loss: Evidence in D-gal -treated and aged rats. *Biomedicine & Pharmacotherapy*, 128, 110304.
- Yuen, C. H. Y., Feliz, D. C., Crisostomo, A. M. A., & Patrella, A. C. (2018).** Treadmill User Centering.
- Zaitoun, M., Ghanem, M., & Harphoush, S. (2018).** Sugars: types and their functional properties in food and human health. *International Journal of Public Health Research*, 6(4), 93.
- Zamyatnin Jr, A. A., Gregory, L. C., Townsend, P. A., & Soond, S. M. (2022).** Beyond basic research: the contribution of cathepsin B to cancer development, diagnosis and therapy. *Expert opinion on therapeutic targets*, 26(11), 963-977

**Zhang, Y. W., Yasui, N., Ito, K., Huang, G., Fujii, M., Hanai, J. I., ... & Ito, Y. (2000).** A RUNX2/PEBP2  $\alpha$ A/CBFA1 mutation displaying impaired transactivation and Smad interaction in cleidocranial dysplasia. *Proceedings of the National Academy of Sciences*, 97(19), 10549-10554.

**Zhang, B., Lian, W., Zhao, J., Wang, Z., Liu, A., & Du, G. (2021).** DL0410 alleviates memory impairment in D-gal -induced aging rats by suppressing neuroinflammation via the TLR4/MyD88/NF- $\kappa$ B pathway. *Oxidative Medicine and Cellular Longevity*, 2021, 1-31.

**Zhang, S., Li, T., Feng, Y., Zhang, K., Zou, J., Weng, X., ... & Zhang, L. (2023).** Exercise improves subchondral bone microenvironment through regulating bone-cartilage crosstalk. *Frontiers in Endocrinology*, 14, 1159393.

**Zhao, H. (2012).** Membrane trafficking in osteoblasts and osteoclasts: new avenues for understanding and treating skeletal diseases. *Traffic*, 13(10), 1307-1314.

**Zhao, B., & Ivashkiv, L. B. (2011).** Negative regulation of osteoclastogenesis and bone resorption by cytokines and transcriptional repressors.

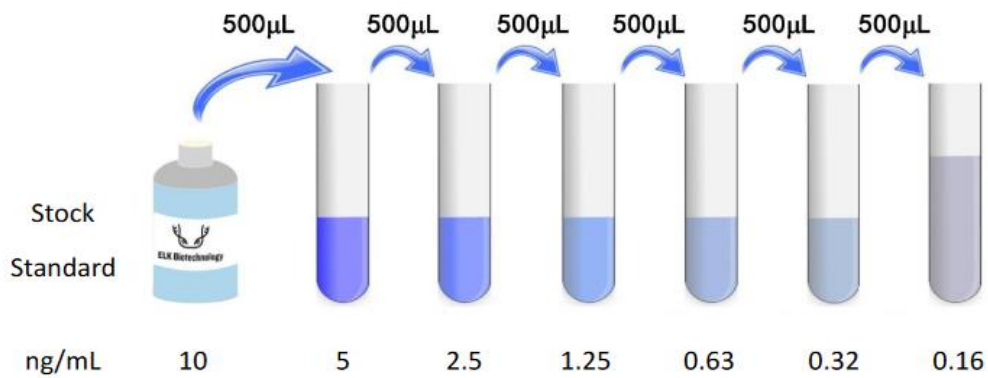
# Appendix

# Appendix I

## Detection of serum RANK

### Reagent Preparation:

1. Bring all kit components and samples to room temperature (18-25°C) before use. Make sure all components are dissolved and mixed well before using the kit.
2. If the kit will not be used up in 1 time, please only take out strips and reagents for present experiment, and save the remaining strips and reagents as specified.
3. Dilute the 25× Wash Buffer into 1× Wash Buffer with double-distilled Water.
4. Standard Working Solution - Centrifuge the Standard at  $1000 \times g$  for 1 minute. Reconstitute the Standard with 1.0 mL of Standard Diluent Buffer, kept for 10 minutes at room temperature, shake gently (not to foam). The concentration of the Standard in the stock solution is 10 ng/mL. Please prepare 7 tubes containing 0.5 mL Standard Diluent Buffer and use the Diluted Standard to produce a double dilution series according to the picture shown below. To mix each tube thoroughly before the next transfer, pipette the solution up and down several times. Set up 7 points of Diluted Standard such as 10 ng/mL, 5 ng/mL, 2.5 ng/mL, 1.25 ng/mL, 0.63 ng/mL, 0.32 ng/mL, 0.16 ng/mL, and the last EP tubes with Standard Diluent is the Blank as 0 ng/mL. In order to guarantee the experimental results validity, please use the new Standard Solution for each experiment. When diluting the Standard from high concentration to low concentration, replace the pipette tip for each dilution. Note: the last tube is regarded as a Blank and do not pipette solution into it from the former tube.



4. Biotinylated Antibody and 1× Streptavidin-HRP - Briefly spin centrifuge the stock Biotinylated Antibody and Streptavidin-HRP before use. Dilute them to working concentration 100-fold with Biotinylated Antibody Diluent and HRP Diluent, respectively.

### **Samples Preparation**

1. Equilibrate all materials and prepared reagents to room temperature prior to use. Prior to use, mix all reagents thoroughly taking care not to create any foam within the vials.
2. The user should calculate the possible amount of the samples used in the whole test. Please reserve sufficient samples in advance.
3. Please predict the concentration before assaying. If values for these are not within the range of the Standard curve, users must determine the optimal sample dilutions for their particular experiments.

### **Assay Procedure**

1. Determine wells for Diluted Standard, Blank and Sample. Prepare 7 wells for Standard, 1 well for Blank. Add 100 μL each of Standard Working Solution (please refer to Reagent Preparation), or 100 μL of samples into the appropriate wells. Cover with the Plate Cover. Incubate for 80 minutes at 37°C. Note: solutions should be added to the bottom of the

micro ELISA plate well, avoid touching the inside wall and causing foaming as much as possible.

2. Pour out the liquid of each well. Aspirate the solution and wash with 200  $\mu$ L of 1 $\times$  Wash Solution to each well and let it sit for 1-2 minutes. Remove the remaining liquid from all wells completely by snapping the plate onto absorbent paper. Totally wash 3 times. After the last wash, remove any remaining Wash Buffer by aspirating or decanting. Invert the plate and blot it against absorbent

paper. Notes: (a) When adding Washing Solution, the pipette tip should not touch the wall of the wells to avoid contamination. (b) Pay attention to pouring the washing liquid directly to ensure that the washing liquid does not contaminate other wells.

3. Add 100  $\mu$ L of Biotinylated Antibody Working Solution to each well, cover the wells with the Plate <http://www.elkbiotech.com> [elkbio@elkbiotech.com](mailto:elkbio@elkbiotech.com)10 Cover and incubate for 50 minutes at 37°C.

4. Repeat the aspiration, wash process for total 3 times as conducted in step 2.

5. Add 100  $\mu$ L of Streptavidin-HRP Working Solution to each well, cover the wells with the plate sealer and incubate for 50 minutes at 37°C.

6. Repeat the aspiration, wash process for total 5 times as conducted in step 2.

7. Add 90  $\mu$ L of TMB Substrate Solution to each well. Cover with a new Plate Cover. Incubate for 20 minutes at 37°C (Don't exceed 30 minutes) in the dark. The liquid will

turn blue by the addition of TMB Substrate Solution. Preheat the Microplate Reader for about 15 minutes before OD measurement.

8. Add 50  $\mu$ L of Stop Reagent to each well. The liquid will turn yellow by the addition of Stop Reagent. Mix the liquid by tapping the side of the plate. If color change does not appear uniform, gently tap the plate to ensure thorough mixing. The insertion order of the Stop Reagent should be the same as that of the TMB Substrate Solution.

9. Wipe off any drop of water and fingerprint on the bottom of the plate and confirm there is no bubble on the surface of the liquid. Then, run the microplate reader and conduct measurement at 450 nm immediately.

### **Calculation of Results**

Average the duplicate readings for each Standard, Control, and Samples and subtract the average zero Standard optical density. Construct a Standard curve with the Rat RANK concentration on the y-axis and absorbance on the x-axis, and draw a best fit curve through the points on the graph. If samples have been diluted, the concentration read from the Standard curve must be multiplied by the dilution.

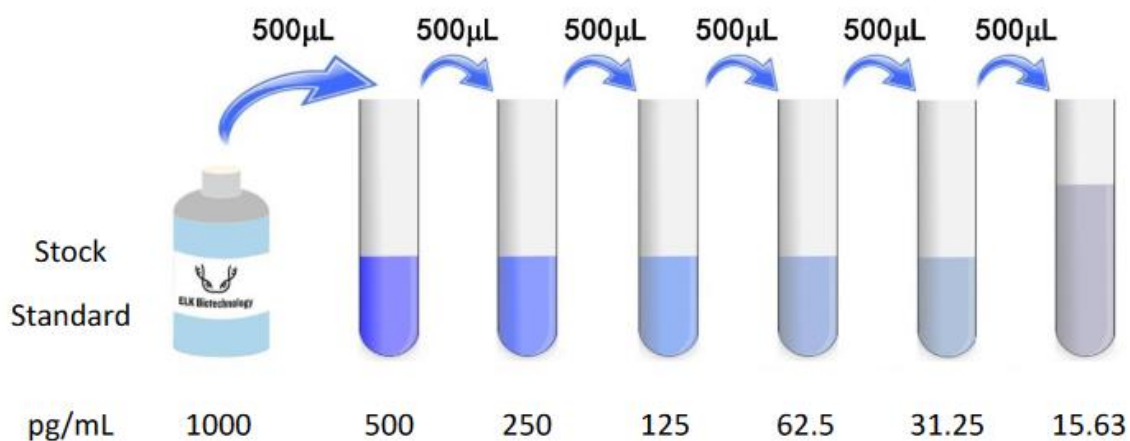


## Appendix II

### Detection of serum RANKL

#### Reagent Preparation:

1. Bring all kit components and samples to room temperature (18-25°C) before use. Make sure all components are dissolved and mixed well before using the kit.
2. If the kit will not be used up in 1 time, please only take out strips and reagents for present experiment, and save the remaining strips and reagents as specified.
3. Dilute the 25× Wash Buffer into 1× Wash Buffer with double-distilled Water.
4. Standard Working Solution - Centrifuge the Standard at  $1000 \times g$  for 1 minute. Reconstitute the Standard with 1.0 mL of Standard Diluent Buffer, kept for 10 minutes at room temperature, shake gently (not to foam). The concentration of the Standard in the stock solution is 10 ng/mL. Please prepare 7 tubes containing 0.5 mL Standard Diluent Buffer and use the Diluted Standard to produce a double dilution series according to the picture shown below. To mix each tube thoroughly before the next transfer, pipette the solution up and down several times. Set up 7 points of Diluted Standard such as 10 ng/mL, 5 ng/mL, 2.5 ng/mL, 1.25 ng/mL, 0.63 ng/mL, 0.32 ng/mL, 0.16 ng/mL, and the last EP tubes with Standard Diluent is the Blank as 0 ng/mL. In order to guarantee the experimental results validity, please use the new Standard Solution for each experiment. When diluting the Standard from high concentration to low concentration, replace the pipette tip for each dilution. Note: the last tube is regarded as a Blank and do not pipette solution into it from the former tube.



5- Biotinylated Antibody and 1× Streptavidin-HRP - Briefly spin centrifuge the stock Biotinylated Antibody and Streptavidin-HRP before use. Dilute them to working concentration 100-fold with Biotinylated Antibody Diluent and HRP Diluent, respectively.

6. TMB Substrate Solution - Aspirate the needed dosage of the solution with sterilized tips and do not dump the residual solution into the vial again.

## **Samples Preparation**

1. Equilibrate all materials and prepared reagents to room temperature prior to use. Prior to use, mix all reagents thoroughly taking care not to create any foam within the vials.
2. The user should calculate the possible amount of the samples used in the whole test. Please reserve sufficient samples in advance.
3. Please predict the concentration before assaying. If values for these are not within the range of the Standard curve, users must determine the optimal sample dilutions for their particular experiments.

## **Assay Procedure**

1. Determine wells for Diluted Standard, Blank and Sample. Prepare 7 wells for Standard,

1 well for Blank. Add 100  $\mu$ L each of Standard Working Solution (please refer to Reagent Preparation), or 100  $\mu$ L of samples into the appropriate wells. Cover with the Plate Cover. Incubate for 80 minutes at 37°C. Note: solutions should be added to the bottom of the micro ELISA plate well, avoid touching the inside wall and causing foaming as much as possible.

2. Pour out the liquid of each well. Aspirate the solution and wash with 200  $\mu$ L of 1 $\times$  Wash Solution to each well and let it sit for 1-2 minutes. Remove the remaining liquid from all wells completely by snapping the plate onto absorbent paper. Totally wash 3 times. After the last wash, remove any remaining Wash Buffer by aspirating or decanting. Invert the plate and blot it against absorbent

paper. Notes: (a) When adding Washing Solution, the pipette tip should not touch the wall of the wells to avoid contamination. (b) Pay attention to pouring the washing liquid directly to ensure that the washing liquid does not contaminate other wells.

3. Add 100  $\mu$ L of Biotinylated Antibody Working Solution to each well, cover the wells with the Plate <http://www.elkbiotech.com> [elkbio@elkbiotech.com](mailto:elkbio@elkbiotech.com)10 Cover and incubate for 50 minutes at 37°C.

4. Repeat the aspiration, wash process for total 3 times as conducted in step 2.

5. Add 100  $\mu$ L of Streptavidin-HRP Working Solution to each well, cover the wells with the plate sealer and incubate for 50 minutes at 37°C.

6. Repeat the aspiration, wash process for total 5 times as conducted in step 2.
7. Add 90  $\mu\text{L}$  of TMB Substrate Solution to each well. Cover with a new Plate Cover. Incubate for 20 minutes at  $37^{\circ}\text{C}$  (Don't exceed 30 minutes) in the dark. The liquid will turn blue by the addition of TMB Substrate Solution. Preheat the Microplate Reader for about 15 minutes before OD measurement.
8. Add 50  $\mu\text{L}$  of Stop Reagent to each well. The liquid will turn yellow by the addition of Stop Reagent. Mix the liquid by tapping the side of the plate. If color change does not appear uniform, gently tap the plate to ensure thorough mixing. The insertion order of the Stop Reagent should be the same as that of the TMB Substrate Solution.
9. Wipe off any drop of water and fingerprint on the bottom of the plate and confirm there is no bubble on the surface of the liquid. Then, run the microplate reader and conduct measurement at 450 nm immediately.

## **Calculation of Results**

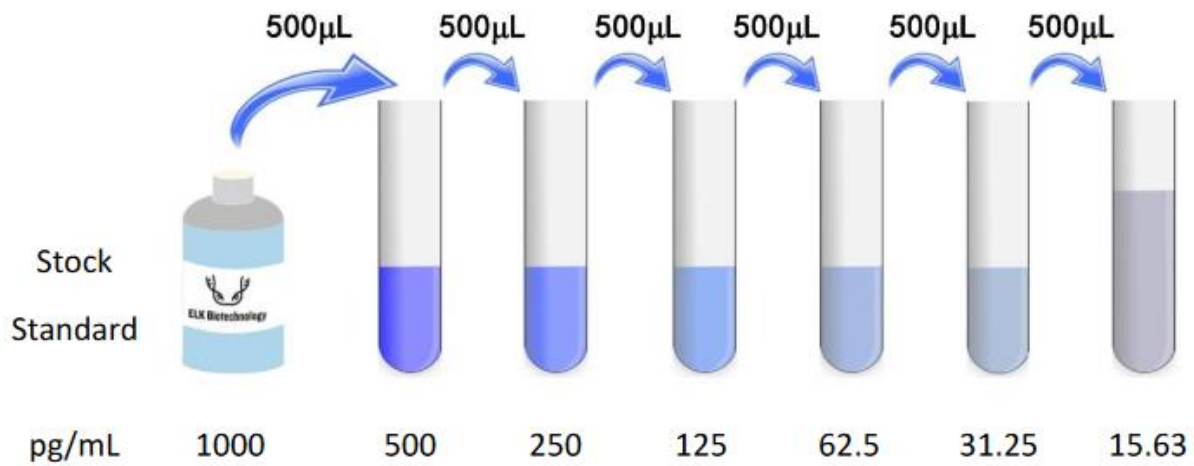
Average the duplicate readings for each Standard, Control, and Samples and subtract the average zero Standard optical density. Construct a Standard curve with the Rat RANKL concentration on the y-axis and absorbance on the x-axis, and draw a best fit curve through the points on the graph. If samples have been diluted, the concentration read from the Standard curve must be multiplied by the dilution.

## Appendix III

### Detection of serum Cathepsin K

#### Reagent Preparation:

1. Bring all kit components and samples to room temperature (18-25°C) before use. Make sure all components are dissolved and mixed well before using the kit.
2. If the kit will not be used up in 1 time, please only take out strips and reagents for present experiment, and save the remaining strips and reagents as specified.
3. Dilute the 25× Wash Buffer into 1× Wash Buffer with double-distilled Water.
4. Standard Working Solution - Centrifuge the Standard at  $1000 \times g$  for 1 minute. Reconstitute the Standard with 1.0 mL of Standard Diluent Buffer, kept for 10 minutes at room temperature, shake gently (not to foam). The concentration of the Standard in the stock solution is 10 ng/mL. Please prepare 7 tubes containing 0.5 mL Standard Diluent Buffer and use the Diluted Standard to produce a double dilution series according to the picture shown below. To mix each tube thoroughly before the next transfer, pipette the solution up and down several times. Set up 7 points of Diluted Standard such as 10 ng/mL, 5 ng/mL, 2.5 ng/mL, 1.25 ng/mL, 0.63 ng/mL, 0.32 ng/mL, 0.16 ng/mL, and the last EP tubes with Standard Diluent is the Blank as 0 ng/mL. In order to guarantee the experimental results validity, please use the new Standard Solution for each experiment. When diluting the Standard from high concentration to low concentration, replace the pipette tip for each dilution. Note: the last tube is regarded as a Blank and do not pipette solution into it from the former tube.



5- Biotinylated Antibody and 1× Streptavidin-HRP - Briefly spin centrifuge the stock Biotinylated Antibody and Streptavidin-HRP before use. Dilute them to working concentration 100-fold with Biotinylated Antibody Diluent and HRP Diluent, respectively.

6. TMB Substrate Solution - Aspirate the needed dosage of the solution with sterilized tips and do not dump the residual solution into the vial again.

## Samples Preparation

1. Equilibrate all materials and prepared reagents to room temperature prior to use. Prior to use, mix all reagents thoroughly taking care not to create any foam within the vials.
2. The user should calculate the possible amount of the samples used in the whole test. Please reserve sufficient samples in advance.
3. Please predict the concentration before assaying. If values for these are not within the range of the Standard curve, users must determine the optimal sample dilutions for their particular experiments.

## Assay Procedure

1. Determine wells for Diluted Standard, Blank and Sample. Prepare 7 wells for Standard,

1 well for Blank. Add 100  $\mu$ L each of Standard Working Solution (please refer to Reagent Preparation), or 100  $\mu$ L of samples into the appropriate wells. Cover with the Plate Cover. Incubate for 80 minutes at 37°C. Note: solutions should be added to the bottom of the micro ELISA plate well, avoid touching the inside wall and causing foaming as much as possible.

2. Pour out the liquid of each well. Aspirate the solution and wash with 200  $\mu$ L of 1 $\times$  Wash Solution to each well and let it sit for 1-2 minutes. Remove the remaining liquid from all wells completely by snapping the plate onto absorbent paper. Totally wash 3 times. After the last wash, remove any remaining Wash Buffer by aspirating or decanting. Invert the plate and blot it against absorbent

paper. Notes: (a) When adding Washing Solution, the pipette tip should not touch the wall of the wells to avoid contamination. (b) Pay attention to pouring the washing liquid directly to ensure that the washing liquid does not contaminate other wells.

3. Add 100  $\mu$ L of Biotinylated Antibody Working Solution to each well, cover the wells with the Plate <http://www.elkbiotech.com> [elkbio@elkbiotech.com](mailto:elkbio@elkbiotech.com)10 Cover and incubate for 50 minutes at 37°C.

4. Repeat the aspiration, wash process for total 3 times as conducted in step 2.

5. Add 100  $\mu$ L of Streptavidin-HRP Working Solution to each well, cover the wells with the plate sealer and incubate for 50 minutes at 37°C.

6. Repeat the aspiration, wash process for total 5 times as conducted in step 2.
7. Add 90  $\mu\text{L}$  of TMB Substrate Solution to each well. Cover with a new Plate Cover. Incubate for 20 minutes at  $37^{\circ}\text{C}$  (Don't exceed 30 minutes) in the dark. The liquid will turn blue by the addition of TMB Substrate Solution. Preheat the Microplate Reader for about 15 minutes before OD measurement.
8. Add 50  $\mu\text{L}$  of Stop Reagent to each well. The liquid will turn yellow by the addition of Stop Reagent. Mix the liquid by tapping the side of the plate. If color change does not appear uniform, gently tap the plate to ensure thorough mixing. The insertion order of the Stop Reagent should be the same as that of the TMB Substrate Solution.
9. Wipe off any drop of water and fingerprint on the bottom of the plate and confirm there is no bubble on the surface of the liquid. Then, run the microplate reader and conduct measurement at 450 nm immediately.

### **Calculation of Results**

Average the duplicate readings for each Standard, Control, and Samples and subtract the average zero Standard optical density. Construct a Standard curve with the Rat CTSK concentration on the y-axis and absorbance on the x-axis, and draw a best fit curve through the points on the graph. If samples have been diluted, the concentration read from the Standard curve must be multiplied by the dilution.

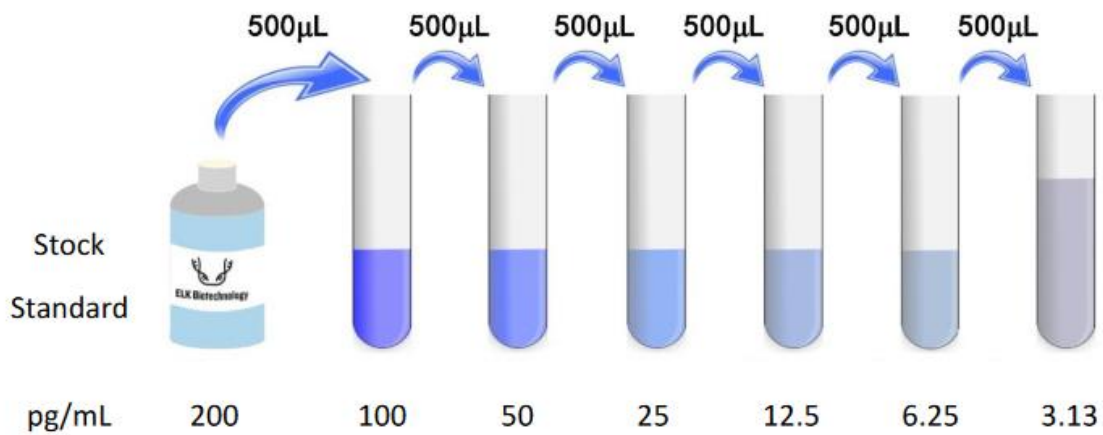


## Appendix IV

### Detection of serum osteoprotegerin

#### Reagent Preparation:

1. Bring all kit components and samples to room temperature (18-25°C) before use. Make sure all components are dissolved and mixed well before using the kit.
2. If the kit will not be used up in 1 time, please only take out strips and reagents for present experiment, and save the remaining strips and reagents as specified.
3. Dilute the 25× Wash Buffer into 1× Wash Buffer with double-distilled Water.
4. Standard Working Solution - Centrifuge the Standard at  $1000 \times g$  for 1 minute. Reconstitute the Standard with 1.0 mL of Standard Diluent Buffer, kept for 10 minutes at room temperature, shake gently (not to foam). The concentration of the Standard in the stock solution is 200 pg/mL. Please prepare 7 tubes containing 0.5 mL Standard Diluent Buffer and use the Diluted Standard to produce a double dilution series according to the picture shown below. To mix each tube thoroughly before the next transfer, pipette the solution up and down several times. Set up 7 points of Diluted Standard such as 200 pg/mL, 100 pg/mL, 50 pg/mL, 25 pg/mL, 12.5 pg/mL, 6.25 pg/mL, 3.13 pg/mL, and the last EP tubes with Standard Diluent is the Blank as 0 pg/mL. In order to guarantee the experimental results validity, please use the new Standard Solution for each experiment. When diluting the Standard from high concentration to low concentration, replace the pipette tip for each dilution. Note: the last tube is regarded as a Blank and do not pipette solution into it from the former tube.



5- Biotinylated Antibody and 1× Streptavidin-HRP - Briefly spin centrifuge the stock Biotinylated Antibody and Streptavidin-HRP before use. Dilute them to working concentration 100-fold with Biotinylated Antibody Diluent and HRP Diluent, respectively.

6. TMB Substrate Solution - Aspirate the needed dosage of the solution with sterilized tips and do not dump the residual solution into the vial again.

## Assay Procedure

1. Determine wells for Diluted Standard, Blank and Sample. Prepare 7 wells for Standard, 1 well for Blank. Add 100 µL each of Standard Working Solution (please refer to Reagent Preparation), or 100 µL of samples into the appropriate wells. Cover with the Plate Cover. Incubate for 80 minutes at 37°C. Note: solutions should be added to the bottom of the micro ELISA plate well, avoid touching the inside wall and causing foaming as much as possible.
2. Pour out the liquid of each well. Aspirate the solution and wash with 200 µL of 1× Wash Solution to each well and let it sit for 1-2 minutes. Remove the remaining liquid

from all wells completely by snapping the plate onto absorbent paper. Totally wash 3 times. After the last wash, remove any remaining Wash Buffer by aspirating or decanting. Invert the plate and blot it against absorbent paper.

Notes: (a) When adding Washing Solution, the pipette tip should not touch the wall of the wells to avoid contamination.

(b) Pay attention to pouring the washing liquid directly to ensure that the washing liquid does not contaminate other wells.

3. Add 100  $\mu$ L of Biotinylated Antibody Working Solution to each well, cover the wells with the Plate <http://www.elkbiotech.com> [elkbio@elkbiotech.com](mailto:elkbio@elkbiotech.com)10 Cover and incubate for 50 minutes at 37°C.

4. Repeat the aspiration, wash process for total 3 times as conducted in step 2.

5. Add 100  $\mu$ L of Streptavidin-HRP Working Solution to each well, cover the wells with the plate sealer and incubate for 50 minutes at 37°C.

6. Repeat the aspiration, wash process for total 5 times as conducted in step 2.

7. Add 90  $\mu$ L of TMB Substrate Solution to each well. Cover with a new Plate Cover. Incubate for 20 minutes at 37°C (Don't exceed 30 minutes) in the dark. The liquid will turn blue by the addition of TMB Substrate Solution. Preheat the Microplate Reader for about 15 minutes before OD measurement.

8. Add 50  $\mu$ L of Stop Reagent to each well. The liquid will turn yellow by the addition of Stop Reagent. Mix the liquid by tapping the side of the plate. If color change does not appear uniform, gently tap the plate to ensure thorough mixing. The insertion order of the Stop Reagent should be the same as that of the TMB Substrate Solution.

9. Wipe off any drop of water and fingerprint on the bottom of the plate and confirm there is no bubble on the surface of the liquid. Then, run the microplate reader and conduct

measurement at 450 nm immediately.

## **Calculation of Results**

Average the duplicate readings for each Standard, Control, and Samples and subtract the average zero Standard optical density. Construct a Standard curve with the Rat CTSK concentration on the y-axis and absorbance on the x-axis, and draw a best fit curve through the points on the graph. If samples have been diluted, the concentration read from the Standard curve must be multiplied by the dilution.

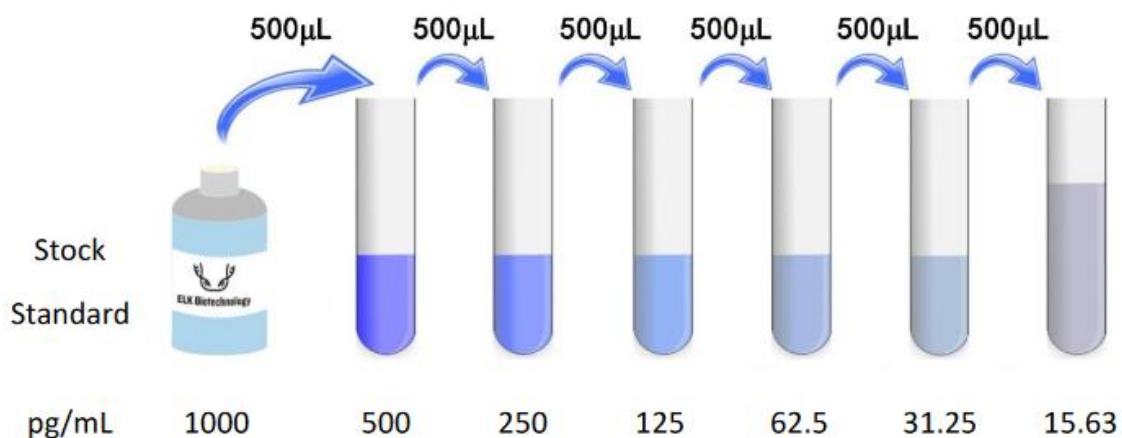
## **Appendix V**

### **Detection of serum Calcitonin**

#### **Reagent Preparation**

1. Bring all kit components and samples to room temperature (18-25°C) before use. Make sure all components are dissolved and mixed well before using the kit.
2. If the kit will not be used up in 1 time, please only take out strips and reagents for present experiment, and save the remaining strips and reagents as specified.
3. Dilute the 25× Wash Buffer into 1× Wash Buffer with double-distilled Water.
4. Standard Working Solution - Centrifuge the Standard at 1000 × g for 1 minute. Reconstitute the Standard with 1.0 mL of Standard Diluent Buffer, kept for 10 minutes at room temperature, shake gently (not to foam). The concentration of the Standard in the stock solution is 1000 pg/mL. Please prepare 7 tubes containing 0.5 mL Standard Diluent

Buffer and use the Diluted Standard to produce a double dilution series according to the picture shown below. To mix each tube thoroughly before the next transfer, pipette the solution up and down several times. Set up 7 points of Diluted Standard such as 1000 pg/mL, 500 pg/mL, 250 pg/mL, 125 pg/mL, 62.5 pg/mL, 31.25 pg/mL, 15.63 pg/mL, and the last EP tubes with Standard Diluent is the Blank as 0 pg/mL. In order to guarantee the experimental results validity, please use the new Standard Solution for each experiment. When diluting the Standard from high concentration to low concentration, replace the pipette tip for each dilution. Note: the last tube is regarded as a Blank and do not pipette solution into it from the former tube



5- Biotinylated Antibody and 1× Streptavidin-HRP - Briefly spin centrifuge the stock Biotinylated Antibody and Streptavidin-HRP before use. Dilute them to working concentration 100-fold with Biotinylated Antibody Diluent and HRP Diluent, respectively.

6. TMB Substrate Solution - Aspirate the needed dosage of the solution with sterilized tips and do not dump the residual solution into the vial again.

### **Assay Procedure:**

1. Determine wells for Diluted Standard, Blank and Sample. Prepare 7 wells for Standard, 1 well for Blank. Add 100  $\mu$ L each of Standard Working Solution (please refer to Reagent Preparation), or 100  $\mu$ L of samples into the appropriate wells. Cover with the Plate Cover. Incubate for 80 minutes at 37°C. Note: solutions should be added to the bottom of the micro ELISA plate well, avoid touching the inside wall and causing foaming as much as possible.

2. Pour out the liquid of each well. Aspirate the solution and wash with 200  $\mu$ L of 1 $\times$  Wash Solution to each well and let it sit for 1-2 minutes. Remove the remaining liquid from all wells completely by snapping the plate onto absorbent paper. Totally wash 3 times. After the last wash, remove any remaining Wash Buffer by aspirating or decanting. Invert the plate and blot it against absorbent paper.

Notes: (a) When adding Washing Solution, the pipette tip should not touch the wall of the wells to avoid contamination.

(b) Pay attention to pouring the washing liquid directly to ensure that the washing liquid does not contaminate other wells.

3. Add 100  $\mu$ L of Biotinylated Antibody Working Solution to each well cover the wells with the Plate <http://www.elkbiotech.com> [elkbio@elkbiotech.com](mailto:elkbio@elkbiotech.com)10 Cover and incubate for 50 minutes at 37°C.

4. Repeat the aspiration, wash process for total 3 times as conducted in step 2.

5. Add 100  $\mu$ L of Streptavidin-HRP Working Solution to each well, cover the wells with

the plate sealer and incubate for 50 minutes at 37°C.

6. Repeat the aspiration, wash process for total 5 times as conducted in step 2.

7. Add 90  $\mu\text{L}$  of TMB Substrate Solution to each well. Cover with a new Plate Cover. Incubate for 20 minutes at 37°C (Don't exceed 30 minutes) in the dark. The liquid will turn blue by the addition of TMB Substrate Solution. Preheat the Microplate Reader for about 15 minutes before OD measurement.

8. Add 50  $\mu\text{L}$  of Stop Reagent to each well. The liquid will turn yellow by the addition of Stop Reagent. Mix the liquid by tapping the side of the plate. If color change does not appear uniform, gently tap the plate to ensure thorough mixing. The insertion order of the Stop Reagent should be the same as that of the TMB Substrate Solution.

9. Wipe off any drop of water and fingerprint on the bottom of the plate and confirm there is no bubble on the surface of the liquid. Then, run the microplate reader and conduct measurement at 450 nm immediately.

### **Calculation of Results:**

Average the duplicate readings for each Standard, Control, and Samples and subtract the average zero Standard optical density. Construct a Standard curve with the Rat CT concentration on the y-axis and absorbance on the x-axis, and draw a best fit curve through the points on the graph. If samples have been diluted, the concentration read from the Standard curve must be multiplied by the dilution factor. Using some plot software, for

instance, curve expert.

## **Appendix VI**

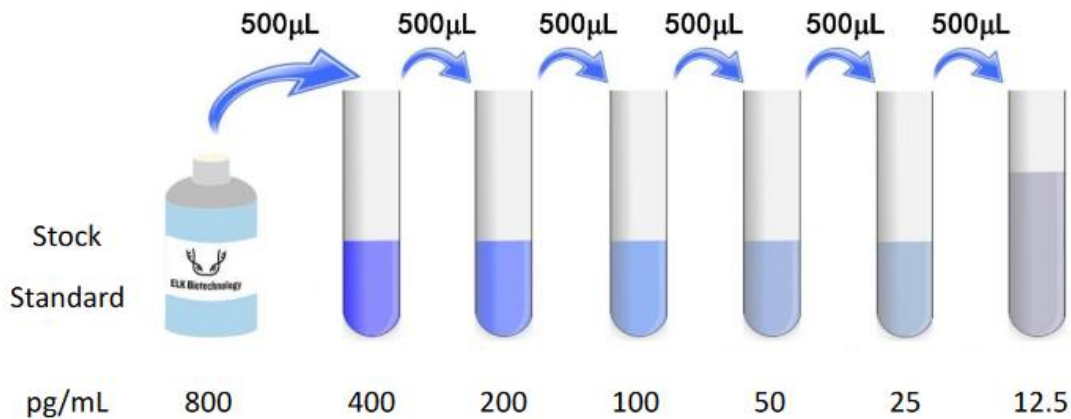
### **Detection of serum parathyroid (PTH)**

#### **Reagent Preparation**

1. Bring all kit components and samples to room temperature (18-25°C) before use. Make sure all components are dissolved and mixed well before using the kit.
2. If the kit will not be used up in 1 time, please only take out strips and reagents for present experiment, and save the remaining strips and reagents as specified.
3. Dilute the 25× Wash Buffer into 1× Wash Buffer with double-distilled Water.
4. Standard Working Solution - Centrifuge the Standard at 1000 × g for 1 minute. Reconstitute the Standard with 1.0 mL of Standard Diluent Buffer, kept for 10 minutes at room temperature, shake gently (not to foam). The concentration of the Standard in the stock solution is 800 pg/mL. Please prepare 7 tubes containing 0.5 mL Standard Diluent Buffer and use the Diluted Standard to produce a double dilution series according to the picture shown below. To mix each tube thoroughly before the next transfer, pipette the solution up and down several times. Set up 7 points of Diluted Standard such as 800 pg/mL, 400 pg/mL, 200 pg/mL, 100 pg/mL, 50 pg/mL, 25 pg/mL, 12.5 pg/mL, and the last EP tubes with Standard Diluent is the Blank as 0 pg/mL. In order to guarantee the experimental results validity, please use the new Standard Solution for each experiment. When diluting



the Standard from high concentration to low concentration, replace the pipette tip for each dilution. Note: the last tube is regarded as a Blank and do not pipette solution into it from the former tube



5- Biotinylated Antibody and 1× Streptavidin-HRP - Briefly spin centrifuge the stock Biotinylated Antibody and Streptavidin-HRP before use. Dilute them to working concentration 100-fold with Biotinylated Antibody Diluent and HRP Diluent, respectively.

6. TMB Substrate Solution - Aspirate the needed dosage of the solution with sterilized tips and do not dump the residual solution into the vial again.

### **Assay Procedure:**

1. Determine wells for Diluted Standard, Blank and Sample. Prepare 7 wells for Standard, 1 well for Blank. Add 100 µL each of Standard Working Solution (please refer to Reagent Preparation), or 100 µL of samples into the appropriate wells. Cover with the Plate Cover. Incubate for 80 minutes at 37°C. Note: solutions should be added to the bottom of the micro

ELISA plate well, avoid touching the inside wall and causing foaming as much as possible.

2. Pour out the liquid of each well. Aspirate the solution and wash with 200  $\mu$ L of 1 $\times$  Wash Solution to each well and let it sit for 1-2 minutes. Remove the remaining liquid from all wells completely by snapping the plate onto absorbent paper. Totally wash 3 times. After the last wash, remove any remaining Wash Buffer by aspirating or decanting. Invert the plate and blot it against absorbent paper.

Notes: (a) When adding Washing Solution, the pipette tip should not touch the wall of the wells to avoid contamination.

(b) Pay attention to pouring the washing liquid directly to ensure that the washing liquid does not contaminate other wells.

3. Add 100  $\mu$ L of Biotinylated Antibody Working Solution to each well cover the wells with the Plate <http://www.elkbiotech.com> [elkbio@elkbiotech.com](mailto:elkbio@elkbiotech.com)10 Cover and incubate for 50 minutes at 37°C.

4. Repeat the aspiration, wash process for total 3 times as conducted in step 2.

5. Add 100  $\mu$ L of Streptavidin-HRP Working Solution to each well, cover the wells with the plate sealer and incubate for 50 minutes at 37°C.

6. Repeat the aspiration, wash process for total 5 times as conducted in step 2.

7. Add 90  $\mu$ L of TMB Substrate Solution to each well. Cover with a new Plate Cover.

Incubate for 20 minutes at 37°C (Don't exceed 30 minutes) in the dark. The liquid will turn blue by the addition of TMB Substrate Solution. Preheat the Microplate Reader for about 15 minutes before OD measurement.

8. Add 50  $\mu\text{L}$  of Stop Reagent to each well. The liquid will turn yellow by the addition of Stop Reagent. Mix the liquid by tapping the side of the plate. If color change does not appear uniform, gently tap the plate to ensure thorough mixing. The insertion order of the Stop Reagent should be the same as that of the TMB Substrate Solution.

9. Wipe off any drop of water and fingerprint on the bottom of the plate and confirm there is no bubble on the surface of the liquid. Then, run the microplate reader and conduct measurement at 450 nm immediately.

### **Calculation of Results:**

Average the duplicate readings for each Standard, Control, and Samples and subtract the average zero Standard optical density. Construct a Standard curve with the Rat CT concentration on the y-axis and absorbance on the x-axis, and draw a best fit curve through the points on the graph. If samples have been diluted, the concentration read from the Standard curve must be multiplied by the dilution factor. Using some plot software, for instance, curve expert.

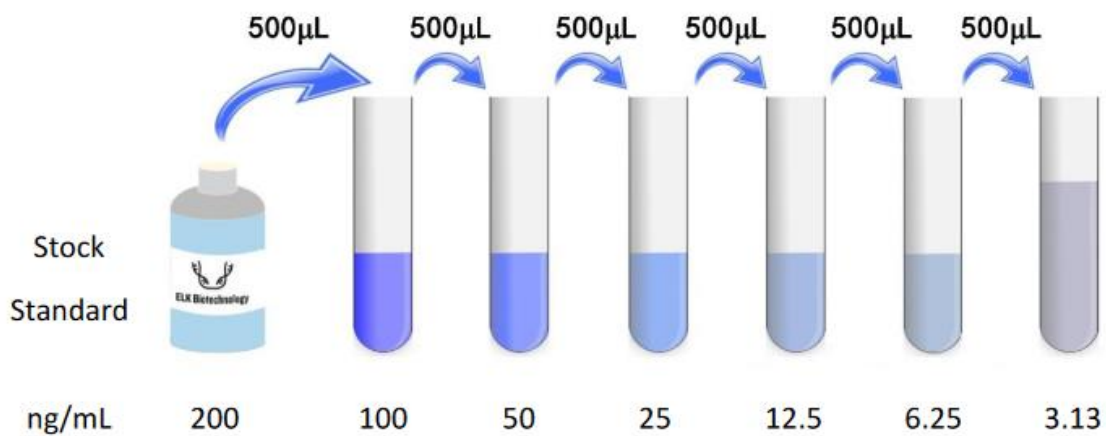
## Appendix VII

### Detection of serum Vit D

#### Reagent Preparation:

1. Bring all kit components and samples to room temperature (18-25°C) before use. Make sure all components are dissolved and mixed well before using the kit.
2. If the kit will not be used up in 1 time, please only take out strips and reagents for present experiment, and save the remaining strips and reagents as specified.
3. Dilute the 25× Wash Buffer into 1× Wash Buffer with double distilled water.
4. Standard Working Solution - Centrifuge the Standard at  $1000 \times g$  for 1 minute. Reconstitute the Standard with 1.0 mL of Standard Diluent Buffer, kept for about 10 minutes at room temperature, shake gently (not to foam). The concentration of the standard in the stock solution is 200 ng/mL. Please prepare 7 tubes containing 0.5 mL Standard Diluent Buffer and use the Diluted Standard to produce a double dilution series according to the picture shown below. To mix each tube thoroughly before the next transfer, pipette the solution up and down several times. Set up 7 points of Diluted Standard such as 200 ng/mL, 100 ng/mL, 50 ng/mL, 25 ng/mL, 12.5 ng/mL, 6.25

ng/mL, 3.13 ng/mL, and the last EP tubes with Standard Diluent is the Blank as 0 ng/mL. In order to guarantee the experimental results validity, please use the new Standard Solution for each experiment. When diluting the Standard from high concentration to low concentration, replace the pipette tip for each dilution. Note: the last tube is regarded as the Blank and do not pipette solution into it from the former tube.



5. 1× Biotinylated-Conjugate and 1× Streptavidin-HRP Working Solution - Briefly spin or centrifuge the stock Biotinylated-Conjugate and Streptavidin-HRP before use. Dilute them to the working concentration 100-fold with Biotinylated-Conjugate Diluent and HRP Diluent, respectively. For <http://www.elkbiotech.com> [elkbio@elkbiotech.com](mailto:elkbio@elkbiotech.com) example, 10 μL of Streptavidin-HRP with 990 μL of HRP Diluent.
6. TMB Substrate Solution - Aspirate the needed dosage of the solution with sterilized tips and do not dump the residual solution into the vial again.

## Assay Procedure

1. Determine wells for Diluted Standard, Blank and Sample. Prepare 7 wells for Standard, 1 well for Blank. Add 50  $\mu$ L of Standard Working Solution (please refer to Reagent Preparation) or Sample into each well (Blank is Standard Diluent). Then, add 50  $\mu$ L of Biotinylated-Conjugate (1 $\times$ ) to each well immediately. Mix well, cover with the Plate Cover. Incubate for 1 hour at 37°C. Note: solutions should be added to the bottom of the micro ELISA plate well, avoid touching the inside wall and causing foaming as much as possible.
2. Pour out the liquid of each well. Aspirate the solution and wash with 200  $\mu$ L of 1 $\times$  Wash Solution to each well and let it sit for 1-2 minutes. After the liquid has been decanted, completely remove the remaining liquid from all wells by snapping the plate onto absorbent paper. Totally wash 3 times. Complete removal of liquid at each step is essential for good performance. After the last wash invert the plate and blot it against clean paper towels to remove excess liquid. Notes: (a) When adding Washing Solution, the pipette tip should not touch the wall of the wells to avoid contamination. <http://www.elkbiotech.com> [elkbio@elkbiotech.com](mailto:elkbio@elkbiotech.com)10 (b) Pay attention to pouring the washing liquid directly to ensure that the washing liquid does not contaminate other wells.
3. Add 100  $\mu$ L of Streptavidin-HRP Working Solution (1 $\times$ ) to each well, cover the wells with the Plate Cover and incubate at 37°C for 60 minutes.
4. Repeat the aspiration, wash process for total 5 times as conducted in step 2.
5. Add 90  $\mu$ L of TMB Substrate Solution to each well. Cover with a new Plate Cover. Incubate for 20 minutes at 37°C (Don't exceed 30 minutes) in the dark. The liquid will turn blue by the addition of TMB Substrate Solution. Preheat the Microplate Reader for about 15 minutes before OD measurement. Avoid placing the plate in direct light.

6. Add 50  $\mu\text{L}$  of Stop Reagent to each well. The liquid will turn yellow by the addition of Stop Reagent. Mix the liquid by tapping the side of the plate. The insertion order of the Stop Reagent should be the same as that of the TMB Substrate Solution.

7. Wipe off any drop of water and fingerprint on the bottom of the plate and confirm there is no bubble on the surface of the liquid. Then, run the microplate reader and conduct measurement at 450 nm immediately.

## **Appendix VIII**

### **Detection of serum Calcium(Ca)**

Total Calcium exists in 3 physiochemical states in plasma, of which approximately 50 % is free or ionised calcium, 40 % is bound to plasma proteins, and 10 % are bound with small anions. The level of serum calcium may be affected by intestinal malabsorption, by alterations in plasma proteins level, especially albumin, which should be measured concurrently with calcium. Hypercalcemia is found in hyperparathyroidism, multiple myeloma, bone and parathyroidal neoplasms and in states with bones demineralisation. Hypocalcemia is encountered in hypoparathyroidism and in several cases of necrosis and acute pancreatitis.

### **PRINCIPLE**

Moorehead and Briggs derived CPC (O-Cresol Phtalein Complexone) method allows to determinate total Calcium concentration in serum, plasma or urines. In alkaline solution CPC reacts with calcium to form a dark-red coloured complex which

absorbance measured at 570 nm is proportional to the amount of calcium in the specimen

## PROCEDURE

Detailed Kenza 240TX procedure is available on request Wavelength: 570 nm

Temperature: 37°C. Temperature should be held constant as the absorbance of the dye is temperature sensitive.

	Automated analyzer	Manual procedure
<b>Reagents</b>	120 µL R1 120 µL R2	WR :1000 µL
<b>Standard, Controls, Specimen</b>	6 µL	25 µL

Mix well. Incubate for 5 minutes at room temperature.  
Read absorbance at 570 nm (550-590) against reagent blank.  
The coloration is stable for 1 hour away from light

## CALCULATION

Calculate the result as follows:

$$\text{Result} = \frac{\text{Abs(Assay)}}{\text{Abs(Standard)}} \times \text{Standard concentration}$$



## Appendix IX

### Detection of serum Phosphorus(p)

1. Bring reagents and samples to room temperature.

2. Pipette into labeled test tubes

TUBES	Blank	Sample	CAL. Standard
Working Reagent	1.0 mL	1.0 mL	1.0 mL
Sample	<input type="checkbox"/>	50 $\mu$ L	<input type="checkbox"/>
CAL. Standard	<input type="checkbox"/>	<input type="checkbox"/>	50 $\mu$ L

3. Mix, let stand the tubes for 1 minute and then pipette:

R3. Developer	0,5 mL	0,5 mL	0,5 mL
---------------	--------	--------	--------

4. Mix and let the tubes stand 10 minutes at room temperature.

5. Read the absorbance (A) of the sample and the standard at 740 nm against the reagent blank.

### CALCULATIONS

Serum, plasma

A Sample

————— x C Standard = mg/dL phosphorus

A Standard

Samples with concentrations higher than 15 mg/dL (4.8 mmol/L) should be diluted 1:2 with saline and assayed again. Multiply the results by 2.

## Appendix X

### Detection of serum sodium(Na)

## Procedure for Measuring Sodium using Kenza Analyzer

### 1. Sample Collection:

- Blood samples were collected in tubes without anticoagulant for serum or in tubes with anticoagulant for plasma.

### 2. Centrifugation:

- The blood samples were centrifuged at an appropriate speed to separate the serum or plasma from the blood cells.

### 3. Sample Transfer:

- The separated serum or plasma was transferred to clean analysis tubes.

### 4. Device Preparation:

- The Kenza Analyzer was turned on and allowed to initialize, ensuring no system errors were present.

### 5. Calibration:

- Calibration of the device was performed using standard solutions with known concentrations of sodium and potassium, following the manufacturer's instructions.

### 6. Sample Analysis:

- The prepared samples were placed into the designated slots on the Kenza Analyzer.

- The specific program for measuring sodium and potassium was selected on the device.

- The analysis process was initiated by pressing the start button.

## 7. Result Reading:

- After the analysis was complete, the concentrations of sodium and potassium were displayed by the device.

- The results were saved or printed as supported by the device.

## 8. Precautions:

- All tools and tubes were ensured to be clean to avoid sample contamination.

- The manufacturer's instructions were closely followed to accommodate specific model variations of the KENZA Analyzer.

- Regular maintenance of the device was performed to ensure accuracy and reliability of result

## Appendix XI

### Detection of serum potassium(K)

#### PROCEDURE

#### Manual method

Let stand reagent and specimens at room temperature.

Reagent 1	800 $\mu$ L
Blank, Standards, control or specimen	20 $\mu$ L
Mix well. Let stand for 5 minutes at 37°C	

Reagent 2	200 $\mu$ L
Mix well. Read at 380 nm absorbance A1 after 60 sec and A2 after 240 sec . Calculate DAbs (Abs A2 – Abs A1) for Blank, Standards and Assays	

1- Performances with manual procedure should be validated by user.

2- KENZA applications and other applications proposal are available on request.

### CALCULATION

Serum or plasma:

DAbs (Assay) - DAbs (Blank)

DAbs (Standard) - DAbs (Blank)

Interpolate the DA in the Calibration Curve

## Appendix XII

### Histopathological examination

The animals were sacrificed via pentobarbital overdose (100 mg/kg). Then, tibia and femur bone were detached and preserved in 10 % neutral buffered formalin for 48 h, and then were fixed in 10 % ethylene diamine tetra-acetic acid (EDTA) for decalcification. Tissue handling was done through graded ethanol, xylol, and paraffin for dehydration, clearing, impregnation, and embedding. Histologic sections with a thickness of 6  $\mu$ m were arranged and afterword they were regularly tainted with hematoxylin and eosin.

## الخلاصة

## الخلاصة :

هشاشة العظام هي احد الامراض التي تصيب العظم و يتميز بفقدانه الكثافة وتدهور في الأنسجة و الخلايا المكونة له وازدياد في الخلايا الهادمة للعظم و قلة في الخلايا البانية و الخلايا العظمية, و ان ممارسة الرياضة و التمارين من الممكن ان تساعد على تحسن بناء العظام و التقليل من حالة الهشاشة .

اجريت التجربة باستخدام 24 جرد حيث تمت تقسيمها الى ثلاث مجاميع متساوية تحتوي كل مجموعة منها على 8 جردان، المجموعة الاولى هي مجموعة السيطرة اما المجموعة الثانية تم اعطاها مادة ال D-gal بجرعة 200 ملغ لكل كيلو غرام من وزن الجسم لمدة 60 يوما، اما المجموعة الثالثة فتم اعطاها مادة ال D-gal بجرعة 200 ملغ لكل كيلو غرام من وزن الجسم مع تمارين المشي بسرعة 25 م/دقيقة لمدة 5 أيام أسبوعياً لمدة ستين يوماً ، كما خضعت الجردان لفحص الاشعة السينية لعظم الفخذ عند اليوم الاول من التجربة و في اليوم ال 30 و في اليوم 60 عند انتهاء التجربة .

سحبت عينات الدم لغرض التحليل البيوكيميائي من خلال قياس ترميم العظام والمؤشرات الحيوية لتكوين العظام ممثلة ب (RANK، RANKL، OPG، CATK) وهرمونات مصل الدم (PTH، calcitonin) و اضافة الى قياس فيتامين D في مصل الدم و قياس نسبة الاملاح في مصل الدم (Ca، P، Na، K). كما تم اخذ عينات من عظم الفخذ و ذلك للفحص بواسطة التقطيع النسيجي والفحص باستخدام المجهر الالكتروني الفاحص (SEM) و الفحص الجيني لجين (Runx 2) عن طريق تصنيع ال cDNA لكشف التعبير الجيني للعظم بين المجاميع الثلاث .

توصلت النتائج الى زيادة واضحة في مستويات كل من RANK و RANK-L و Cathepsin-K في الفئران المصابة ب هشاشة العظام ب استخدام D-gal ، في حين كشف تحليل OPG عن انخفاض كبير في هذه المجموعة. في حين أن تأثير ( D-gal+treadmill ) أظهر انخفاضا كبيرا في مستويات RANK و RANK-L ، و Cathepsin-K مقارنة بمجموعة D-gal. كما ان هناك زيادة كبيرة في المصل في PTH، فيتامين D، الكالسيوم و الكالسيوم في الفئران المصابة بهشاشة العظام مع مجموعات أخرى ، في حين أظهرت المصل انخفاضا كبيرا في كل

من NA و K في مجموعة الفئران المصابة بالهشاشة مقارنة بالمجاميع الأخرى . من ناحية أخرى ، في الناحية الأخرى أظهر تأثير ( D-gal + treadmill ) انخفاضًا كبيرًا في مستوى المصل (PTH و VIT D و Calcitonin و Ca) بالمقارنة مع مجموعة التحكم|. في مجموعة ال D-gal كان هناك اختلال في تركيز هرمون ( Ca وPTH و calcitonin) التي تؤدي إلى اختلال التوازن في Ca بالجسم ، أظهرت النتائج أيضا ان التمارين الرياضية تحفز تكوين العظام وتمنع ارتشاف العظام. و أظهر التعبير الجيني (RUNX 2) زيادة كبيرة في مجموعة D-gal عند مقارنتها بالمجموعات الأخرى . أظهر التصوير الفوتوغرافي للأشعة السينية انخفاضًا كبيرًا في كثافة العظام في مجموعة D-gal كما هو مقارن مع (treadmill + D-gal) ومجموعة التحكم.

أظهر الفحص النسيجي لعظم الفخذ لجرذان مجموعة هشاشة العظام اعادة امتصاص لنسيج العظم مع ترقق في الصفائح العظمية ووجود العديد من الخلايا الهادمة للعظم. بينما أظهرت مجموعات (D-gal +treadmill) العديد من الصفائح المضافة حديثًا وعدد من الخلايا العظمية مع تجويفات أقل في اللوحات العظمية المفحوصة باستخدام المجهر الإلكتروني ، يزيد التمرين من كتلة العظام من خلال زيادة تكوين العظام مع التقليل من امتصاص العظام ، وايضا يسبب زيادة كتلة العظام القشرية بسبب زيادة تكوين العظام. أظهرت نتائج العظام التي تم فحصها تحت المجهر الضوئي وجود اختلافات بين مجموعة السيطرة ومجموعة D-gal ، حيث أن مجموعة D-gal قد قامت بتنشيط خلايا الهمد العظمي ، والتي تسبب نخر العظام والفشل في أداء وظائفها بشكل صحيح ، مما يؤدي إلى ضعف في أنسجة العظم بينما أظهرت مجموعات (D-gal +Treamill) صفيحة عظمية أكثر كثافة داخل القنوات هافرس (تجاويف داخل العظم).

الاستنتاج: استنتجت الدراسة الحالية بانه يمكن أن تقلل التمارين الرياضية من مستوى مسار OPG RANKL و RANKL وتسبب انخفاض مستوى المصل Cathepsin K مع تنظيم للتعبير الجيني لجين RUNX2 على هشاشة العظام الناجمة عن D-galactose.



جمهورية العراق

وزارة التعليم العالي و البحث العلمي

جامعة كربلاء /كلية الطب البيطري

فرع الفلسفة و الكيمياء الحياتية و الادوية

التحري عن بنية العظام ودور تمارين الجري في ذكور الجرذان المصابة بهشاشة العظام بواسطة  
مسار RANKL/RANK-OPG

رسالة

مقدمة إلى مجلس كلية الطب البيطري جامعة كربلاء كجزء من متطلبات درجة الماجستير في الطب البيطري /  
الفلسفة البيطرية

اعداد

تبارك بسيم بليبص

بأشراف

أ. د. رنا فاضل موسى

أ.د وفاق جبوري البازي